Fall 2010

Bioremediation and biocatalysis with Polaromonas sstrain JS666

Anne Kathryn Alexander
University of Iowa

BIOREMEDIATION AND BIOCATALYSIS WITH *POLAROMONAS* SP. STRAIN JS666

by

Anne Kathryn Alexander

An Abstract

Of a thesis submitted in partial fulfillment
of the requirements for the Doctor of
Philosophy degree in Civil and Environmental Engineering
in the Graduate College of
The University of Iowa

December 2010

Thesis Supervisor: Associate Professor Timothy E. Mattes

ABSTRACT

Polaromonas sp. strain JS666 is the only isolated bacterium capable of aerobic growth using the groundwater pollutant *cis*-1,2-dichloroethene (cDCE) as a sole carbon source. Its genome has a wealth of evidence of recent gene acquisition through horizontal gene transfer, and contains gene clusters predicted to encode enzymes allowing the metabolism of a wide variety of xenobiotic compounds. Culture growth using each of these hypothesized substrates was tested experimentally, and many were confirmed as sole carbon sources for strain JS666. In addition to pollutant degradation, many of these metabolic pathways have applicability in the field of biocatalysis, as does the genome-assisted pathway prediction approach to biocatalyst discovery.

During (or immediately following) growth on cDCE, cultures of *Polaromonas* sp. strain JS666 oxidize ethene to epoxyethane at an increased rate, and also cometabolically oxidize several other chlorinated ethenes. Given the involvement of a monooxygenase in other species' 1-chloroethene (vinyl chloride) oxidation, it was hypothesized that alkene oxidation in strain JS666 was due to the activity of a monooxygenase that also was responsible for the first step in cDCE oxidation. The alkene oxidation activity of strain JS666 was investigated using gene expression analysis, proteomics, and whole-cell kinetic assays. Results of these experiments pointed to the upregulation of a cyclohexanone monooxygenase (CHMO) during growth on cDCE and during oxidation of ethene.

To determine the activity of this cyclohexanone monooxygenase, its gene was cloned and heterologously expressed in an *E. coli* host. Our CHMO expression system exhibited activity on cyclohexanone, but not cDCE or ethene, disproving the hypothesis about its involvement in alkene oxidation. The heterologously expressed monooxygenase was also investigated for enantioselective oxidation of racemic cyclic

ketones to chiral lactones, and was discovered to have very high enantioselectivity with the tested compounds. Chiral lactones and other single-enantiomer oxidation products are valuable for fine chemical synthesis, and their biocatalytic production is more environmentally sustainable and often less expensive than traditional techniques.

The research described in the following chapters illustrates the many opportunities that arise when the fields of bioremediation and biocatalysis converge. The shared research goals and methods of these two areas lend themselves to interdisciplinary research, and increased communication and crossover between them should provide benefits for both environmental remediation and sustainable chemical synthesis.

Abstract Approved: _____

Thesis Supervisor

_____

Title and Department

_____

Date

BIOREMEDIATION AND BIOCATALYSIS WITH *POLAROMONAS* SP. STRAIN JS666

by

Anne Kathryn Alexander

A thesis submitted in partial fulfillment
of the requirements for the Doctor of
Philosophy degree in Civil and Environmental Engineering
in the Graduate College of
The University of Iowa

December 2010

Thesis Supervisor: Associate Professor Timothy E. Mattes

Graduate College
The University of Iowa
Iowa City, Iowa

CERTIFICATE OF APPROVAL

_____

PH.D. THESIS

_____

This is to certify that the Ph.D. thesis of

Anne Kathryn Alexander

has been approved by the Examining Committee
for the thesis requirement for the Doctor of Philosophy
degree in Civil and Environmental Engineering at the December 2010
graduation.

Thesis Committee: _____
Timothy E. Mattes, Thesis Supervisor

_____
Jerald Schnoor

_____
Michelle Scherer

_____
Tonya Peeples

_____
John Rosazza

In the end, we will conserve only what we love,
we will love only what we understand,
and we will understand only what we are taught.

Baba Dioum,
Speech to the
General Assembly
of the International
Union for
Conservation of
Nature, 1968

ACKNOWLEDGMENTS

Funding for this work was provided by the University of Iowa's Center for Biocatalysis and Bioprocessing, the Iowa Biotechnology Byproducts Consortium, the Center for Environmental Beneficial Catalysis, and a National Science Foundation Graduate Research Fellowship.

All of this research was made possible by the excellent facilities and welcoming environment of the Department of Civil and Environmental Engineering, and thanks are due to all of its encouraging faculty and extremely helpful staff. In particular, Collin Just provided assistance and expertise in the use of many different laboratory instruments and procedures. Fellow environmental engineering graduate students have always been friendly and willing to help, and Yang Oh Jin, Adina Chuang, Carmen Owens, and Joshua Livermore deserve specific recognition for many insightful and instructive conversations about hypotheses and research methods.

My research advisor, Dr. Timothy Mattes, has provided invaluable guidance and support throughout my Ph.D. training. His unflagging enthusiasm for both teaching and research has been an inspiration, and the individual attention and consideration he gives to each one of his students is truly appreciated.

Encouragement from my family has been a great source of strength and sanity throughout this effort, and my husband Erik has been a wonderful partner. From teaching me chemistry on our first dates to patiently and lovingly supporting me during the preparation of this dissertation, he has always supported me and pushed me to achieve greater things.

I also need to thank Dr. Andrew Lamm of the University of Technology, Jamaica (formerly of the Center for Biocatalysis and Bioprocessing) for guidance in the initial construction of our heterologous enzyme expression system, and Dr. Marko Mihovilovic

of the Vienna University of Technology for graciously providing plasmid pMM4 containing the *Acinetobacter* NCIMB 9871 cyclohexanone monooxygenase gene.

ABSTRACT

Polaromonas sp. strain JS666 is the only isolated bacterium capable of aerobic growth using the groundwater pollutant *cis*-1,2-dichloroethene (cDCE) as a sole carbon source. Its genome has a wealth of evidence of recent gene acquisition through horizontal gene transfer, and contains gene clusters predicted to encode enzymes allowing the metabolism of a wide variety of xenobiotic compounds. Culture growth using each of these hypothesized substrates was tested experimentally, and many were confirmed as sole carbon sources for strain JS666. In addition to pollutant degradation, many of these metabolic pathways have applicability in the field of biocatalysis, as does the genome-assisted pathway prediction approach to biocatalyst discovery.

During (or immediately following) growth on cDCE, cultures of *Polaromonas* sp. strain JS666 oxidize ethene to epoxyethane at an increased rate, and also cometabolically oxidize several other chlorinated ethenes. Given the involvement of a monooxygenase in other species' 1-chloroethene (vinyl chloride) oxidation, it was hypothesized that alkene oxidation in strain JS666 was due to the activity of a monooxygenase that also was responsible for the first step in cDCE oxidation. The alkene oxidation activity of strain JS666 was investigated using gene expression analysis, proteomics, and whole-cell kinetic assays. Results of these experiments pointed to the upregulation of a cyclohexanone monooxygenase (CHMO) during growth on cDCE and during oxidation of ethene.

To determine the activity of this cyclohexanone monooxygenase, its gene was cloned and heterologously expressed in an *E. coli* host. Our CHMO expression system exhibited activity on cyclohexanone, but not cDCE or ethene, disproving the hypothesis about its involvement in alkene oxidation. The heterologously expressed monooxygenase was also investigated for enantioselective oxidation of racemic cyclic

ketones to chiral lactones, and was discovered to have very high enantioselectivity with the tested compounds. Chiral lactones and other single-enantiomer oxidation products are valuable for fine chemical synthesis, and their biocatalytic production is more environmentally sustainable and often less expensive than traditional techniques.

The research described in the following chapters illustrates the many opportunities that arise when the fields of bioremediation and biocatalysis converge. The shared research goals and methods of these two areas lend themselves to interdisciplinary research, and increased communication and crossover between them should provide benefits for both environmental remediation and sustainable chemical synthesis.

TABLE OF CONTENTS

LIST OF TABLES

Table

LIST OF FIGURES

Figure

CHAPTER I

INTRODUCTION

Background

The research described in this dissertation focuses on investigations of the bacterium *Polaromonas* sp. strain JS666 and its potential application in the fields of both bioremediation and biocatalysis. This species was originally isolated and studied because of its unique ability to grow aerobically using a recalcitrant groundwater pollutant (*cis*-1,2-dichloroethene) as a sole carbon source. However, the research described here demonstrates that the xenobiotic-degrading properties that make this bacterium a notable prospect in bioremediation also make it a potentially valuable source of industrial biocatalysts. The overlap of goals and methods between these two fields has been a common theme throughout the research presented here, and should be taken advantage of in future studies to discover the hidden applications of biocatalyst-providing organisms to bioremediation, and vice versa.

This introductory chapter contains general material about evolution of xenobiotic-degrading bacteria, remediation of chlorinated ethenes, the occurrence, activity, and detection of chlorinated ethene degraders in the environment, and contributions of xenobiotic-degrading bacteria to industrial biocatalysis. Some of these sections were prepared for a recent review article about the ecology and evolution of aerobic chlorinated ethene degraders (T. E. Mattes, Alexander, & Coleman, 2010), while other sections are included here solely to provide important background material and context for the research described in the later chapters.

Portions of this chapter were published in: Mattes, T.E.; Alexander, A.K.; and Coleman, N.V. 2010. "Aerobic Biodegradation of the Chloroethenes: Pathways, Enzymes, Ecology, and Evolution." FEMS Microbiology Reviews. 34:445-475.

Evolution of Xenobiotic-Degrading Bacteria from Natural Product Degraders

The term “xenobiotic” refers to something foreign to living organisms, and in the case of environmental pollution, it is used to describe contaminants that natural populations have not previously encountered. In their strictest definition, xenobiotic compounds are those that never appeared in nature before being introduced by human activity, but a more useful designation from an evolutionary standpoint is one that includes compounds occurring in nature at an elevated concentration due to anthropogenic release (Leisinger, 1983). Examples of strictly-defined xenobiotic compounds include polychlorinated biphenyls, while more loosely-defined xenobiotics include heavy metals, petroleum-derived compounds, and chlorinated alkenes (Abrahamsson, Ekdahl, Collen, & Pedersen, 1995; Myneni, 2002). For the purposes of an evolutionary analysis, it is most helpful to discuss xenobiotic compounds in the broader sense because the introduction of pollutants to new locations or at drastically elevated concentrations presents the same evolutionary challenges to microorganisms that entirely new compounds would.

In spite of the novelty of xenobiotic compounds, microbiological degradation of a wide variety of pollutants has been confirmed at many contaminated sites. Classic examples include microbial oxidation of nitroorganic explosives (Gorontzy et al., 1994), reduction of heavy metals (Lloyd, Nolting, Sole, Bosecker, & Macaskie, 1998; Lovley & Phillips, 1992), and reductive dechlorination of polychlorinated biphenyls (Brown et al., 1987; Wiegel & Wu, 2000). The ability of microorganisms at these sites to switch from natural product degradation to xenobiotic degradation likely develops through one of

three mechanisms. First, a species or individual within a species may already possess an enzyme(s) whose activity on a naturally occurring compound(s) fortuitously extends to the pollutant. This species (or individual) is strongly selected for in the contaminated environment, reproduces, and degrades the xenobiotic compound. Some enzymes, such as cytochrome P450s and methane monooxygenase are known to have broad substrate ranges, and enzymes of these types are frequently implicated in pollutant degradation (Lewis & Wiseman, 2005; Lipscomb, 1994). For example, a cytochrome P450 in soil bacterium *Rhodococcus rhodochrous* strain 11Y has been found to denitrify the explosive hexahydro-1,3,5-trinitro-1,3,5-triazine (RDX) (Seth-Smith et al., 2002). Overlapping enzyme functionality cannot account for most xenobiotic degradation, however, because of several limitations. Many xenobiotic compounds require more than one enzymatic step before they can be incorporated into normal metabolism, so the odds that a cell would already contain all of the necessary enzymes are low. Also, pollution events often involve a mixture of contaminants, and any xenobiotic-degrading species must be resistant to all of them in order to thrive. For these reasons, development of xenobiotic degradation abilities frequently must proceed through one or both of the remaining two mechanisms: mutation and horizontal gene transfer.

Genetic changes to catabolic genes such as insertions, deletions, and point mutations can result in an enzyme with altered substrate specificity and/or activity, allowing the organism to adapt to new growth substrates. For example, haloalkane dehalogenase (DhlA) from *Xanthobacter autotrophicus* was expressed in a *Pseudomonas* host that could already grow on long-chain alcohols. The *Pseudomonas* host could not initially grow on 1-chlorohexane, but eventually acclimated to it as a growth substrate. Subsequent molecular analysis of 6 *dhlA* mutant genes indicated that point mutations, insertions, and deletions had occurred in a domain of the enzyme that facilitated altered enzyme specificity for 1-chlorohexane, though the active site residues remained unchanged (Pries, Wijngaard, Bos, Pentenga, & Janssen, 1994).

Other genetic changes with the potential to convert a microorganism to a xenobiotic-degrading phenotype include gene duplications, DNA rearrangement through the activity of transposons and integrons, and mutations in regulatory genes (Top & Springael, 2003). Gene duplication can contribute to xenobiotic-degradation abilities by enabling a cell to cope with higher-than-natural concentrations of a toxic intermediate, as in *Burkholderia cepacia* AC1100, which uses the chlorinated aromatic compound 2,4,5-trichlorophenoxyacetic acid as a sole source of carbon and energy. The first step in its degradation produces 2,4,5-trichlorophenol, a toxic intermediate that is subsequently dechlorinated. The gene cluster responsible for 2,4,5-trichlorophenol dechlorination was found to be present in two copies, potentially increasing the enzyme expression level and protecting the cell from an accumulation of this compound (Hubner, Danganan, Xun, Chakrabarty, & Hendrickson, 1998).

DNA rearrangements within a cell can lead to newly organized gene clusters under altered regulatory control. Changes in gene regulation (through gene rearrangement or mutations in regulatory genes) are often essential in adaptation to xenobiotic compounds; the microorganism may have the necessary catabolic genes, but must be able to transcribe them at appropriate levels in response to the pollutant. Increased enzyme expression levels can provide a means for acclimation to a new growth substrate, especially if metabolic intermediates are unstable or toxic to the mediating organism. For example, organisms that grow on 2-chloroethanol are well known, but organisms that grow on 2-bromoethanol are not, because of 2-bromoethanol toxicity. It was determined that the bromoacetaldehyde intermediate inactivated a NAD-dependent aldehyde deydrogenase that participated in the 2-chloroethanol pathway (J. R. van der Ploeg, Kingma, De Vries, Van der Ven, & Janssen, 1996). *Pseudomonas* strain GJ1, which was initially capable of growth on 2-chloroethanol but not 2-bromoethanol, adapted to growth on 2-bromoethanol by overexpressing NAD-dependent aldehyde

dehydrogenase to compensate for inactivation by the bromoacetaldehyde intermediate (J. R. van der Ploeg et al., 1996).

The third mechanism through which a microorganism may acquire xenobiotic-degrading capability is horizontal gene transfer (HGT), which includes plasmid conjugation, phage transduction, and transformation. Recognition of the importance of HGT in microbial evolution first began with the discovery of the spread of antibiotic resistance genes (Cohen, 1992). Catabolic genes can be distributed rapidly throughout a microbial community by HGT, increasing the likelihood that a cell will acquire the genes necessary to degrade a given pollutant. This may happen all at once, as in the transfer of a catabolic gene cluster on a plasmid, or incrementally, as acquired and pre-existing genes are "patchworked" together to create a new metabolic pathway (Top & Springael, 2003). Integration of mobile genetic elements into the chromosome can also be involved in the evolution of xenobiotic-degrading pathways (van der Meer & Sentchilo, 2003). For example, highly similar plasmid-encoded haloalkane dehalogenase (*dhaA*) gene clusters were found in several geographically distinct haloalkane-degrading *Rhodococcus* strains (Poelarands et al., 2000). The DhaA gene, which was 100% identical in all strains studied, was used as a probe in Southern blots. DNA sequences recovered from the Southern blots revealed that a 12.5 kb gene cluster containing *dhaA* genes was conserved in the *Rhodococcus* strains. Agarose gel electrophoresis revealed the presence of plasmids in the strains, and additional Southern blotting indicated that *dhaA* genes were encoded on the plasmids as well as on the chromosome. The presence of highly conserved, plasmid-encoded *dhaA* genes suggests that a recent plasmid-mediated lateral gene transfer event provided for recruitment of the encoded catabolic enzymes for haloalkane utilization in the strains (Poelarands et al., 2000).

Linear plasmids as well as circular ones have been implicated in the transfer of important gene clusters. Bacterial linear plasmids can confer phenotypes such as autotrophy, metal resistance, antibiotic synthesis, virulence, and degradation of

xenobiotics (Meinhardt, Scharath, & Larsen, 1997). Linear plasmids have been detected in several Actinomycetes including *Streptomyces* (Meinhardt et al., 1997), *Rhodococcus* (Meinhardt et al., 1997; H. Saeki, Akira, Furuhashi, Averhoff, & Gottschalk, 1999; Stecker, Johann, Herzberg, Averhoff, & Gottschalk, 2003), *Mycobacterium* (Coleman & Spain, 2003; Lorah & Voytek, 2004; Louarn, Aulenta, Levantesi, Majone, & Tandoi, 2006), *Nocardioides* (T. E. Mattes, Coleman, Gossett, & Spain, 2005), and *Planobispora* (Polo, Guerini, Sosio, & Deho, 1998), and in the Gram-negative genera *Xanthobacter* (Krum & Ensign, 2001), *Pseudomonas* (Danko, Luo, Bagwell, Brigmon, & Freedman, 2004), and *Ochrobactrum* (Danko et al., 2004). Linear plasmids are often conjugative, even among different species, indicating a high potential for HGT among diverse bacteria (Meinhardt et al., 1997).

The adaptation mechanisms of overlapping enzyme functionality, mutation, and horizontal gene transfer can work together to expand the possibilities for xenobiotic degradation in the environment. Evidence of these mechanisms has been found to be at work in the evolution of many xenobiotic-degrading bacteria, including chlorinated ethene degraders.

Remediation of Chlorinated Ethenes in Groundwater

The class of compounds known as chlorinated ethenes comprises those molecules with the same structure as ethene, but with one or more chlorines substituted in the hydrogen position(s). These include perchloroethene (PCE), trichloroethene (TCE), three forms of dichloroethene (DCE): 1,1-DCE, *cis*-1,2-DCE, and *trans*-1,2-DCE, and vinyl chloride (VC). (Figure 1.1) PCE and TCE are produced for worldwide use as solvents and degreasers, and are particularly commonly used in dry cleaning and metal fabrication

(USEPA, 2010). VC is produced for polymerization into the plastic polyvinylchloride (PVC) (Y. Saeki & Emura, 2002). Release of these compounds to the environment from leakage or improper disposal often results in groundwater contamination, which puts people at risk of exposure through their drinking water. Chlorinated ethenes have been shown to have serious liver and central nervous system effects, and several are proven carcinogens (USEPA, 2010). For this reason, the federal government has set very low limits for chlorinated ethene pollution in groundwater. (Table 1.1)

Once chlorinated ethenes have entered the groundwater, it can be very difficult to bring their concentrations down to safe levels. With the exception of VC (which occurs only in the dissolved and gaseous phases), they are dense, non-aqueous phase liquids (DNAPLs), and tend to sink below the water table. Here, they serve as a difficult-to-reach long term source of dissolved pollution. In the face of these challenges, several different treatment strategies have been introduced over the years.

Conventional pump-and-treat remediation has been applied to chlorinated ethene pollution, but has many drawbacks. This process involves pumping large volumes of groundwater out of the sediment, followed by on-site treatment with chemical oxidation or adsorption onto activated carbon, then return of the treated water to the ground. While the systems are usually able to contain the pollution within specified boundaries, they are only able to treat the dissolved phase of the contaminants and often must be operated for long periods of time, and at great expense (De Wildeman & Verstraete, 2003).

Permeable reactive barriers have also been used to treat chlorinated ethene pollution by reductive dechlorination to ethene, a more benign compound that occurs naturally in the environment. (Figure 1.2) These barriers consist of trenches filled with an electron donor (such as zero-valent iron) that will reduce the contaminants as the groundwater plume flows through. This strategy has the advantage of lower operational costs than pump-and-treat remediation, but can run into problems when geological site particulars make the construction of a barrier difficult, and may lose long-term efficacy

with the less oxidized of the chlorinated ethenes (DCE and VC) (De Wildeman & Verstraete, 2003; Gavaskar, 1999).

Bioremediation, the removal or detoxification of pollution by living organisms, is currently a popular and much-studied strategy for sites contaminated with chlorinated ethenes. Three main incarnations of bioremediation have been used in various pollution-treatment situations. The first is monitored natural attenuation (MNA), which utilizes the existing microbial or plant life present at a contaminated site. This approach incorporates thorough monitoring to prove disappearance of the pollutant, increase in metabolites, and presence of microbes or enzymes responsible for the degradation. MNA can be cost-effective, but is often slow and may not be feasible at every site, due to variations in microbial communities and pollutants (Grandel & Dahmke, 2004). The second type, enhanced natural attenuation, adopts the principles of MNA, but also attempts to accelerate the process. Biological degradation of pollutants can be limited by the availability of nutrients, carbon sources, or electron donors; these are added to the groundwater in enhanced natural attenuation to speed up the remediation. The effectiveness and applicability of this strategy is still limited by the existing consortium of microbes at the site, however, and a thorough understanding of the effects of the "enhancements" on the microbial community is required. The third form of bioremediation is bioaugmentation, which overcomes the limitations of the first two by the addition of one or more microbial species (or plants) known to possess the required degradation activity. This approach can also incorporate nutrient and electron donor addition, as in enhanced natural attenuation. The advantage provided by bioaugmentation is a more predictable degradation mechanism, no longer limited by the species that happen to be present at the contaminated site. Problems with this method include failure of the introduced species to thrive in the new environment, competition with existing microbial populations, and public resistance to the use of recombinant organisms.

Bioremediation has been applied to chlorinated ethene contamination in a variety of ways. The most common takes advantage of the ability of some microbes to reductively dechlorinate these compounds as permeable reactive barriers do. In microbial reductive dechlorination (which occurs anaerobically), the chlorinated ethene molecule is used as the terminal electron acceptor as oxygen would be in an aerobic environment (Freedman & Gossett, 1989). A separate carbon source (and electron donor) is still required for growth. Microbes capable of dechlorinating PCE and TCE are fairly common, but only members of the genus *Dehalococcoides* have been shown to achieve complete reductive dechlorination to ethene and chloride ion (Christ, Ramsburg, Abriola, Pennell, & Löffler, 2005). Complete biological reductive dechlorination therefore requires several things: presence (or addition) of *Dehalococcoides*, sufficient electron donors (such as hydrogen, lactate, or acetate), and an anaerobic environment. The absence of any one of these essentials will result in incomplete reductive dechlorination; in practice, reductive bioremediation of chlorinated ethene plumes frequently stalls, resulting in accumulation of VC and/or cDCE (the most common form of DCE) (T. D. DiStefano, Gossett, & Zinder, 1991; T. D. Distefano, 1999). (Figure 1.3)

Farther from the contamination source, VC and cDCE can migrate into aerobic areas, where they can often be degraded by existing or added bacteria. This can be done in a cometabolic way, in which microbes fortuitously oxidize the chlorinated ethene, but are unable to convert the product of this oxidation into a useful compound for the cell. Cometabolic VC-oxidizing bacteria have been used successfully for bioremediation, but have several limitations (McCarty et al., 1998). In addition to requiring an additional carbon source for growth, cometabolic degraders can encounter toxicity problems due to accumulation of the mutagenic chlorinated epoxide products of their oxidation (Habets-Crützen & de Bont, 1985). They can also exhibit slower degradation rates due to competition between the chlorinated ethene and carbon-source substrate for enzyme active sites (van Hylckama Vlieg, de Koning, & Janssen, 1996).

An alternative to cometabolic oxidation of chlorinated ethenes is assimilative oxidation, in which microbes utilize the chlorinated ethene as a carbon and energy source. Vinyl chloride-assimilating microbes accomplish this by oxidizing the VC molecule with an alkene monooxygenase (AkMO), then conjugating the toxic chlorinated epoxide metabolite with coenzyme M (CoM) using a CoM transferase, and incorporating it into the metabolism of the cell (T. E. Mattes et al., 2010). In the end, this process yields carbon dioxide and chloride ions as products (Coleman, Mattes, Gossett, & Spain, 2002b; Coleman, Spain, & Duxbury, 2002). Vinyl chloride assimilators are found in a wide variety of genera, including *Pseudomonas, Mycobacterium, Nocardioides, Ralstonia, and Ochrobactrum* (T. E. Mattes et al., 2010), but currently the only isolated cDCE-assimilating microbe is *Polaromonas* sp. strain JS666 (Coleman, Mattes, Gossett, & Spain, 2002a). (Figure 1.4) Since accumulation of cDCE in aerobic subsurface environments is a common problem in the remediation of contaminated sites, strain JS666 is the focus of much attention and research.

Occurrence and Activity of Aerobic Chlorinated Ethene Assimilators in the Environment

While *Polaromonas* sp. strain JS666 is the only confirmed cDCE-assimilating microbe isolated to date, the phylogeny of growth-coupled VC-degrading bacteria has proven to be varied. Isolated VC-assimilating strains have thus far been discovered in genera *Pseudomonas*, *Mycobacterium*, *Nocardioides*, *Ralstonia*, and *Ochrobactrum* (Coleman, Mattes, Gossett, & Spain, 2002b; Danko et al., 2004; Elango, Liggenstoffer, & Fathepure, 2006; Verce, Ulrich, & Freedman, 2001). All reported growth-coupled VC-degraders are also ethene-assimilators, and strains from all five genera listed above have

been found to grow aerobically on both ethene and VC. Aerobic ethene-assimilating bacteria (de Bont, 1976; Habets-Crützen, Brink, van Ginkel, de Bont, & Tramper, 1984) and VC-assimilators (Coleman, Mattes, Gossett, & Spain, 2002b) appear to be fairly widespread in the environment. VC-assimilating strains are found in soil, groundwater, activated sludge, and activated carbon, including some sites with no detectable chlorinated ethene contamination (Coleman, Mattes, Gossett, & Spain, 2002b; Elango et al., 2006; Fathepure, Elango, Singh, & Bruner, 2005).

In spite of their shared metabolic characteristics, the genera containing chlorinated ethene assimilating bacteria are not necessarily closely related to one another. For instance, the *Mycobacterium* genus is a member of the Gram-positive *Actinobacteria* class, while the *Pseudomonas* and *Ralstonia* genera belong to the Gram-negative *Gamma-* and *Beta-Proteobacteria* classes, respectively. This diversity is consistent with the diversity of ecological niches in which aerobic chlorinated ethene oxidation takes place in the environment, and may be a result of plasmid-mediated horizontal gene transfer among disparate species. Competition with other microbes, co-contamination with other pollutants, and physical site characteristics like redox potential, pH, and nutrient availability can all affect which (if any) VC-assimilating species are present at a site. Another important factor affecting VC assimilation at a contaminated site is the presence or absence of ethene in the groundwater. As a substrate, ethene is preferred over vinyl chloride by all VC-assimilators, so available ethene at a site may slow or prevent VC degradation (Coleman, Mattes, Gossett, & Spain, 2002b). Additionally, the presence of ethene may remove the selective pressure necessary for existing ethene-assimilating bacteria to adapt to growth on vinyl chloride (Jin & Mattes, 2008).

Isolation of VC-assimilating microbes from environmental samples is also dependent upon the selection of sampling and enrichment techniques. The choice to sample groundwater instead of soil, for example, may lead to an underestimation of the role of surface-associated microbes in chloroethene oxidation, whereas sampling an

engineered environment like activated sludge may select for species that are not competitive in the groundwater plume. Studies identifying VC-assimilating strains have also varied in their choice of the initial selective substrate; ethane, ethene, and vinyl chloride with and without nutrient agar have all been used (Coleman, Mattes, Gossett, & Spain, 2002b; Danko et al., 2004; Elango et al., 2006; Verce, Ulrich, & Freedman, 2000; Verce et al., 2001). It is very likely that this choice could have an effect on the strains discovered through enrichment. Vinyl chloride assimilating strains with long starvation-induced lag times, such as *Nocardioides* strain JS614, may also be discriminated against in isolation procedures with short cut-off times or with other, more competitive strains (Coleman, Mattes, Gossett, & Spain, 2002b).

Isotopic Fractionation to Confirm and Characterize Chlorinated Ethene Bioremediation

From a practical standpoint, it is desirable to distinguish between aerobic and anaerobic chlorinated ethene degradation in the field as this information could be useful in the design of bioremediation strategies. Since the products of aerobic VC and cDCE oxidation (CO_2 and Cl^-) are essentially ubiquitous in the environment, it is impractical to try to use the accumulation of these compounds as proof of chlorinated ethene oxidation *in situ*. The products of reductive dechlorination (ethane and ethene) are also common, so it is difficult to discriminate between aerobic and anaerobic degradation in the field using their metabolic products (Hunkeler, Aravena, & Cox, 2002). Advances in isotopic fractionation analyses of these processes are revealing the promise of compound specific isotope analysis (CSIA) for characterization of degradation activity at sites contaminated with chlorinated ethenes.

CSIA is based on the observation that enzymatic activity tends to favor substrate molecules composed only of lighter isotopes ahead of those containing one or more heavy atoms (e.g. ^{13}C or ^{37}Cl). This phenomenon is a result of the kinetic isotope effect (KIE), in which a bond involving a heavier isotope is stronger than one between two light isotopes, resulting in a higher activation energy required to break the bond. CSIA can be used as evidence of real pollutant degradation (either biotic or abiotic) because purely physical processes that only affect the concentration of contaminants (e.g. sorption, volatilization, and dilution) exhibit very minimal isotope fractionation (Chartrand et al., 2005; Chu, Mahendra, Song, Conrad, & Alvarez-Cohen, 2004; Tiehm, Schmidt, Pfeifer, Heidinger, & Ertl, 2008). Because the effect of a heavy isotope on the kinetics of a reaction depends on the atoms involved in the rate-limiting step, the magnitude of the observed fractionation may also allow discrimination between aerobic and anaerobic chlorinated ethene degradation; particular reaction mechanisms (e.g. dechlorination or epoxidation) can even be implicated, especially if more information-rich dual isotope analysis is utilized (Abe et al., 2009; Chu et al., 2004).

Substrate isotope ratios are measured by mass spectrometry and reported using the delta notation as $\delta = (R/R_{std} - 1) \times 1000‰$ where R and R_{std} are the isotope ratios of the sample and a reference standard, respectively (Abe et al., 2009). $\delta^{13}C$ values are always reported relative to Vienna PeeDee Belemnite ($\delta^{13}C_{VPDB}$), and $\delta^{37}Cl$ values are reported relative to Standard Mean Ocean Chloride ($\delta^{37}Cl_{SMOC}$) (Abe et al., 2009; Chu et al., 2004). While delta values serve as units of measurement for isotope ratios and can be used to track changes, a value referred to as the fractionation factor (α) is used to quantify isotope fractionation during the initial transformation of a compound (Hunkeler et al., 2002).

$$\alpha = \frac{dP_{heavy}/dP_{light}}{S_{heavy}/S_{light}}$$

where dP_{heavy} and dP_{light} are instantaneous product, and S_{heavy} and S_{light} are the substrate concentrations

If this fractionation factor remains constant over the course of the experiment, the transformation will fit the Rayleigh model, which allows for the calculation of the isotopic enrichment factor ε, defined by the equation $\varepsilon = (\alpha - 1) \times 1000$ (Hunkeler et al., 2002). A negative ε value (corresponding to $\alpha < 1$) indicates enrichment of the remaining substrate in the heavier isotope, which is the observed pattern for much biological activity. Larger negative ε values indicate greater degrees of fractionation. The change in isotope ratios as a function of time can be calculated for transformations that fit the Rayleigh model via the following equation (Hunkeler et al., 2002).

$\delta R_S = \delta R_{S0} + \varepsilon \ln f$ where δR_S is the isotope ratio of the substrate at a remaining fraction f, and δR_{S0} is the initial isotope ratio of the substrate

This equation has been adapted for two-step processes by Hunkeler, et al. (Hunkeler et al., 2002) using the assumption of first-order kinetics for both steps of the transformation. This permits the isotope effects of biodegradation processes to be modeled, as long as ε values and the reaction kinetics are known. This may help when estimating the rate of biodegradation in the field, because the isotope data (unlike concentration data) will be unaffected by physical processes.

The degree of isotopic fractionation observed during a reaction is a result of the kinetic isotope effect (KIE).

$KIE = {}^{L}k / {}^{H}k$ where ${}^{L}k$ and ${}^{H}k$ are the rate constants for reaction of molecules with a light or heavy isotope, respectively

The basis of the difference in reaction rate constants lies in the difference in energy required to go from the ground state to the transition state for molecules with light versus heavy isotopes. When a heavy isotope is involved in a bond that is broken during this transition, the KIE is larger due to the higher energy required to break a bond with the heavy isotope than one with the lighter isotope. Bonds involving heavier isotopes are

slightly stronger than those with their lighter counterparts because of differences in vibrational frequency and their reduced masses ($m_1m_2/[m_1 + m_2]$) (Chartrand et al., 2005). When the heavy isotope is adjacent to the affected bond instead of directly involved, the KIE is much less pronounced and is referred to as "secondary" (Abe et al., 2009).

The effect of a heavy isotope on the kinetics of a reaction depends upon the reaction mechanism, so different degradation pathways for the same compound will potentially exhibit different KIEs, which are related to enrichment factors via the following equation (Chartrand et al., 2005).

$$KIE = {}^{L}k / {}^{H}k = 1 / (1 + \varepsilon/1000)$$

The range of ^{13}C enrichment factors for the reductive dechlorination of VC has been reported from –21.5 to –31.1‰ (Abe et al., 2009; Chartrand et al., 2005; Hunkeler et al., 2002; P. K. H. Lee, Conrad, & Alvarez-Cohen, 2007; Tiehm et al., 2008). ^{13}C enrichment factors for aerobic oxidation of VC tend to be smaller, which reflects a difference in reaction mechanism. Metabolic (assimilative) aerobic VC oxidation has exhibited ^{13}C enrichment factors from –5.7‰ for *Mycobacterium aurum* L1 (Chu et al., 2004) to –7.0 to –8.2‰ for *Mycobacterium* JS60, JS61, JS617, and *Nocardioides* JS614 (Abe et al., 2009; Chartrand et al., 2005). Cometabolic aerobic VC oxidation has yielded ^{13}C enrichment factors from -3.2‰ for *Methylosinus trichosporium* OB3b to -4.8‰ for *Mycobacterium vaccae* JOB5 (Chu et al., 2004). ^{13}C enrichment factors for aerobic VC-oxidizing enrichment cultures have fallen within the range of those observed for metabolic and cometabolic species; values of ε from -4.5‰ to -6.5‰ have been reported (Chu et al., 2004; Tiehm et al., 2008). This is consistent with the expectation that VC-degrading enrichment cultures may contain a mixture of VC-assimilating and non-assimilating strains. The small difference in the degree of isotopic fractionation between cometabolic and metabolic VC oxidation indicates that it would be very difficult to use

CSIA to discriminate between these two processes in the field, especially since they may often be operating simultaneously.

A similar pattern of ^{13}C isotopic fractionation is seen for anaerobic and aerobic cDCE degradation as for VC degradation. Anaerobic enrichment factors are higher, with reported values from -14.1‰ to -29.7‰ for various isolates and enrichment cultures (Hunkeler et al., 2002; P. K. H. Lee et al., 2007; Tiehm et al., 2008). Metabolic aerobic oxidation of cDCE by *Polaromonas* JS666 exhibited an ε of -8.5‰ ± 0.10 in a recent study by Abe, et al. (Abe et al., 2009). Cometabolic cDCE oxidation by *Methylosinus trichosporium* OB3b yielded an ε of only -0.4‰ ± 0.5 in one study (Chu et al., 2004), yet cDCE cometabolism by aerobic enrichment cultures from a contaminated site gave a range of enrichment factors from -7.1‰ to -9.8‰ (Tiehm et al., 2008). Further work to characterize isotopic fractionation during cometabolic oxidation of cDCE would be helpful, but so far it appears that as with VC oxidation, metabolic and cometabolic oxidation of cDCE are difficult to distinguish using CSIA.

Single isotope analysis has several issues that limit its applicability in field settings. Analysis of only one isotope leaves the results vulnerable to the mixed effects of multiple degradation pathways occurring simultaneously. Also, calculation of the enrichment factor ε requires the contaminant concentration to not be significantly affected by non-biological processes such as sorption, volatilization, or dilution, which may be impossible in a contaminated site (Abe et al., 2009). Analysis of the isotope ratios of two elements simultaneously has been found to yield correlations characteristic of particular reaction mechanisms that are independent of changes in contaminant concentrations (Abe et al., 2009; Elsner, Zwank, Hunkeler, & Schwarzenbach, 2005). This technique, known as the dual isotope approach, makes use of the fact that two reaction mechanisms that involve cleavage of two different bonds during the initial step will show differing magnitudes of the kinetic isotope effect for certain elements. For example, a reaction in which a C-Cl bond is broken will likely show a greater preference

for molecules with no "heavy" Cl (^{37}Cl) than will a reaction which first breaks a C=C bond with an adjacent Cl. This phenomenon was exploited by Abe, et al. to study the differences between anaerobic dechlorination and aerobic oxidation of VC and cDCE (Abe et al., 2009). They plotted δ^{37}Cl versus δ^{13}C and found a significant difference in slope at the 95% confidence level for metabolic aerobic oxidation and reductive dechlorination for both VC and cDCE. This illustrates that dual isotope CSIA may be capable of distinguishing between these processes in the field. A second observation of this study was that both chlorine and carbon isotope enrichment factors are very similar for VC and cDCE metabolic oxidation. Chlorine isotopic fractionation was very small for both compounds (-0.3‰ ± 0.04 for VC; -0.3‰ ± 0.07 for cDCE), lending strength to the hypothesis that metabolic aerobic degradation of these two compounds may proceed by the same mechanism (Abe et al., 2009). Low fractionation of chlorine isotopes is an expected observation for a reaction in which the rate-determining step does not involve a C-Cl bond, which is the case with the epoxidation of the C=C bond in VC oxidation.

Ecology and Evolution of cDCE-Assimilating Bacteria

Ecological Context of cDCE Degradation

Prior to isolation of *Polaromonas* sp. strain JS666, microbial mineralization of cDCE as a sole carbon source had only been reported in enrichment cultures from organic-rich, streambed sediments. In that study, supernatant from a microcosm showing high cDCE-degrading activity was inoculated into minimal media and retained activity through a 10^{-7} dilution (Bradley & Chapelle, 2000). Despite evidence of cDCE mineralization as the sole carbon substrate, no evidence of growth (i.e. no change in absorbance values at 460 and 600 nm) was observed (Coleman, Mattes, Gossett, & Spain,

2002a). The authors speculated that the low concentrations of cDCE used might have limited growth.

A subsequent search for cDCE-assimilating bacteria in environmental samples yielded only two active cDCE-degrading enrichment cultures out of 18 initial samples from diverse media such as soil, groundwater, sediments, sewage sludge, and activated carbon, suggesting that aerobic cDCE-assimilating bacteria are rare in nature and calling into question the environmental relevance of cDCE-assimilating bacteria. *Polaromonas* sp. strain JS666 was isolated from a sample of granular activated carbon originally used to process groundwater contaminated with PCE, TCE, and cDCE (Coleman, Mattes, Gossett, & Spain, 2002a). Strain JS666 is a member of the family *Comamonadaceae* in the β-proteobacteria class. It is yellow, non-motile, devoid of vacuoles, prefers growth at 20°C, and does not grow at 30°C, classifying the strain as psychrotrophic (Coleman, Mattes, Gossett, & Spain, 2002a). Based on analysis of 16S rRNA sequences, the cultured organism most closely related to strain JS666 is the psychrotrophic arsenite-oxidizing isolate *Polaromonas* sp. GM1, with a 99% sequence identity (Osborne et al., 2010; Zhang, Schwartz, Wagner, & Miller, 2000).

A recent study found *Polaromonas* to be the most commonly occurring genus in granular activated carbon filters treating surface and ground water (Magic-Knezev, Wullings, & Van der Kooij, 2009). This is consistent with the common observation of *Polaromonas* species in extremely oligotrophic environments, such as Crater Lake (Page, Connon, & Giovannoni, 2004), tap water (Kampfer, Busse, & Falsen, 2006), and bottled mineral water (Loy, Beisker, & Meier, 2005). In addition, *Polaromonas* species tend to be slow-growing and psychrotrophic, which hinders their isolation from environmental samples by customary methods (Irgens, Gosink, & Staley, 1996). However, several species from this genus have already proven to be xenobiotic degraders, so it appears to be a worthy focus of future study, in spite of culturing challenges (Alfreider, Vogt, & Babel, 2002; Connon et al., 2005; Jeon et al., 2003).

cDCE Degradation in *Polaromonas* sp. strain JS666

The growth yield of strain JS666 on cDCE is 6.1 ± 0.4 g protein/mole cDCE, which is comparable to VC-assimilating bacteria, despite the lower energy content of cDCE (Coleman, Mattes, Gossett, & Spain, 2002a). A maximum specific substrate utilization rate (k) of 12.6 ± 0.3 nmol/min/mg protein and a half-velocity constant for cDCE transformation (K_s) of 1.6 ± 0.2 µM were determined (Coleman, Mattes, Gossett, & Spain, 2002a). In addition, cDCE was degraded routinely to below 0.03 µg/L, which is below current drinking water standards (see Table 1-1) (Coleman, Mattes, Gossett, & Spain, 2002a). These data suggest that two important features of strain JS666 warrant its further investigation in the context of bioaugmentation or natural attenuation potential: first, it can extract enough energy from cDCE for reasonable growth, and second, it can degrade cDCE to a concentration below the MCL without significant effects on substrate utilization rate (Coleman, Mattes, Gossett, & Spain, 2002a; Verce et al., 2001). A recent study found that strain JS666 degraded cDCE in microcosms constructed with contaminated sediment and groundwater, even when presented with alternative carbon sources or competitive/predatory microbes (C. G. S. Giddings, Liu, & Gossett, 2010). This activity was also reliably correlated with the abundance of a DNA probe for the JS666 chromosomal gene encoding isocitrate lyase, an enzyme that is not suspected of involvement in cDCE degradation (C. G. Giddings, Jennings, & Gossett, 2010).

The metabolic pathway of cDCE oxidation and the relationship of strain JS666 to other chlorinated alkene degraders are, at this point, unknown, although a very recently published dissertation reports that the first step of cDCE degradation in JS666 uses a P450 monooxygenase (Shin, 2010). The background work and hypotheses for the research discussed in this manuscript were developed before the publication of Shin's

dissertation, so the pre-existing state of knowledge in the field is discussed here, and the implications of this new advance are explored in later sections.

Due to the structural similarities between cDCE, VC, and ethene, JS666 was expected to also grow on VC and ethene. Evidence that ethene-degrading *Pseudomonas* strains developed the ability to use VC as a source of carbon and energy after exposure to VC strengthened this expectation (Coleman, Mattes, Gossett, & Spain, 2002a). Surprisingly, strain JS666 is capable of transforming VC and ethene only in a cometabolic way, suggesting that JS666 may employ enzymes other than those employed by VC- and ethene-degraders or that growth of JS666 on VC or ethene is not possible because of regulatory limitations.

Pathway prediction using the University of Minnesota Biocatalysis and Biodegradation Database (Ellis, Roe, & Wackett, 2006) deemed plausible through genome inspection for the requisite initial and downstream genes indicated that the initial attack on cDCE could be made by one of three types of enzyme: a monooxygenase, a hydratase, or a hydrolytic dehalogenase. Epoxidation of cDCE by a monooxygenase is a reasonable hypothesis supported by the observation that strain JS666 produces epoxyethane from ethene at an increased rate after growth on cDCE (Coleman, Mattes, Gossett, & Spain, 2002a). There is no homolog of the typical downstream enzyme epoxyalkane coenzyme M transferase in the JS666 genome, but the toxic epoxide created by this reaction could be degraded by an epoxide hydrolase or a glutathione S-transferase, or proceed through abiotic decomposition to dichloroacetaldehyde (Jennings et al., 2009). This would be further metabolized via an aldehyde dehydrogenase or haloacid dehalogenase, followed by abiotic rearrangement to glyoxalate. Alternatively, attack on cDCE by a hydratase would produce 1,2-dichloroethanol, which could be converted to chloroacetyl chloride by an alcohol dehydrogenase and then abiotically decomposed to chloroacetate. A haloacid dehalogenase could then convert chloroacetate to glycolate, which enters the glyoxalate pathway. Attack on cDCE by a hydrolytic dehalogenase

would generate (*Z*)-2-chloroethylenol, which would interconvert with chloroacetaldehyde due to keto/enol tautomerism. Degradation of chloroacetaldehyde to glycolate could occur by at least two different combinations of dehalogenase and dehydrogenase steps.

Evolution of cDCE Assimilation in Strain JS666

Elucidation of the metabolic pathway responsible for cDCE assimilation in strain JS666 will provide important insights into the evolutionary history of this particular ability, but analysis of the strain's sequenced genome has already yielded clues as to how this evolution may have occurred. The genome of strain JS666 contains a wealth of mobile genetic elements and potential evidence of horizontal gene transfer, including two plasmids (360 and 338 kb), fifty-five transposases, one phage, eight genomic islands, six retrons, and two inteins (T. E. Mattes et al., 2008). The two self-transmissible plasmids encode putative pathways for the metabolism of many types of anthropogenic pollutants, including alkanes, cycloalkanes, cyclic alcohols, haloalkanoates, and amino-aromatic compounds (T. E. Mattes et al., 2008). Replication genes on the 338 kb plasmid exhibit similarity to those of *Burkholderia* small chromosomes, indicating likely gene transfer between strain JS666 and members of *Burkholderia*, an important genus in bioremediation and in human and plant pathogenicity (Chain et al., 2006; T. E. Mattes et al., 2008).

A putative haloalkane biodegradation gene cluster is present in nearly identical copies on the chromosome and the 360 kb plasmid within a 9.9 kb duplicated region. This duplication may have been mediated by two nearby transposases, and the increase in gene dosage could have played a role in the adaptation of strain JS666 to growth on chlorinated alkenes or aromatics (Janssen, Pries, & Van der Ploeg, 1994; T. E. Mattes et al., 2008). Many other catabolic genes are found closely associated with transposable elements throughout the JS666 genome, indicating recent acquisition and/or

rearrangement of genes necessary for the degradation of various xenobiotic compounds, including alkanes, cycloalkanes, and cyclic alcohols (T. E. Mattes et al., 2008).

While the specifics remain to be determined, it appears likely that the acquisition of the two plasmids by strain JS666 was a major step in the evolution of its cDCE-assimilating capability. This hypothesis is supported by the observation that these two plasmids have been maintained by the strain throughout enrichment, isolation, and many generations of growth in the laboratory, suggesting that they are necessary for growth on cDCE (Coleman, Mattes, Gossett, & Spain, 2002a; T. E. Mattes et al., 2008). The cDCE-degrading phenotype has also been found to be unstable (Alexander & Mattes, Unpublished data), which would be consistent with plasmid or transposon-carried genes, but may also be due to imperfect regulatory control of the newly constructed pathway. More clues to the evolutionary background of cDCE assimilation in strain JS666 will be illuminated by the identification of the genes responsible for this unique ability, and the associations with plasmids and transposable elements discovered by genome analysis will be invaluable in deciphering the pathway's evolutionary past.

Applications of Xenobiotic-Degrading Bacteria in Biocatalysis

In addition to deepening our understanding of bioremediation processes, the study of xenobiotic degrading bacteria has had beneficial applications in industrial biocatalysis. Biocatalysis, which is the use of enzymes or whole microorganisms to catalyze valuable reactions, has grown significantly in the last few decades as better molecular biology tools have been developed and more genomic information has become available (Thomas, DiCosimo, & Nagarajan, 2002). Chemical industries have shown interest in

incorporating biocatalysis into their operations for three main reasons. First, enzymes can be capable of catalyzing reactions to produce compounds that have no feasible organic synthesis pathway. This point is especially significant for the pharmaceutical industry, as it is in the business of creating compounds of high complexity and often of a single enantiomer. The second advantage of biocatalysis is that it sometimes is able to improve the economics of a chemical synthesis. This is becoming increasingly important as energy and petrochemical costs rise globally. The final benefit of biocatalysis is its vast improvement in sustainability over many organic syntheses. The use of biological catalysts often reduces the need for extremes in pH, temperature, and pressure, the volume and toxicity of byproducts, and the use of rare metal catalysts.

Xenobiotic degrading organisms are a rich source of potential biocatalysts because they possess enzymes with activity on unique compounds. These xenobiotic degrading enzymes often have wide substrate ranges, as they have evolved to be able to handle new and varied molecular structures (Gillam, 2005). For instance, dehalogenases that were originally studied for their use in bioremediation of halogenated pollutants have found applications in the chemical industry for manufacture of chiral intermediates (Swanson, 1999).

Traditionally, researchers screened large collections of microbes for their desired chemical conversion by enrichment cultures, then isolated individual strains and attempted to optimize the reaction from there (Thompson, Van Der Gast, Ciric, & Singer, 2005). Today, the increasing availability of genome sequences and the ease of genome database searches lend themselves well to a genome-oriented approach to biocatalyst discovery, both for chemical synthesis and pollutant degradation (Steele & Streit, 2005). Once a class of enzymes is known to catalyze the reaction of a particular type of compound, sequenced organisms containing this enzyme can be identified through online searching and subsequently tested for their activity on the compound under environmental or reactor conditions. The steric limitations and enantioselectivity of an

enzyme can vary from organism to organism, meaning that laboratory testing is still required, but the initial genome search narrows the candidates to a manageable "toolbox" of strains. In addition, the DNA of entire environmental consortia of unsequenced microbial life can be probed for genes of the correct type, providing assistance in the creation of useful gene libraries and the isolation of new microorganisms (Steele & Streit, 2005). This method adds specificity and direction to the traditional enrichment culture approach, while not replacing its use for novel pathway discovery.

The sequenced genome of *Polaromonas* sp. strain JS666 has facilitated the identification of many genes whose enzyme products have potential for use in biocatalysis. Many of these reside on its two plasmids (Figure 1.5), including pathways for the oxidation of *n*-alkanes and cyclic alcohols. These reactions are useful industrially for (among other things) the production of anti-cancer drugs and lactones, respectively (Thomas et al., 2002; van Beilen et al., 2005). Study into the substrate range of these enzymes will help to define their potential industrial uses and opportunities for improvement.

Research Overview and Hypotheses

The main objective of this work was to explore the unique enzyme functionality and associated bioremediation and biocatalysis potential of *Polaromonas* sp. strain JS666. This exploration drew from the fields of environmental microbiology, molecular biology, genetics, and biochemistry to discover and understand the novel activities exhibited by this distinctive organism. Specifically, three main hypotheses were proposed and tested.

Hypothesis #1

The genome of *Polaromonas* sp. strain JS666 can be used to predict its substrate range, efficiently adding to the collection of interesting enzymes that can be examined for use in bioremediation and biocatalysis.

This hypothesis was addressed through growth experiments of strain JS666 on a wide variety of substrates selected using genome annotation. Experimental design and results are discussed in Chapter II.

Hypothesis #2

Alkene oxidation activity observed in cDCE-grown JS666 cells is catalyzed by the cyclohexanone monooxygenase on plasmid pPol338 (Bpro_5565; GenBank accession number ABE47414.1).

This hypothesis was evaluated using a variety of molecular biology techniques, including gene expression studies, proteomics, kinetic assays, and heterologous expression of the cyclohexanone monooxygenase gene. The basis for the hypothesis, specific experimental approaches, and results are discussed in Chapters III and IV.

Hypothesis #3

The plasmid-encoded cyclohexanone monooxygenase in *Polaromonas* sp. strain JS666 has enantioselective activity on industrially relevant compounds.

Heterologous expression of the cyclohexanone monooxygenase and analytical detection of chiral molecules were used to test this hypothesis. Background on enantioselective catalysis by cyclohexanone monooxygenases, experimental design, and results are discussed in Chapter V.

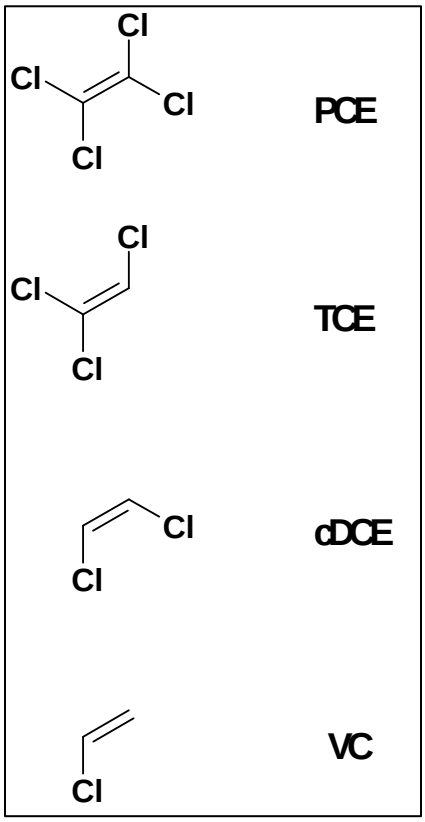

Figure 1.1. Chlorinated ethenes perchloroethene (PCE), trichloroethene (TCE), *cis*-1,2-dichloroethene (cDCE), and vinyl chloride (VC); 1,1-dichloroethene and *trans*-1,2-dichloroethene are less commonly observed in the environment.

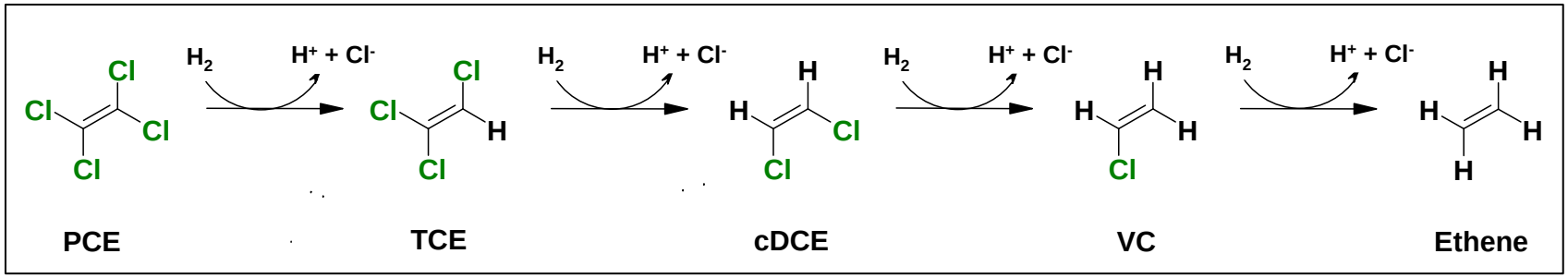

Figure 1.2. Reductive dechlorination of PCE.

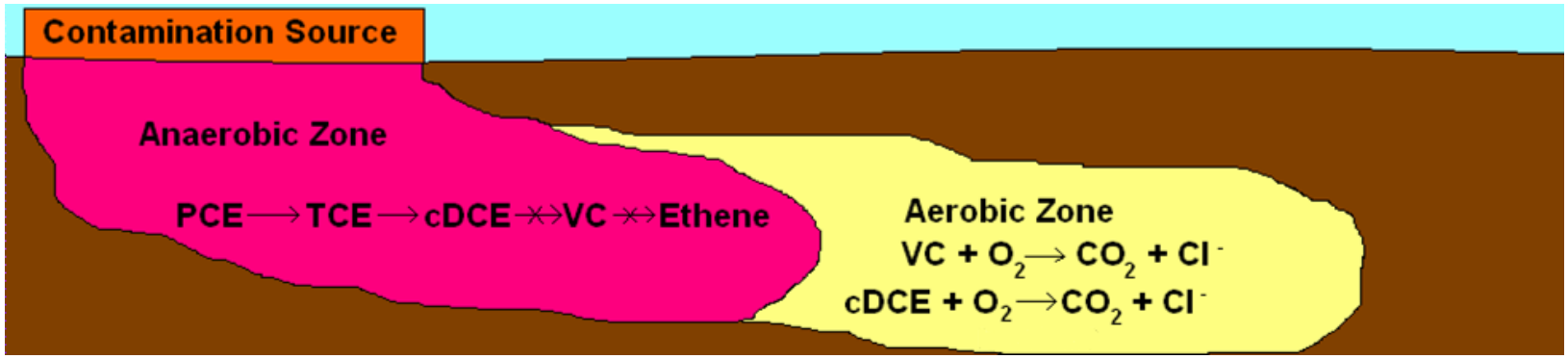

Figure 1.3. Illustration of the treatment of a chlorinated ethene groundwater plume using coupled anaerobic and aerobic biological treatment. Anaerobic reductive dechlorination often does not proceed all the way to ethene, resulting in accumulation of cDCE. Subsequent aerobic conditions can promote the oxidative mineralization of cDCE and VC.

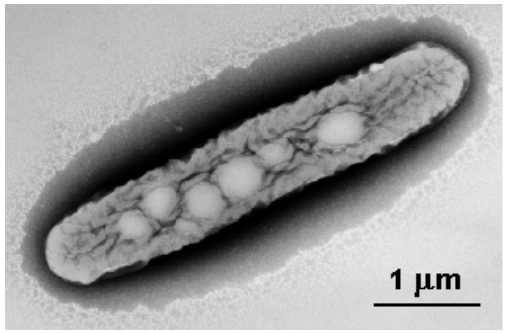

Figure 1.4. Transmission electron micrograph of *Polaromonas* sp. strain JS666.

Figure 1.5. (Following page) The two plasmids of *Polaromonas* sp. strain JS666: 360-kb plasmid pPol360, and 338-kb plasmid pPol338..

Approximate locations of important metabolic gene clusters, plasmid replication, and conjugation genes are indicated outside of the first circle, which depicts coding regions on the plus strand colored by functional category:
plasmid transfer (orange);
plasmid replication and maintenance (yellow);
transport (light green);
DNA replication, recombination, and repair (red);
metabolism (cyan);
biosynthesis (dark blue);
regulators (purple);
cell envelope and membrane biogenesis (pink);
general function prediction (brown);
conserved hypothetical (dark gray);
no COG (light gray).
Moving toward the center, the second circle depicts coding regions on the minus strand (with the same color scheme as the plus strand).
The third circle shows G+C content (deviation from average).
The fourth circle shows G+C skew in purple and olive.

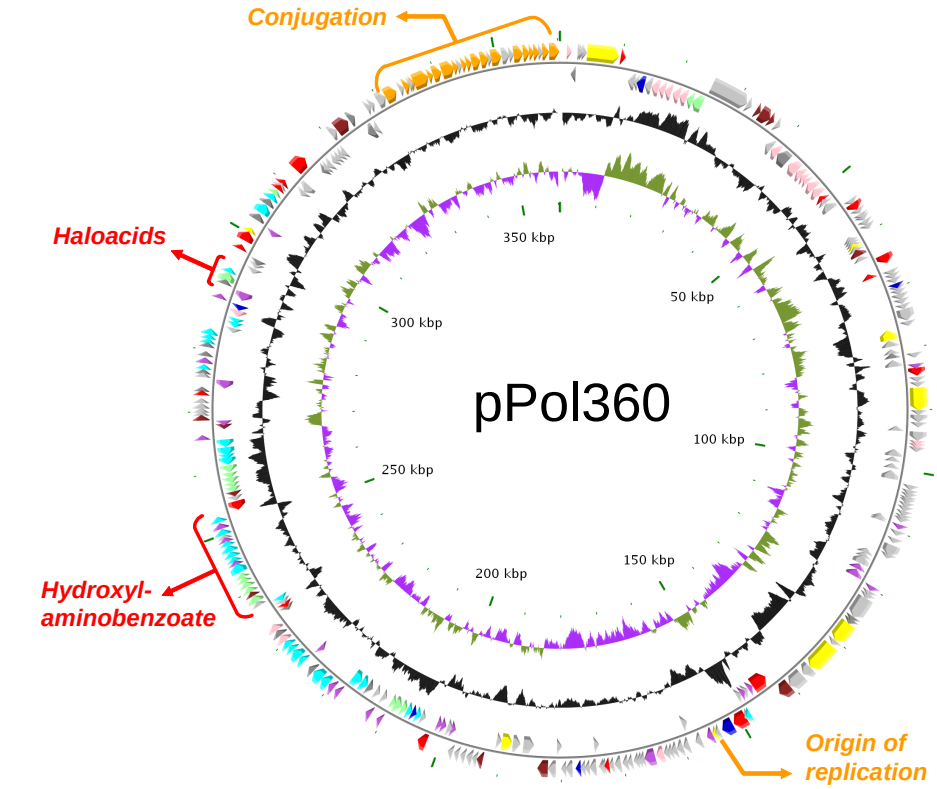
Conjugation
Haloacids
Hydroxyl-
aminobenzoate
Origin of
replication
pPol360
350 kbp
50 kbp
300 kbp
100 kbp
250 kbp
150 kbp
200 kbp

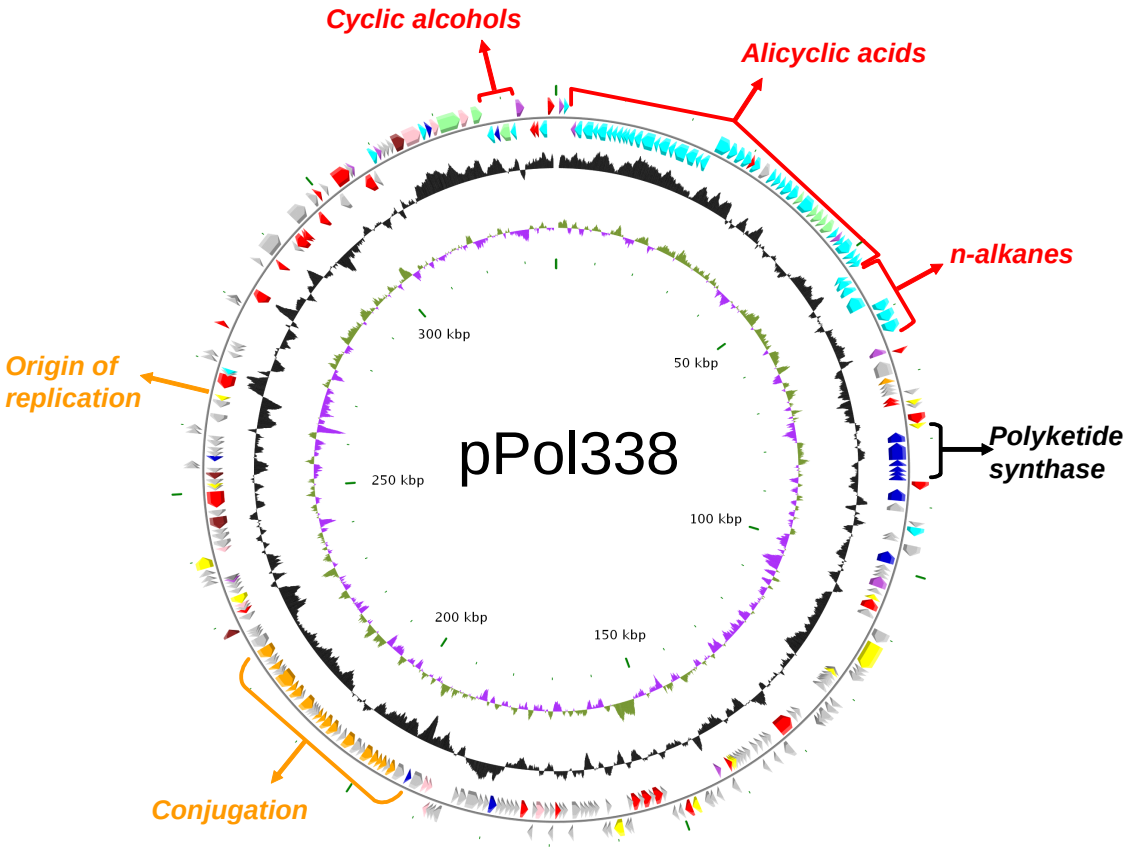
Cyclic alcohols
Alicyclic acids
n-alkanes
Origin of
replication
Polyketide
synthase
Conjugation
pPol338
300 kbp
50 kbp
250 kbp
100 kbp
200 kbp
150 kbp

Table 1.1. Maximum Contaminant Level Goals (MCLGs) and Maximum Contaminant Levels (MCLs) for chlorinated ethenes in water, in parts per billion (ppb) (USEPA, 2010).

	MCLG (ppb)	**MCL (ppb)**
VC	0	2
1,1-DCE	7	7
***cis*-1,2-DCE**	70	70
***trans*-1,2-DCE**	100	100
TCE	0	5
PCE	0	5

CHAPTER II

GENOME-ASSISTED PREDICTION OF XENOBIOTIC SUBSTRATES

Background

Microbial degraders of xenobiotic substrates have traditionally been discovered through enrichment cultures or fortuitous testing of laboratory-cultured strains (Widada, Nojiri, & Omori, 2002). The enrichment culture approach limits the discovery of potential xenobiotic degraders to those present at a sampling location and responsive to enrichment conditions, while the second tactic relies on luck and an appropriate match between a cultured strain and the research focus of the laboratory containing it. An alternative technique makes use of increasingly available genome sequence information to discover probable xenobiotic degraders through rational searches, and has the potential to aid in the discovery of novel biocatalysts, as well. Genome-assisted prediction of substrates relies on our knowledge of enzymes involved in various degradation pathways, and utilizes a search of annotated genomes for the associated genes. In this work, we used the recently sequenced genome of *Polaromonas* sp. strain JS666 to evaluate the efficacy of genome-assisted substrate prediction (T. E. Mattes et al., 2008).

A wide variety of possible substrates for strain JS666 was predicted by Dr. Timothy Mattes and Dr. Nicholas Coleman through curation and examination of the annotated genome sequence, particularly of the two plasmids. Operons containing genes necessary for the degradation of compounds and their incorporation into the central metabolism of the cell were identified by comparison with other known gene clusters and

---

Portions of this chapter were published in: Mattes, T.E.; Alexander, A.K.; Richardson, P.M.; Munk, C.M.; Han, C.S.; Stothard, P.; and Coleman, N.V. 2008. "The Genome of *Polaromonas* sp. Strain JS666: Insights into the Evolution of a Hydrocarbon- and Xenobiotic-Degrading Bacterium, and Features of Relevance to Biotechnology." Applied and Environmental Microbiology. 74:6405-6416.

with online tools, such as the University of Minnesota's Biocatalysis/Biodegradation Database Pathway Prediction System (Ellis et al., 2006). Many of the putative pathways identified through this work are noted on the plasmid diagrams in Figure 1.5, and some of the more significant gene clusters are discussed in the following paragraphs.

Haloalkanes and Haloacids

Haloalkanes and haloacids are chemical groups that include many important groundwater polluants, such as chlorinated alkanes and aromatics. Putative biodegradative pathways for haloalkanes and haloacids in strain JS666 were identified through comparison with known genes in the 1,2-dichloroethane-degrading *Xanthobacter autotrophicus* strain GJ10 (T. E. Mattes et al., 2008; J. van der Ploeg, Willemsen, van Hall, & Janssen, 1995). The genes predicted to be involved in the metabolism of haloalkanes and haloacids include homologs of haloalkane dehalogenase DhlA, haloalkanoate dehalogenase DhlB, the regulator DhlR, and the uptake protein DhlC (T. E. Mattes et al., 2008). This gene cluster is present in nearly identical copies on strain JS666's chromosome and 360 kb plasmid, close to transposases that could have mediated its transfer. This indicates that gene duplication may have played a role in adaptation of this strain to growth on these xenobiotic compounds, as discussed in Chapter 1. Substrates tested in the laboratory to confirm the activity of these genes included 1,2-dichloroethane (1,2-DCA), chloroacetate, and the herbicide Dalapon (2,2-dichloropropionic acid).

n-Alkanes, Alicyclic Acids, and Cyclic Alcohols

Proposed metabolic pathways for *n*-alkanes, alicyclic acids, and cyclic alcohols are located on strain JS666's 338 kb plasmid. (Figure 1.5) This region is associated with several transposase genes, which is consistent with acquisition by horizontal gene

transfer. Metabolism of *n*-alkanes was predicted to begin with the product of a cytochrome P450 gene similar to that in a *Mycobacterium* strain that attacks C5 to C10 alkanes (T. E. Mattes et al., 2008). Strain JS666's P450 gene product has also been the focus of study into its cDCE degradation capability, and will be discussed in later chapters. Downstream gene products in the *n*-alkane pathway include an aldehyde dehydrogenase (AlkH), an alcohol dehydrogenase (AlkJ), and an acyl-CoA synthetase (AlkK) that are similar to those found in *Pseudomonas putida* GPo1 (T. E. Mattes et al., 2008). Substrates chosen to test this predicted pathway in the laboratory included ethane, propane, hexane, heptane, and octane.

Alicyclic acids, which occur in the environment as metabolites of petroleum hydrocarbons, were predicted to be metabolized in *Polaromonas* sp. strain JS666 by a gene cluster very similar to one found in *Rhodopseudomonas palustris* strain CGA009 whose products degrade cyclohexanecarboxylate (T. E. Mattes et al., 2008). The alignment and comparison of the alicyclic acid gene clusters in these two species is illustrated in Figure 2.1. Cyclohexanecarboxylate and cyclohexaneacetate were tested as substrates for strain JS666 in the laboratory to evaluate the activity of this gene pathway.

A complete cyclic alcohol degradation pathway predicted to convert cyclohexanol to adipic acid was discovered in the same region on the 338 kb plasmid as the pathways for *n*-alkanes and alicyclic acids. (Figure 2.6) This gene cluster was identified based on its similarity to the cyclohexanol-degrading pathway in *Acinetobacter* sp. strain SE19 (Cheng, Thomas, Kostichka, Valentine, & Nagarajan, 2000; T. E. Mattes et al., 2008). This pathway is of interest to biocatalysis because the end product, adipic acid, is produced in enormous quantities worldwide for use as the monomer in 6,6-nylon, and its chemical manufacture releases nitrous oxide, a greenhouse gas (USEPA, 2006). The gene labeled ChnB (Figure 2.6) encodes a cyclohexanone monooxygenase, which is discussed in great detail in later chapters. The activity of this cyclic alcohol degradation

pathway was tested experimentally by presenting cyclohexanol as a growth substrate for JS666 cultures.

Ferulate

Ferulate (or ferulic acid) is a ubiquitous phenolic compound in plant cell walls, and is of interest to biocatalysis because it is a common agricultural byproduct with the potential to be converted to a variety of valuable aromatic chemicals, including the flavoring vanillin (Balasundram, Sundram, & Samman, 2006; Gasson et al., 1998; Rosazza, Huang, Dostal, Volm, & Rousseau, 1995). *Polaromonas* sp. strain JS666 contains a ferulate catabolic gene cluster similar to those described for *Pseudomonas* sp. strains HR199 and KT2440 (T. E. Mattes et al., 2008). In the case of strain JS666, ferulate was predicted to proceed through a vanillyl-CoA intermediate instead of vanillin, because no vanillate dehydrogenase gene was discovered in the genome. JS666 growth on ferulate was tested in the laboratory.

Salicylate

The pathway predicted to code for salicylate degradation enzymes is located on the chromosome in *Polaromonas* sp. strain JS666, and its similarity to the analogous pathway in *Ralstonia* sp. strain U2 is illustrated in Figure 2.2 (T. E. Mattes et al., 2008). Both pathways contain genes for large and small salicylate 5-hydroxylase subunits. The *Ralstonia* salicylate gene cluster also includes a naphthalene dioxygenase, but this is missing in strain JS666's genome (T. E. Mattes et al., 2008). The function of the salicylate pathway in JS666 was tested experimentally with salicylate, gentisate, 3-hydroxybenzoate, and naphthalene as substrates.

Alternative Electron Donors and Acceptors

Polaromonas sp. strain JS666 was predicted to use nitrate as an alternative electron acceptor in the absence of oxygen because it contains a gene cluster similar to the *E. coli* K-12 *nar* operon (*narGHJI*) (T. E. Mattes et al., 2008). This hypothesis was tested in anaerobic cultures with nitrate and ethanol as a carbon source. The identification of potential sulfur oxidation genes, similar to those of the sulfur-oxidizing species *Paracoccus pantotrophus*, led to the prediction that strain JS666 may be able to grow chemolithotrophically (or mixotrophically) by using thiosulfate, sulfite, hydrogen sulfide, and/or elemental sulfur as electron donors (T. E. Mattes et al., 2008). In chemolithotrophic growth, energy for ATP production would be obtained by oxidizing one of the chemicals listed above, and carbon for cell growth would be collected through carbon fixation. This was tested in the laboratory with thiosulfate and bicarbonate as the carbon source. Mixotrophic growth would proceed in the same way, but with some carbon obtained from organic sources (ethanol in the laboratory cultures). The ability to use alternative electron donors or acceptors would increase the ecological niches available to strain JS666, and therefore also increase its potential applicability in bioaugmentative treatment of contaminated sites.

Other predicted substrates not discussed here are listed in Table 2.1, which shows the results of the growth experiments. Thorough descriptions of the JS666 gene clusters used to make these substrate predictions can be found in Mattes, et al. (2008).

Materials and Methods

Chemicals and Media

Ferulic acid (*trans*-4-hydroxy-3-methoxy-cinnamic acid, 99%), ethylcyclohexane (99%), cyclohexanecarboxylic acid (98%), cyclohexaneacetic acid (99%), heptane (99%), hexane (99%), propane (98%), chloroacetaldehyde (~50 wt.% in H_20), chloroacetic acid (99%), 1,2-dichloroethane (99.8%), and *cis*-1,2-dichloroethene (97%) were obtained from Sigma-Aldrich. Cyclohexane (99.5%), cyclohexanol (99%), and octane (99%) were obtained from Fluka, Dalapon (2,2-dichloropropionate, 97%) was obtained from Chem Service, and sodium succinate (99%) was obtained from Alfa Aesar. All other chemicals were reagent grade. Minimal salts medium (MSM) used for growth experiments was as described by Coleman (Coleman, Mattes, Gossett, & Spain, 2002a), and the pH was adjusted to 7.0.

Growth Experiments

Polaromonas sp. strain JS666 cultures were grown with *cis*-1,2-dichloroethene (cDCE) as the sole carbon source to ensure maintenance of the plasmids in the cell. Neat cDCE was added to cultures in MSM to a final aqueous concentration of 0.46 mM (based on a dimensionless Henry's constant of 0.1232 (Coleman, Mattes, Gossett, & Spain, 2002a)), and quantified using a gas chromatography-based standard curve (see Analytical Methods, this chapter). The cDCE was replenished to 0.46 mM when its concentration neared or reached zero. Culture pH was monitored and maintained near 7.0 by adjustment with NaOH, and cultures were grown at room temperature (23°C) with 200 rpm shaking. Once a cDCE-grown culture had doubled in cell density (measured by optical density at 600 nm [OD_{600}], see Analytical Methods), it was transferred to 20 mM succinate for one fed-batch culture to achieve vigorous growth and a high count of

healthy cells. Succinate-grown JS666 cultures were harvested during exponential growth (between one and two doublings of cell density) and stored in dense ($OD_{600} \approx 10$) 1 mL stocks at -80°C for long-term storage. Culture stocks were frozen in a 20% glycerol suspension to preserve the integrity of the outer cell membrane; each thawed stock was washed with ≥45 mL MSM to remove the glycerol prior to inoculation. One culture stock was diluted for each experimental culture to an initial OD_{600} of approximately 0.05. Each culture consisted of 40 mL of MSM plus the inoculum and chosen growth substrate in a 160 mL serum bottle sealed with a Teflon-coated rubber septum and crimp cap. Growth experiments with *n*-alkanes demonstrated the necessity of Teflon-coated septa to avoid loss of nonpolar substrates into the rubber; initial experiments with uncoated septa showed a large decrease in all *n*-alkanes with no accompanying cell growth. Identical experiments with coated septa showed no such decrease. No carbon sources were included other than the stated substrate for each experiment. Cultures were incubated upright at 23°C with shaking at 190-300 rpm. Duplicate growth experiments were conducted for each substrate at concentrations ranging from 8 μmoles/bottle to 400 μmoles/bottle (0.2 to 10.0 mM if completely aqueous), including a control with no carbon source for each test, and uninoculated controls for compounds yielding colored breakdown products (catechol, protocatechuate, ferulate, and gentisate).

Chemolithotrophic thiosulfate oxidation cultures were also prepared as described above with the following exceptions: sodium thiosulfate (0 to 40 mM) was added as the energy source, and sodium bicarbonate (10 mM) was added as a carbon source. Duplicate sets of growth experiments were conducted for both lithotrophic and mixotrophic growth; in the latter case, ethanol (5 mM) was provided as a limited source of organic carbon.

Anaerobic nitrate reduction cultures were prepared as described above, except 160 mL of MSM was used, leaving no headspace in the serum bottles, and the medium was purged with nitrogen gas to create anaerobic conditions. Ethanol (5 mM) was provided as

a carbon source, and samples were removed while the bottles were being purged with nitrogen gas in order to maintain anaerobic conditions.

Auxanography plates were prepared with 1.5% Noble agar in MSM (made with high-performance liquid chromatography grade water) to minimize the contribution of any other carbon source to colony growth. Auxanography refers to a plate culture (an auxanogram) used to investigate the effects of varying conditions on cell growth. In this case, our varying condition was the substrate provided to the cultures. Exponentially growing succinate cultures were diluted in MSM to an OD_{600} of 0.1, and 100 µL was spread on each plate. Solid-phase test compounds (5 mg) were deposited on the edges of the plates to allow a concentration gradient to form in the agar, and the starting locations of the compounds were marked. Substrate concentration gradients allowed the cells the opportunity to grow at any substrate concentration, depending on the distance from the solid-phase compounds. It also eliminated practical concerns about detecting growth in liquid cultures with extremely low substrate concentrations. The plates were sealed with Parafilm, inverted, and incubated at 20 to 22°C for 2 to 8 weeks. All compounds were tested with duplicate plates in two independent experiments, as were the no-carbon and no-inoculum controls.

Analytical Methods

Growth was estimated in liquid cultures by measuring the absorbance at 600 nm (optical density, OD_{600}). Changes in OD_{600} of less than 0.02 were considered to be insignificant, and in order to confirm growth, an increase in OD_{600} had to be maintained over consecutive days. Following auxanography, cells were scraped from the plates and then resuspended in MSM and washed, and total protein was analyzed by a UV protein assay, described in more detail in Chapter III (Kalb, 1977). Propane, hexane, heptane, octane, 1,2-dichloroethane, and cDCE were analyzed in headspace samples (100 µL)

using an isothermal method on an Agilent 6890N gas chromatographer with flame ionization detection, nitrogen carrier gas, and a J&W GSQ capillary 30m x 250 μm x 0.53 μm i.d.) column. Nitrate and nitrite concentrations in anaerobic cultures were measured on a Dionex DX600 ion chromatographer with a Dionex IonPac AS18 hydroxide-selective anion-exchange column.

Results and Discussion

Results of these growth tests are given in Table 2.1, which reports maximum OD_{600} doublings and ideal substrate concentrations for liquid cultures, and uses a plus-minus system to characterize growth on auxanography plates. Figures 2.3 and 2.4 are growth curves for cyclohexanecarboxylate and salicylate, respectively. These substrates gave positive results; their growth curves are presented here as representative examples, and also to illustrate the large variation in culture response to substrates. Growth on cyclohexanecarboxylate was much more vigorous than growth on salicylate, although both were predicted to have complete gene pathways for their degradation. Representative auxanography plates for catechol (one demonstrating cell growth and one negative control) are shown in Figure 2.5.

Many predicted substrates were indeed used for growth by strain JS666, but not all of the predictions were confirmed in the laboratory. The negative responses may be due to a number of factors. First, the genomic annotation could be incorrect, in that the enzyme encoded by the gene may not have the stated function. This is a limitation of genome annotation, which predicts gene product function based on statistically significant sequence matches to proteins with known function. This technique cannot discriminate between sequence variation in unimportant regions of the peptide and

variations in essential amino acid residues. Also likely, however, is that the reaction conditions were not conducive to growth on these substrates. The concentrations may have been toxic to the cells, or perhaps some other environmental cue is necessary to turn on the transcription of the appropriate genes, as is the case in Nocardioides sp. strain JS614, where the toxic metabolite epoxyethane was found to induce the degradation of ethene and vinyl chloride (T. E. Mattes et al., 2007). One substrate for which this explanation has been confirmed is 1,2-dichloroethane (1,2-DCA). A complete set of haloalkane degradation genes was found, but JS666 cultures did not grow on 1,2-DCA in our study, and GC analysis showed no significant decrease in concentration over control bottles. A recent dissertation from another research group, however, reported growth of strain JS666 on 1,2-DCA (Shin, 2010). These conflicting results indicate the strong influence of laboratory conditions and/or regulatory issues on outcomes in growth studies, and demonstrate that a negative result is not necessarily the final word for a given substrate.

The high proportion of positive responses out of the number of substrates tested, however, proves that genome prediction of bacterial substrates is a much more high-yield approach than random testing. Without the genome sequence, many of the substrates that strain JS666 readily degraded would probably never have been tested. An example is cyclohexanecarboxylic acid, whose vigorous degradation is encoded in strain JS666 by genes in the alicyclic acid region on the pPol338 plasmid (Bpro_5258 and Bpro_5273; GenBank accession numbers ABE47117.1 and ABE47132.1). (Figures 1.4 and 2.1) This compound is relevant to bioremediation because cyclohexanecarboxylate is formed oxidatively from *n*-alkyl-cycloparaffins, which are components of petroleum pollution (Küver, Xu, & Gibson, 1995). Other genomically-predicted and experimentally confirmed substrates with interest for biocatalysis and bioremediation are the *n*-alkanes (components of petroleum pollution), ferulate (biocatalysis of valuable chemicals from agricultural waste), and cyclohexanol (conversion to adipic acid, Figure 2.6). Overall,

the results of this work suggest that genome-assisted prediction of substrates (for both bioremediation- and biocatalysis- related applications) is a promising new technique, and will only become more useful as the number of annotated microbial genomes increases.

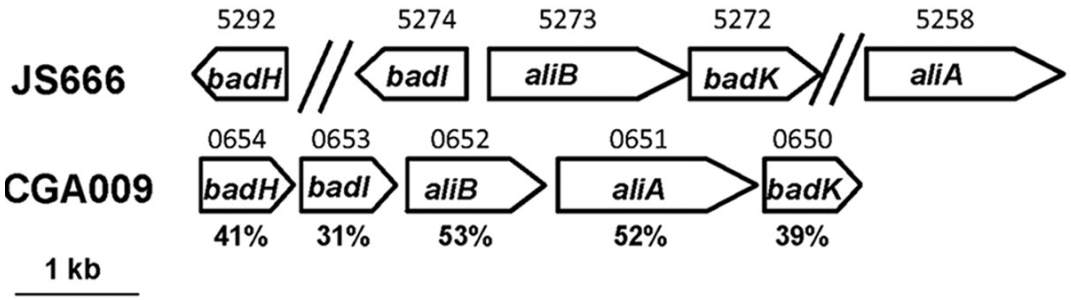

Figure 2.1. Organization of alicyclic acid biodegradation genes of JS666 and *R. palustris* CGA009.
badH, 2-hydroxycyclohexanecarboxyl-CoA dehydrogenase
badI, 2-ketocyclohexanecarboxyl-CoA hydrolase
aliB, cyclohexanecarboxyl-CoA dehydrogenase ABE47132.1
badK, enoyl-CoA hydratase
aliA, cyclohexanecarboxylate-CoA ligase. (ABE47117.1)
JS666 gene numbers (Bpro) are shown above the JS666 genes, CGA009 gene numbers (RPA) are shown above the genes, and percentage amino acid identities to JS666 homologs are shown under the CGA009 genes.

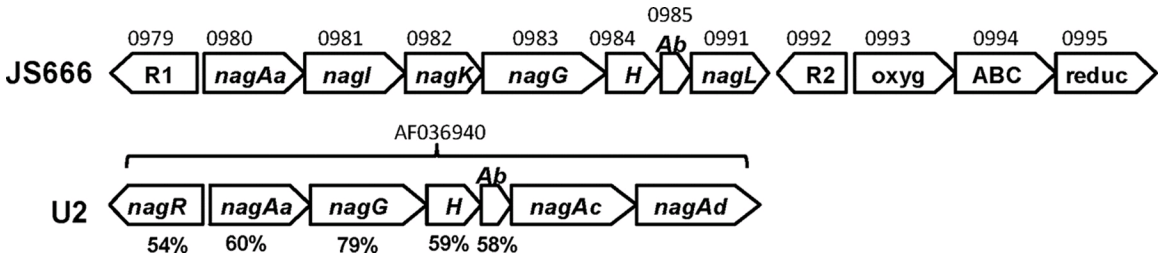

Figure 2.2. Organization of salicylate/gentisate biodegradation genes in JS666 and *Ralstonia* sp. strain U2.
R1, LysR family regulator;
nagAa, ferredoxin reductase;
nagI, gentisate 1,2-dioxygenase;
nagK, fumarylpyruvate hydrolase;
nagG, salicylate 5-hydroxylase large oxygenase component;
H, salicylate 5-hydroxylase small oxygenase component (*nagH*);
Ab, ferredoxin *nagAb*;
nagL, maleylpyruvate isomerase;
R2, TetR regulator;
oxyg, oxygenase;
ABC, ABC transporter;
reduc, reductase;
nagR, LysR family regulator;
nagAc, napththalene dioxygenase large subunit;
nagAd, napththalene dioxygenase small subunit.
JS666 gene numbers (Bpro) are shown above the JS666 genes, GenBank nucleotide accession numbers are shown above the U2 genes, and percentage amino acid identities to JS666 homologs are shown under the U2 genes.

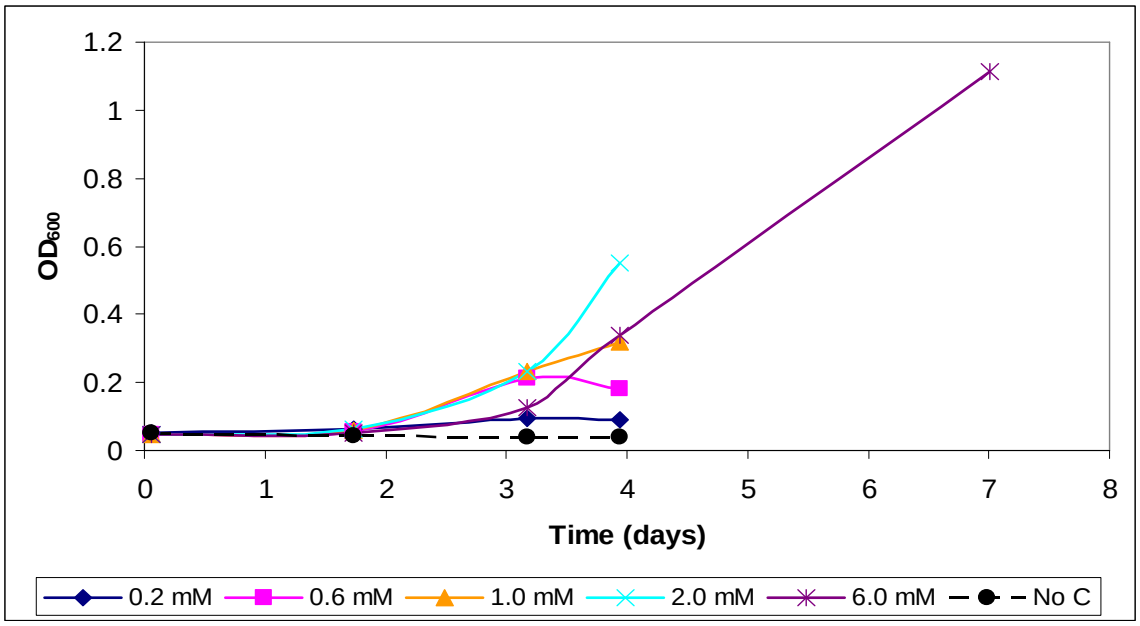

Figure 2.3. Growth of *Polaromonas* sp. strain JS666 batch cultures in MSM with cyclohexanecarboxylate as the sole carbon source. Legend values indicate initial concentration of cyclohexanecarboxylate.

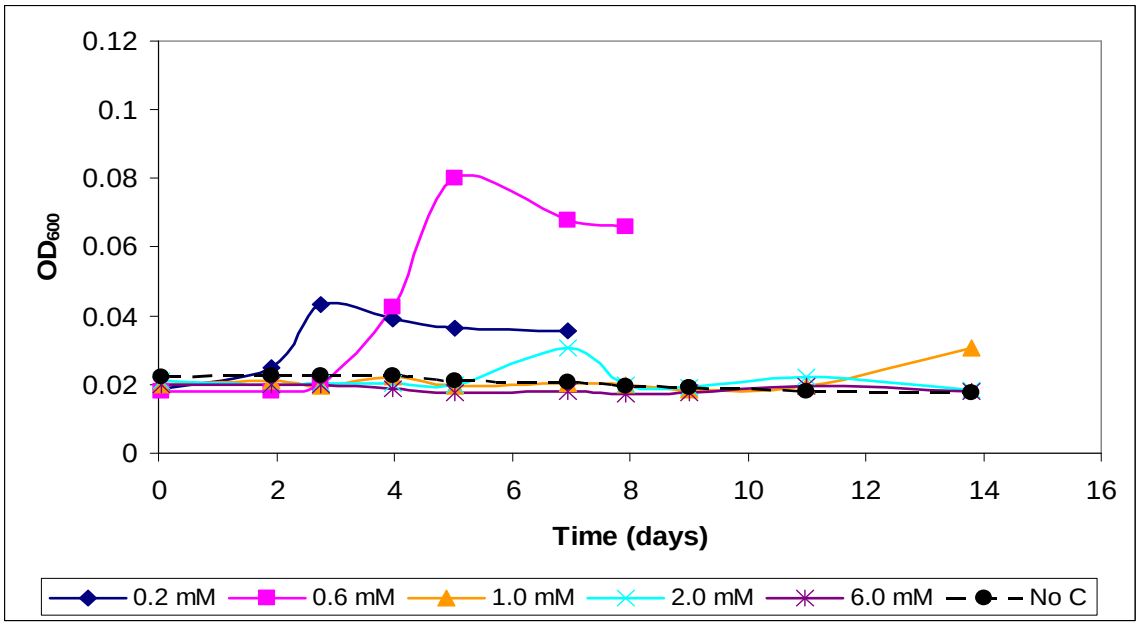

Figure 2.4. Growth of *Polaromonas* sp. strain JS666 batch cultures in MSM with salicylate as the sole carbon source. Legend values indicate initial concentration of salicylate.

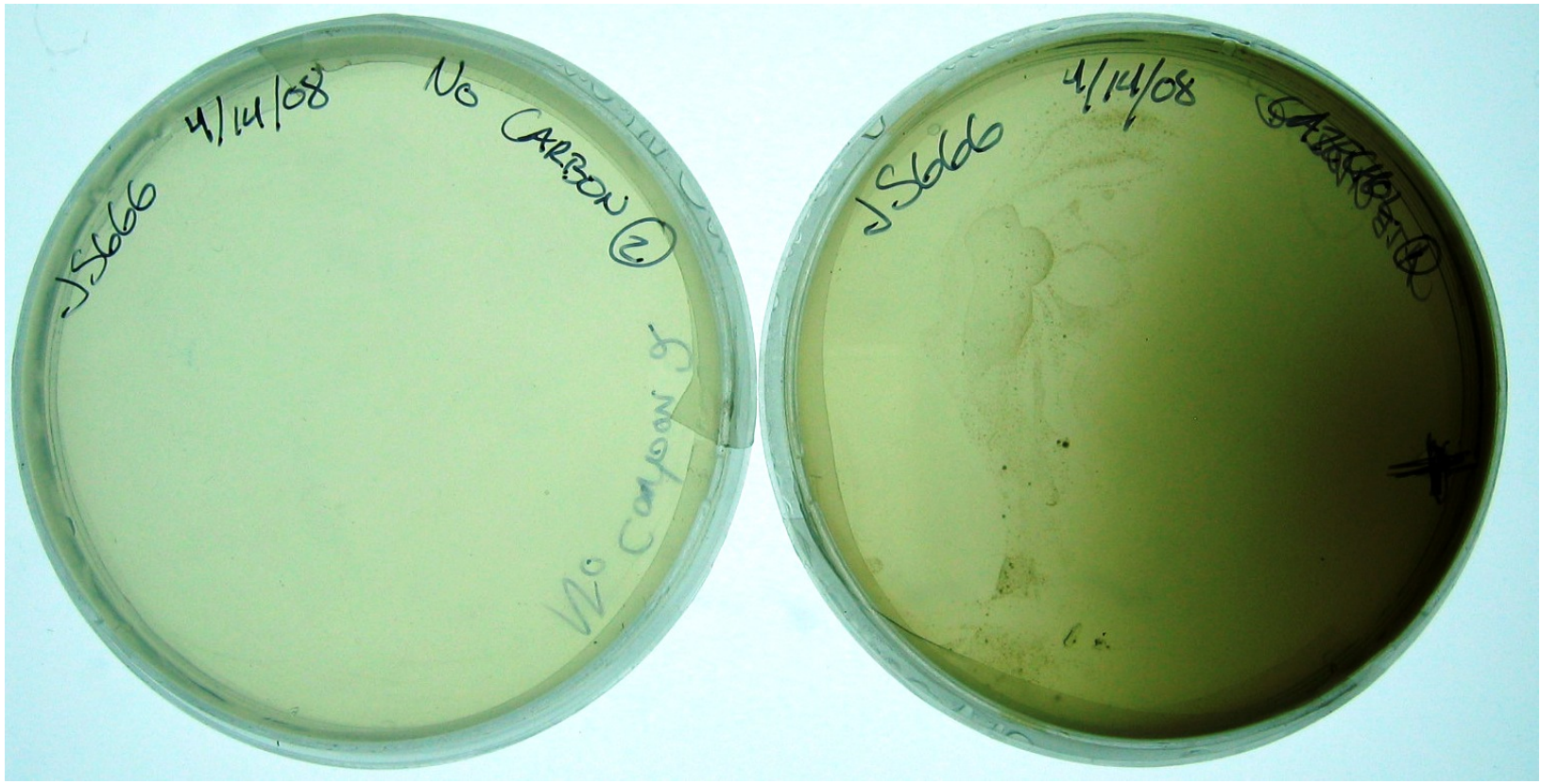

Figure 2.5. Auxanography plates with strain JS666 and no carbon source (left) or catechol as the sole carbon source (right). On the right-hand plate, 5 mg catechol was placed at the "X," and cell growth can be observed at the edges of the dark catechol dispersion gradient.

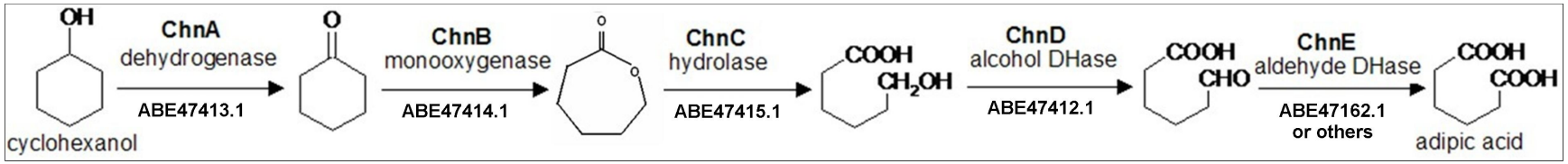

Figure 2.6. Pathway for conversion of cyclohexanol to adipic acid; numbers below reaction arrows correspond to GenBank accession numbers for genes in Polaromonas sp. strain JS666.

Table 2.1. Growth substrate range of *Polaromonas* sp. strain JS666.

Substrate	**Growth**[a]	**Initial Conc. (mM)**[b]	**Incubation Time (days)**[c]
Acetate	6.5[d]	10	5
Benzoate	-	2	30
Benzoate	+	Auxanography	30
Carbon Monoxide	-	10% Headspace	17
Carbon Monoxide (+10 mM ethanol)	-	10% Headspace	17
Catechol	-	2	30
Catechol	+	Auxanography	30
Chloroacetaldehyde	-	0.2-10	50
Chloroacetate	2.2	6	35
Cyclohexane	-	0.2-10	19
Cyclohexaneacetate	-	0.2-10	33
Cyclohexanecarboxylate	4.6	6	7
Cyclohexanol	2.7	1.2	8
1,2-Dichloroethane	-	0.2-10	14
cis-1,2-Dichloroethene	4.6	1.3	15
Dalapon (2,2-Dichloroproprionate)	-	0.2-10	57
Ethane	-	0.2-10	30
Ethanol (aerobic)	5.3	10	17
Ethanol (anaerobic + nitrate)	-	5-35 ($NO3^-$)	41
Ethylcyclohexane	-	0.2-10	54
Ferulate	1.8	2	15
Gentisate	4.1	2	15
Heptane	2.1	0.9	13
Hexane	-	0.2-10	6
3-Hydroxybenzoate	4.7	2	17
4-Hydroxybenzoate	-	2	30
Hydroxyquinol	+/-	Auxanography	30
Naphthalene	-	2	30
2-Nitrobenzoate	-	2	30
4-Nitrobenzoate	-	2	30
Octane	0.6	0.2	7

Table 2.1 continued

Substrate	Growth[a]	Initial Conc. (mM)[b]	Incubation Time (days)[c]
o-Phthalate	-	2	30
Propane	-	0.2-10	34
Protocatechuate	4.9	2	15
Salicylate	2.1	0.6	5
Succinate	4.8	10	6
Thiosulfate	-	10-40	29
Thiosulfate (+ 5 mM ethanol)	-	10-40	29

a) The numbers indicate the highest number of observed exponential doublings of OD_{600} in liquid medium.
+, positive for growth on auxanography plates
–, negative for growth
+/–, growth was inconclusive.

b) The concentration range tested is reported in cases where growth was negative. When growth was confirmed, the concentration showing the highest number of exponential doublings is reported.

c) In cases where growth was negative, the time when the experiment was abandoned is reported. In cases where growth was positive, the time when a maximum OD_{600} was observed is reported.

d) The starting OD_{600} was 0.002 in this experiment.

CHAPTER III

ANALYSIS OF ALKENE OXIDATION ACTIVITY IN *POLAROMONAS* SP. STRAIN JS666

Background

During initial studies of *Polaromonas* sp. strain JS666, it was discovered that after growth on cDCE, resting cells were able to aerobically degrade the alkenes cDCE, ethene, VC, *trans*-DCE (tDCE), and TCE (Coleman, Mattes, Gossett, & Spain, 2002a). Stoichiometric transformation of ethene to epoxyethane was observed in these cells, indicating the activity of a monooxygenase. (Figures 3.1, 3.2) Subsequent genome sequencing and annotation showed no evidence of an alkene monooxygenase (the enzyme used by VC-assimilating microbes (Hartmans & de Bont, 1992; Verce et al., 2000)) in strain JS666 or of any genes encoding other known alkene- epoxidizing enzymes. There are sixteen monooxygenases encoded in the genome of strain JS666, one of which is annotated as a "putative ammonia monooxygenase" (Bpro_0442; GenBank accession number ABE42406.1). Some ammonia monooxygenases have been found to have cometabolic alkene-oxidizing activity, but they are typically encoded in three-gene operons (one for each subunit of the enzyme) (Arciero, Vannelli, Logan, & Hopper, 1989; Arp, Sayavedra-Soto, & Hommes, 2002). The gene annotated as an ammonia monooxygenase in strain JS666 only corresponds to a single subunit (the transmembrane AmoA), so if the annotation is correct, it would be insufficient to exhibit the activity of the full enzyme.

Alkene oxidation is important to the field of bioremediation because it is essential for the degradation of many pollutants (chlorinated ethenes, unsaturated petroleum hydrocarbons, pesticides, etc.) (Bhatt, Kumar, Mudliar, & Chakrabarti, 2007; Stroud,

Paton, & Semple, 2007). It is also a focus of research in biocatalysis because of the value of alkene oxidation products (enantiopure epoxides, etc.) (Leak, Sheldon, Woodley, & Adlercreutz, 2009).

The observation of alkene oxidizing activity in an organism with no clear alkene-oxidizing enzymes is interesting because it could mean the discovery of a new function for a class of enzymes. A novel alkene-oxidizing enzyme could have very different substrate acceptance and enantioselectivity properties than well-studied alkene oxygenases, leading to new applications in bioremediation and biotechnology. Since strain JS666's ethene-oxidizing enzyme is expressed during growth on cDCE, there is also a strong possibility that it is capable of oxidizing cDCE, perhaps as the first step in a degradation pathway. Or, since the organism was isolated from a mixture of pollutants including cDCE, this enzyme may have activity on other xenobiotic compounds and is expressed during exposure to cDCE by co-regulation of pollutant degradation pathways. Regardless of its role in strain JS666, a novel alkene-oxidizing enzyme has the potential to increase our understanding of bioremediation processes and add to the toolbox of enzymes used in biocatalysis.

In the absence of a clear candidate for the observed alkene oxidation activity, a few hypotheses about the identity of the responsible enzyme were made. Since xenobiotic degradation abilities often are the result of horizontal gene transfer and rearrangement, genes on the two plasmids (which have evidence of transposase activity) were closely scrutinized for alkene-oxidizing possibilities. Two leading candidate genes were picked off of plasmid pPol338: a cytochrome P450 monooxygenase (Bpro_5301; GenBank accession number ABE47160.1) and a cyclohexanone monooxygenase (Bpro_5565; GenBank accession number ABE47414.1). The P450 monooxygenase is part of the proposed *n*-alkane oxidation pathway (T. E. Mattes et al., 2008), and was chosen because P450 enzymes are often associated with detoxification of xenobiotic compounds (Lewis & Wiseman, 2005). The cyclohexanone monooxygenase (CHMO) is

found in a genetic pathway coding for the conversion of cyclohexanol to the nylon monomer adipic acid (Figure 2.2), and was chosen because cyclohexanone monooxygenases are known to have wide substrate ranges (Carrea et al., 1992; Kamerbeek, Janssen, van Berkel, & Fraaije, 2003; Kyte, Rouvière, Cheng, & Stewart, 2004; Stewart, Reed, Zhu, Chen, & Kayser, 1996). The quest to identify the enzyme responsible for alkene oxidation in strain JS666 began with a three-pronged approach: gene expression, proteomics, and kinetics.

We studied the expression levels of the genes encoding the P450 and cyclohexanone monooxygenases using reverse-transcriptase PCR, after extracting RNA from cultures growing on various substrates. This approach made use of the expectation that expression levels of a given gene would be higher during growth conditions that required the activity of the enzyme encoded by that gene. Protein abundance was studied using SDS-PAGE to evaluate total protein extracted from cultures growing on various substrates. This approach relied on the same relationship between enzyme expression and growth conditions, but was less targeted than reverse-transcriptase PCR, allowing for discoveries outside of our anticipated results. Additionally, direct observation of increased amounts of an enzyme is more rigorous than noting increased amounts of specific RNA, as the quantity of RNA transcripts is not always strictly correlated to enzyme abundance in the cell (Gygi, Rochon, Franza, & Aebersold, 1999). Kinetic oxidation assays were used to investigate the relationship between growth substrate and the rate of ethene epoxidation. This approach made use of the observation that cells grown under conditions promoting the expression of an alkene-oxidizing enzyme exhibit higher rates of ethene oxidation in subsequent resting cell assays.

Materials and Methods

In gene expression studies, strain JS666 was grown to mid-exponential phase in minimal salts medium (MSM) with various carbon sources, including cDCE and substrates not expected to induce expression of an alkene-oxidizing enzyme (such as succinate and ethanol). Mid-exponential phase was defined as 1.0 to 1.5 doublings of cell density at 600 nm (OD_{600}); for example, a culture with an initial OD_{600} of 0.04 would be harvested for RNA extraction at an OD_{600} near 0.1. Normally, mid-exponential phase is determined based on the exponential shape of a culture's growth curve, but a set number of doublings was chosen because cultures of strain JS666 often did not exhibit exponentially-shaped growth curves, especially during slow growth on cDCE. Culturing with cDCE was performed as described in the Chapter II Materials and Methods section, and succinate and ethanol cultures were grown in MSM with 20 mM and 10 mM initial concentrations, respectively.

RNA was extracted from each culture using TRIzol reagent (guanidinium thiocyanate-phenol-chloroform extraction) from Invitrogen, then purified using the Qiagen RNEasy Mini kit. RNA preps were quantified with the Qubit fluorometer Quant-iT assay in later experiments, as it was found to have higher reproducibility than UV spectrophotometric methods used initially. Purified RNA samples were diluted with nuclease-free water to achieve identical RNA concentrations, and used in reverse transcriptase polymerase chain reaction (rtPCR) experiments with primers designed for the P450 and cyclohexanone monooxygenase (CHMO) genes. Primers were designed using Primer3 (Rozen & Skaletsky, 2000) and analyzed for possible side reactions with NetPrimer (Premier Biosoft International, 2010). Agarose gel electrophoresis (1.5% gels, TBE running buffer, 130V, 1 hr. run time) was run with the resulting amplified DNA for qualitative comparison. Gels were stained in dilute ethidium bromide solution (0.5

μg/mL) for thirty minutes, rinsed in deionized water for thirty minutes, then visualized using a Fisher BioTech UV light box and a Kodak EDAS 290 digital camera.

JS666 RNA extracts for real-time rtPCR experiments were prepared as above, followed by amplification with the Qiagen One-Step SYBR Green kit. The SYBR Green reagent fluoresces upon binding double-stranded DNA, allowing the quantification of reverse-transcribed RNA transcripts as they are amplified in the PCR. Primers were designed specifically for real-time PCR with minimized runs of repeated nucleotides, no more than two G and/or C bases in the five nucleotides at the 3' end, and predicted product sizes of 50-150 bp. Adherance to these guidelines minimizes non-specific product formation and improves amplification efficiency (University of Iowa Carver College of Medicine DNA Facility, 2010). Real-time rtPCR amplification was performed using an ABI PRISM 7000 Sequence Detection System.

For the complementary proteomic approach, cultures of strain JS666 were grown to mid-exponential phase in MSM with various carbon sources, including cDCE and non-inducing substrates. Crude cell extracts were obtained by lysing concentrated culture suspensions three consecutive times in a mini French pressure cell at 9000 psi, then centrifuging the lysate for three minutes at maximum speed (14,800 rpm; 21,000 x g) in a microcentrifuge to remove nucleic acids and cell wall debris. These protein extracts from different substrates were then resolved simultaneously with sodium dodecyl sulfate polyacrylamide gel electrophoresis (SDS-PAGE), using precast Criterion 12.5% polyacrylamide gels from Bio-Rad, at a constant 200 V for 55 minutes. This method separates proteins on the basis of size, and differences in the band pattern (or "protein fingerprint") represent the presence of different proteins in the cells.

Protein bands observed at greater intensity in cells grown on cDCE than in cells grown on other substrates were excised from the gels with a clean razor blade and sent to the University of Iowa Molecular Analysis Facility for trypsin digestion and analysis with matrix-assisted laser desorption/ionization – time of flight mass spectrometry (MALDI-

TOF MS). The trypsin digestion breaks the proteins down at predictable locations (the carboxyl side of lysine and arginine residues not immediately followed by a proline). These fragments are then vaporized, ionized, and separated by their mass/charge ratio, which is measured by the time it takes each fragment to travel the length of a tube under the influence of an electric field to reach a detector (time of flight). The consortium of mass/charge ratios observed for each protein band was then compared to the NCBInr database of predicted mass spectra of proteins whose gene sequences (and therefore amino acid sequences) are known (Chuang & Mattes, 2007), using the MASCOT search tool from Matrix Science (Matrix Science, 2010). Parameters selected for the database search included: trypsin digestion, the "Bacteria (Eubacteria)" taxon, the fixed carboxymethylation (C) modification, up to one missed cleavage, and a peptide mass tolerance of ±0.2 Da. A protein match was not considered to be correct unless its probability-based Mowse score exceeded the significance threshold of 77, which corresponded to a probability of 0.05 or less that the observed match was a random event.

Our third approach to identifying the alkene-oxidizing enzyme expressed during growth on cDCE was to study the kinetics of alkene oxidation in resting cells that had been grown on various substrates. This approach mimicked the initial experiment that exposed the ethene oxidation activity of cDCE-grown JS666 in the first place, but expanded it to include substrates that could illuminate potential enzymes involved in the oxidation. The underlying assumption here was that if alkene oxidation was increased after growth on a given substrate, then enzymes involved in assimilating that substrate may also be involved in alkene oxidation, as they would have been more highly expressed in those cells. Specifically, we chose to test cyclohexanol-grown cells to see if increased expression of the cyclohexanone monooxygenase was correlated with increased alkene oxidation activity.

Cultures of strain JS666 were grown to mid-exponential phase in MSM with 10 mM acetate (not expected to induce alkene oxidation (T. E. Mattes et al., 2005)), 1.0 mM

cyclohexanol, or cDCE (known to induce alkene oxidation; grown as described in Chapter II Materials and Methods), then pelleted and resuspended at a much higher density ($OD_{600} \approx 10$) in nitrogen-free potassium/phosphate (KP) buffer to prevent further growth (yielding "resting" cells). Resting cell suspensions (1 mL) were sealed in 20 mL glass serum bottles with rubber stoppers and crimp caps. Ethene (0.1 mL at ambient pressure; 0.115 mg; 2.6 μmoles) was injected into these dense cell suspensions and the increase in epoxyethane was measured over three hours using headspace samples and flame-ionization detection gas chromatography on a 1% SP-1000 60/80 Carbopack B packed column (Supelco). Following the kinetic assay, the cell suspensions were lysed and the protein concentration was calculated from UV measurements using the following equation (Kalb, 1977).

$$\text{Protein } (\mu g/mL) = (183 \times A_{230}) - (75.8 \times A_{260})$$

where $A_{###}$ is absorbance at the indicated wavelength (in nm)

Kinetic data was then normalized to the total amount of protein in the test bottle. Triplicate cultures were grown on each substrate, and triplicate resting cell suspensions were created from each culture.

Results and Discussion

Growth on cDCE and Unstable Phenotype Observations

Polaromonas sp. strain JS666 is known to have an unstable cDCE-assimilating phenotype when cultured without cDCE, which has been hypothesized to be due to plasmid loss or poorly developed regulatory control of the necessary enzymes (T. E. Mattes et al., 2008). Good cDCE-assimilating behavior is characterized by degradation of several successive cDCE injections (as described in Chapter II), with concurrent

increases in OD_{600} (at least one doubling of the initial value). Bad behavior is marked by some initial degradation of cDCE (less than two injections to a final concentration of 0.5 mM each) without an increase in OD_{600}, then a slowing and eventual stopping of cDCE degradation altogether; cDCE assimilation activity is not restored by transferring these cultures to fresh media. It is possible that this pattern is indicative of a cometabolic cDCE degradation pathway that may predominate when the proper regulatory response for the assimilative pathway has failed. This explanation would be consistent with non-growth-coupled degradation of cDCE that eventually ceases due to accumulation of a toxic intermediate such as an epoxide. The unstable cDCE-assimilation phenotype complicated gene expression and proteomic analyses by making it difficult to attain reliable replicate culture conditions.

During growth experiments for this work, it was observed that certain substrates preserved cDCE oxidation activity in strain JS666 better than others. Succinate and acetate, while good substrates for producing large quantities of healthy cells, did not maintain the cDCE-assimilating phenotype well. Growing strain JS666 for two or more successive fed-batch cultures on one of these substrates frequently resulted in poor behavior when the cultures were transferred back to cDCE as a sole substrate. For this reason, experimental cultures required to be grown on succinate and acetate for comparative purposes were always inoculated from cDCE-grown stock. In contrast, cultures grown on ethanol or cyclohexanol, with few exceptions, did not exhibit bad behavior when transferred back to cDCE as a sole substrate. The observation of good cDCE-assimilating behavior following growth on ethanol was confirmed by Jennings, et al. (2009). The implications of the good cDCE-assimilating behavior following growth on cyclohexanol were explored using kinetic assays described later in this chapter.

Gene Expression Analysis

The results of the rtPCR experiments are illustrated by the agarose gels shown in Figure 3.3. Expression of the P450 gene actually appears to be lower in cells grown on cDCE than cells grown on other substrates (based on gel band intensity), which is not consistent with the increased oxidation activity found in cDCE-grown cells. This result was sufficient to remove the P450 gene from the top of our list of contenders. However, given a recent dissertation report of JS666 P450 monooxygenase activity on cDCE, this removal now appears to have been premature (Shin, 2010). Recent evolution of the cDCE degradation pathway in strain JS666 may cause poor regulatory control of the genes involved, which could reconcile this new discovery with our observation of decreased P450 expression during growth on cDCE. Expression of the CHMO gene appears to be high during growth on all substrates (Figure 3.3); this could mean one of two things. The first possibility is that the CHMO gene is constitutively expressed under all substrate conditions, which would make it an unlikely candidate for the alkene epoxidation activity we observed to increase after growth on cDCE. The second prospect is that the CHMO is more highly expressed during growth on cDCE, but rtPCR is not sensitive enough to detect this increase over its basal expression level.

Reverse transcriptase PCR is good for discriminating between “on” and “off” gene expression, but the qualitative nature of the results (band intensity in agarose gels) and the point at which analysis is done (the tail end of a logarithmic amplification curve) reduce its ability to illuminate more subtle differences in expression levels. Highly improved quantification can be obtained with real-time (quantitative) reverse transcriptase PCR, which uses a DNA-binding fluorescent dye and real-time detection to quantify DNA concentration over the entire amplification curve (Bustin, Benes, Nolan, & Pfaffl, 2005). The number of PCR cycles it takes for the DNA concentration-dependent fluorescence to cross a set threshold is inversely proportional to the starting RNA copy number of the gene. This relationship is used to construct standard curves and calculate

the starting RNA gene copy number of each sample with high sensitivity and accuracy (Bustin et al., 2005). A model real-time PCR amplification curve is shown in Figure 3.4.

Real-time rtPCR experiments with JS666 RNA extracts used a relative quantification method that compared varying sample gene expression to the hypothetically consistent expression levels of a "housekeeping" gene in all samples. While many challenges in method optimization (including real-time PCR-specific primer design, issues with cycle time and temperature choices, and inconsistent JS666 culture growth patterns) were overcome, a recurring problem was inconsistency in the expression levels of the 16S rRNA and RNA Polymerase β subunit genes (two commonly used housekeeping genes for bacterial real-time PCR). Measured expression levels of these genes varied by more than ten-fold among cultures grown on the same substrates, and even more between those grown on different substrates. Variation in housekeeping gene expression levels has been documented to be a much larger problem in real-time rtPCR with prokaryotic cells than in eukaryotic cells (Eleaume & Jabbouri, 2004; Fey et al., 2004). This variation was likely exacerbated in this case by the difficulty in identifying a consistent mid-exponential growth phase during strain JS666's slow growth on cDCE, as discussed in the previous section. Without a consistent expression level of at least one of these genes throughout all of the tested substrates, it is impossible to derive meaning from the variations observed in the other genes we tested.

One promising solution to this problem would have been the use of an absolute quantification method, as described by Dr. Lisa Alvarez-Cohen's research group (Johnson, Lee, Holmes, & Alvarez-Cohen, 2005). In this technique, an internal reference mRNA standard (*ref* mRNA) is added to each sample at the beginning of the extraction procedure to quantify loss of RNA, and is also used to create a standard curve, enabling absolute quantification in RNA gene copy number per cell instead of relative x-fold expression. During preparations to begin absolute quantification with JS666 RNA extracts, however, another research group confirmed our gene expression, proteomic, and

kinetic results using a genetic microarray (Jennings et al., 2009), so it was determined that additional real-time rtPCR experiments were unnecessary for this particular gene expression question.

Proteomic Analysis

A representative polyacrylamide gel from the proteomic studies is shown in Figure 3.5. Here it can be seen that the protein fingerprint of JS666 cultures noticeably changed depending on the growth substrate. It is also clear that certain protein bands are quite intense under all conditions; for example, using the MASCOT search tool (with a threshold Mowse score of 77), the very dark band at approximately 40 kilodaltons (kDa) was identified as a porin, which is an outer membrane-spanning protein that allows water and other molecules to freely pass between the interior and exterior of the cell. Our work with this method did not yield the identity of the oxygenase responsible for alkene oxidation, but did confirm that the downstream fate of cDCE in the cell is the glyoxylate pathway. The glyoxylate pathway is a modification of the Krebs cycle that allows a cell to synthesize carbohydrates from fatty acids or two-carbon precursors; we identified elevated levels of a few of these enzymes in cDCE extracts, including hydroxypyruvate isomerase and 2-hydroxy-3-oxopropionate reductase. Common proteins that were more highly expressed during growth on cDCE, but had no obvious involvement in its metabolism included an extracellular ligand-binding receptor, a twin-arginine translocation pathway signal, a chaperonin, and an aldehyde dehydrogenase. The product of Bpro_5566 (GenBank accession number ABE47415.1; annotated as an epoxide hydrolase or esterase in the JS666 genome) was also found to be more highly expressed during growth on cDCE than during growth on the other tested substrates, and was identified with a Mowse score of 88. This was a significant discovery because this gene is immediately adjacent to the cyclohexanone monooxygenase on plasmid pPol338, and

regulated in the same operon. As discussed in Chapter I, an epoxide hydrolase is one of the possible enzymes a cell might use to detoxify the chlorinated epoxide that would be produced by a cDCE-degrading monooxygenase. In the cyclohexanol to adipic acid pathway, the function of this hydrolase is to hydrolyze ε-caprolactone to 6-hydroxyhexanoic acid (Brzostowicz et al., 2005; Cheng et al., 2000).

While we did not find the cyclohexanone monooxygenase itself in our proteomic studies, our confidence in our hypothesis that it was involved in alkene oxidation was boosted by the observation of increased levels of the adjacent hydrolase. The complexity of the proteome and limited resolution of the single dimension SDS-PAGE method make identification of every single expressed protein in the cell essentially impossible, so there is a high likelihood that an enzyme more highly expressed in cDCE-grown cells could have been missed.

Kinetic Analysis

Figure 3.6 presents representative single-culture, triplicate-assay results for whole-cell ethene oxidation assays with acetate, cDCE, and cyclohexanol as the growth substrates used immediately prior to resting cell ethene exposure. The slopes of the lines are proportional to epoxyethane production rates, and although the data in these graphs is not normalized to the amount of protein in the bottles, it can clearly be seen that epoxyethane was produced much faster by cDCE- and cyclohexanol-grown cultures than by the acetate-grown culture. The detection limit of epoxyethane with the GC method was near 0.1 μmole per bottle, which is why the data points and trendlines do not extend all the way to the origin of the graphs.

The compiled results of the kinetic studies, normalized for protein concentration, are summarized in Table 3.1. It is clearly apparent that the ethene epoxidation activity of cyclohexanol-grown cells is higher than that of acetate-grown cells, and very close to the

value obtained for cDCE-grown cells. Since the operon containing the CHMO would almost certainly be upregulated during growth on cyclohexanol, this result is consistent with the hypothesis that the CHMO is responsible for ethene oxidation in strain JS666. It is not conclusive proof of alkene oxidation by the CHMO, however, because the kinetic assay results reflect the activity of the entire group of proteins expressed in the cells, not just the CHMO.

General Conclusions from Alkene-Oxidation Analysis in *Polaromonas* sp. Strain JS666

Experiments measuring P450 and cyclohexanone monooxygenase gene expression using reverse transcriptase PCR showed decreased expression of the P450 gene during growth on cDCE, and unchanged expression of the CHMO. Proteomic experiments did not prove increased abundance of any monooxygenase, but did illustrate that expression of the epoxide hydrolase enzyme (in the same operon as the CHMO) was increased during growth on cDCE. Kinetic resting cell assays demonstrated that ethene epoxidation activity was similarly increased after culture growth on cyclohexanol as on cDCE. While no one of these results conclusively demonstrated the involvement of strain JS666's CHMO in alkene oxidation, the sum of the three approaches provided strong circumstantial evidence that it was upregulated in response to cDCE, and possibly involved in its degradation and in ethene oxidation. This inference was supported by subsequent microarray data and additional proteomic results from Jennings, et al. (Jennings et al., 2009). Given these converging lines of evidence, our next step was to attempt to definitively determine if the CHMO from strain JS666 had activity on ethene or cDCE. This approach (heterologous expression) is discussed in Chapter IV.

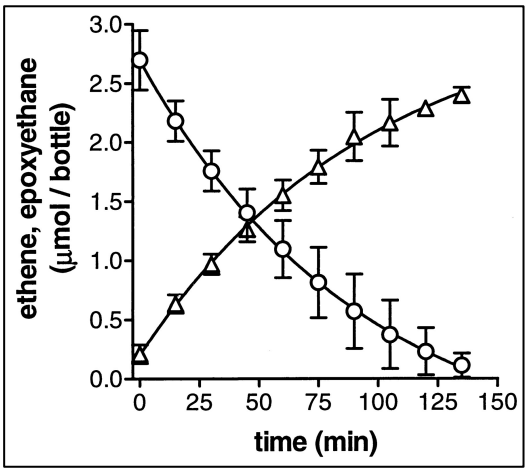

Figure 3.1. Oxidation of ethene to epoxyethane by strain JS666, where "Δ" represents epoxyethane and "O" is ethene (Coleman, Mattes, Gossett, & Spain, 2002a).

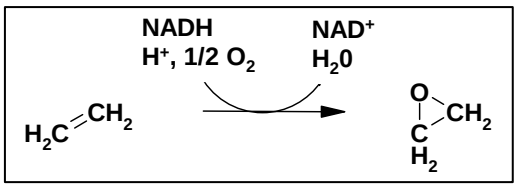

Figure 3.2. Epoxidation of ethene by a monooxygenase.

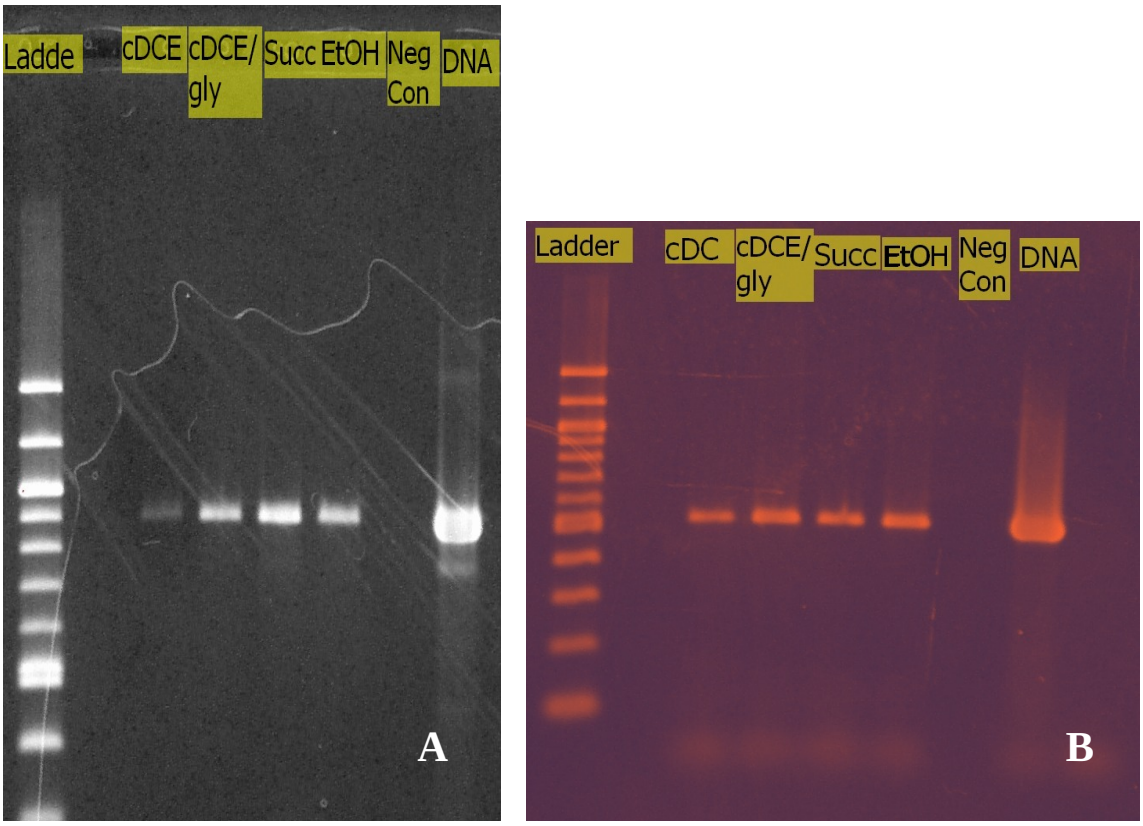

Figure 3.3. Agarose gels with products of rtPCR using JS666 RNA extracts (50 ng template per 25 μL reaction; 5.0 μL PCR product per lane). Band intensity is proportional to RNA concentration of the target gene; vertical migration is dependent on the size of the transcript.

Ladder: New England BioLabs DNA size reference ladder (100 – 1500 bp; 1.0 μL per lane)
cDCE: RNA from JS666 culture grown on cDCE only (as described in Chapter II)
cDCE/gly: RNA from JS666 culture grown on cDCE and residual glycerol from frozen stock
Succ: RNA from JS666 culture grown on 20 mM succinate
EtOH: RNA from JS666 culture grown on 10 mM ethanol
Neg Con: Negative Control, rtPCR prep with all reagents and no RNA template
DNA: Positive control, rtPCR with 50 ng JS666 genomic DNA

A) P450 monooxygenase primers (expected product size: 893 bp)
B) Cyclohexanone monooxygenase (CHMO) primers (expected product size: 572 bp)

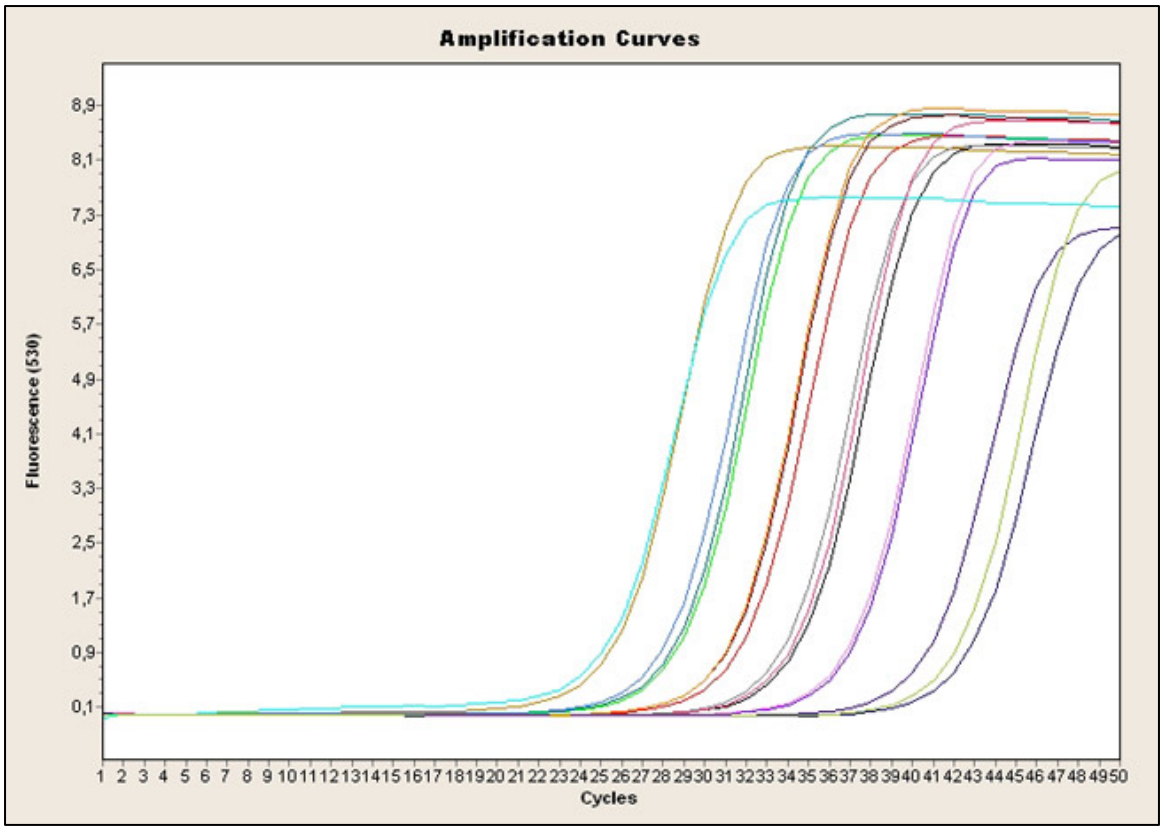

Figure 3.4. Model real-time rtPCR amplification curves.
Colored lines correspond to individual sample wells, “Cycles” refers to the number of PCR amplification cycles, and “Fluorescence” is the fluorescence of the reporter dye, SYBR Green.

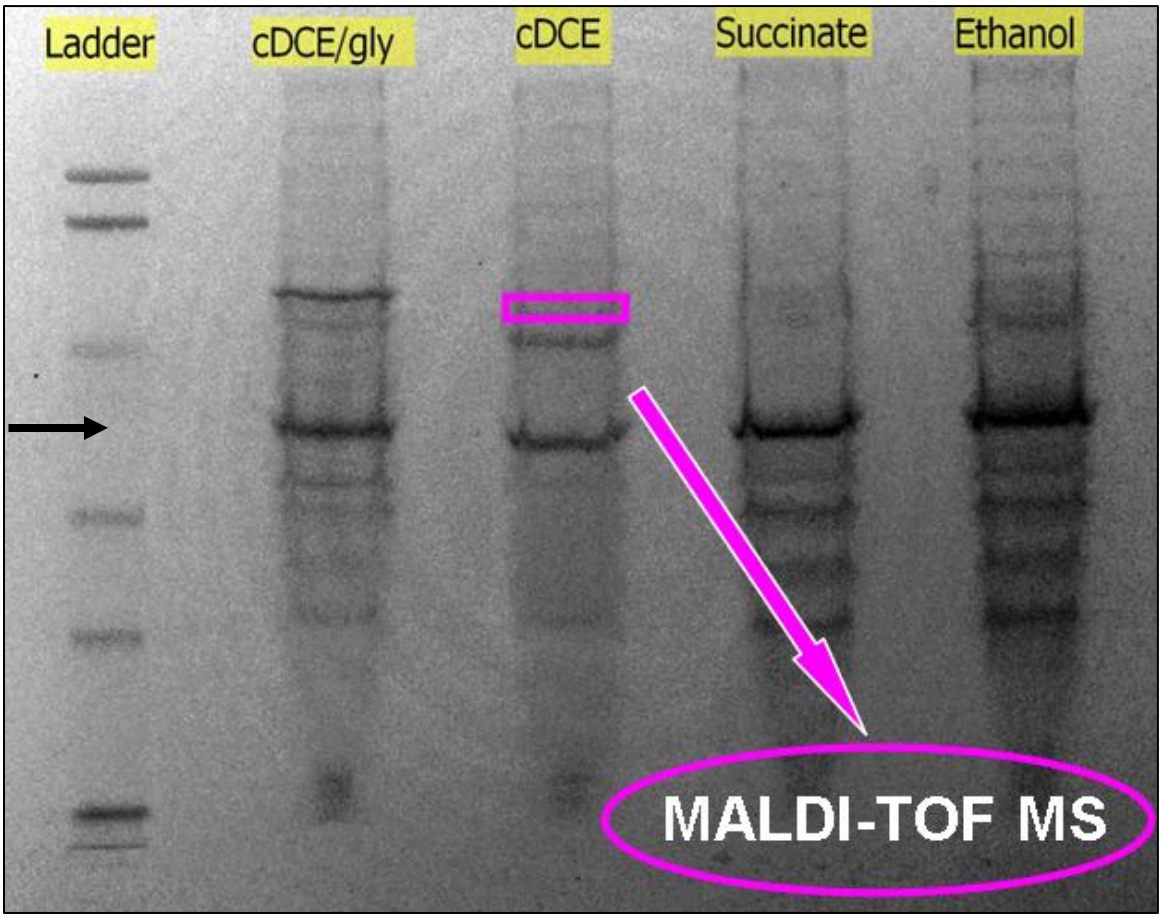

Figure 3.5. SDS-PAGE gel with total protein extracts from JS666 cultures (32 μg protein per well). Band intensity is proportional to concentration of a given protein, and vertical migration is dependent upon protein size.

Ladder: 10 μL Bio Rad Prestained SDS-PAGE Standards, Low Range (20-105 kD)
cDCE/gly: Protein extract from JS666 grown on cDCE and glycerol
cDCE: Protein extract from JS666 grown on cDCE
Succinate: Protein extract from JS666 grown on succinate
Ethanol: Protein extract from JS666 grown on ethanol

The pink box represents an example slice of gel that was digested and analyzed by MALDI-TOF MS, and the arrow points to the dark band that was identified as a porin (~40 kDa).

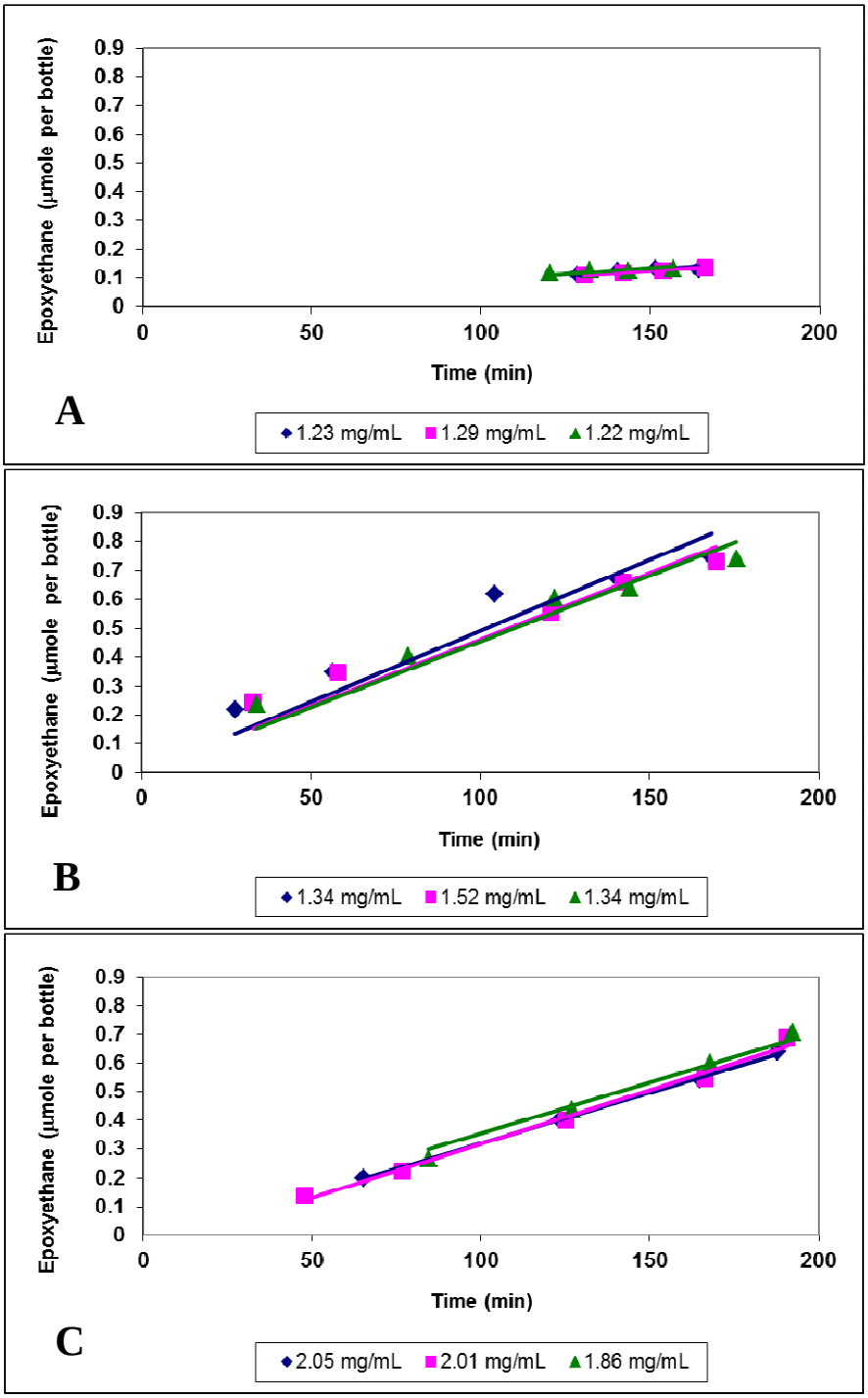

Figure 3.6. Epoxyethane production in JS666 resting cell assays by cultures grown on
A) Acetate (10 mM)
B) cDCE (Grown as described in Chapter II)
C) Cyclohexanol (1.0 mM)
Protein concentration of each assay bottle is noted in the legend. No epoxyethane was detected in control bottles with no cells.

Table 3.1. Epoxyethane production rates in resting cell assays (values are the means from triplicate assays of triplicate cultures).

Substrate	**[nmol epoxyethane produced] / [min. – mg protein]**	**Standard Deviation**
Acetate	0.64	0.34
cDCE	1.82	0.46
Cyclohexanol	1.62	0.65

CHAPTER IV

CREATION AND OPTIMIZATION OF A HETEROLOGOUS CYCLOHEXANONE MONOOXYGENASE EXPRESSION SYSTEM

Background

The results of the initial three-pronged approach to identify the alkene-oxidizing enzyme in strain JS666 supported the hypothesis that the plasmid-encoded cyclohexanone monooxygenase is upregulated in response to cDCE exposure. This hypothesis was confirmed independently with microarray experiments by Jennings, et al. (Jennings et al., 2009). Evidence of CHMO upregulation, however, does not prove that this enzyme has activity on cDCE or ethene, and there were still other possible alkene-oxidizing candidates present in strain JS666's genome.

To address this problem, a heterologous CHMO expression system was created to isolate the activity of the CHMO from that of other enzymes in strain JS666. Heterologous expression also facilitates significant over-expression of the CHMO, thereby making its activity easier to detect over relatively short timescales. Whole-cell expression in *Escherichia coli* was chosen over production of purified enzyme in this study in order to maintain a typical intracellular environment for proper enzyme activity, and to ensure availability of the necessary NADPH and FAD cofactors. *E. coli* was chosen as the expression host because as a Gram-negative bacterium, it should provide an intracellular physiology similar to that of strain JS666. Also, since it is not naturally capable of the predicted CHMO reactions (or downstream reactions to consume their products), a comparison of activity between *E. coli* cells expressing the CHMO and those not expressing the CHMO was straightforward.

Materials and Methods

Vector Construction and Analysis

The target CHMO gene was amplified as a blunt-end PCR product using the proofreading Pfx DNA polymerase, and 5 ng of this product was ligated into a pET101/D-TOPO vector (Invitrogen) as per the vector-specific instructions. (Figures 4.1 and 4.2) Directional TOPO (D-TOPO) cloning makes use of a 3' phosphate bond between a cleaved strand of DNA and a residue of the enzyme topoisomerase I. The bound topoisomerase protects the cleaved DNA until a DNA molecule with a coordinating overhang sequence binds to the free single-stranded segment and displaces the topoisomerase (Figure 4.2). The desired gene insert (for the JS666 CHMO) was designed with a "CACC" sequence addition immediately preceding the start codon in order to promote directionally-correct ligation into this spot by base-pairing with the "GTGG" single-stranded segment in the vector.

The pET101/D-TOPO vector was selected for this expression system to take advantage of the simplicity of directional cloning, and for its collection of regulatory and selective features. The expression of the cloned gene in this vector is tightly controlled by the bacteriophage T7 promoter, which is recognized by T7 RNA polymerase. T7 polymerase must be supplied by the host strain, and this in itself is done in a regulated manner (see the description of the expression strain, below). The pET101/D-TOPO vector also contains genes for ampicillin resistance (Figure 4.2), allowing for easy selection of cells containing the vector, and easy maintenance of the vector in cultures grown with ampicillin. The vector contains sequences coding for protein fusion "tags" (Figure 4.2), but our PCR product was designed to include the native stop codon in order to eliminate the influence of these sequences. The normal purpose of a protein fusion tag

is to facilitate identification and isolation of the heterologously expressed protein. As enzyme purification was not planned for this study, native peptide ends were chosen to avoid any potential fusion tag interference with the enzyme's native activity.

Once the CHMO gene was ligated into the pET101/D-TOPO vector, the vector was transformed into chemically competent One Shot TOP10 *E. coli* cells (Invitrogen) for vector maintenance. This *E. coli* strain does not contain the T7 RNA polymerase, so is incapable of expressing the heterologous gene at high levels. Some heterologous gene products can be harmful to *E. coli* cells, so a non-expressing strain is often used for maintenance of the plasmid in ampicillin-containing cultures. After transformation of One Shot TOP 10 *E. coli* (as per manufacturer instructions) with the CHMO-containing vector, the *E. coli* cells were plated on pre-warmed 37°C Luria Bertani (LB) agar plates containing 75 μg/mL ampicillin, and incubated overnight at 37°C. Five colonies were picked from these plates, and plasmid extraction was conducted using the Zyppy Plasmid Miniprep kit from Zymo Research. Plasmid DNA was incubated at 37°C with the PstI restriction enzyme from New England BioLabs (0.5 μg plasmid DNA, 0.5 μL PstI, 5 μL 10X NEBuffer, and 0.5 μL of 10 mg/mL BSA, all in 50 μL total reaction volume) for three hours, then deactivated at 80°C for 20 minutes. The PstI digests were analyzed with agarose gel electrophoresis to determine if the gene insert was present in the correct orientation. Digested fragment lengths for successful and unsuccessful ligations were predicted using the restriction enzyme map of vector pET101/D-TOPO (Invitrogen, 2010b) and the known sequence of the CHMO gene insert. Out of the five colonies picked from the selective plates, four contained the gene insert in the correct orientation, and one of these (CHMO3) was chosen for use in expression studies as described below.

After several expression attempts with pET101(CHMO3) failed to exhibit monooxygenase activity, the CHMO3 plasmid extract was submitted to the University of Iowa DNA Facility for sequencing with the T7 primers provided with the vector (see Figure 4.2 for primer binding sites). It was discovered that in spite of our choice of a

high-fidelity proofreading DNA polymerase in our blunt-ended PCR, the CHMO3 insert contained a single base pair mutation that changed the coding of the gene for one amino acid residue. Sequencing of the remaining vectors with the correctly oriented insert found pET101(CHMO4) to have the correct CHMO gene sequence (as compared to the genome sequence), and this vector (named plasmid pAA2) was used for all subsequent expression studies.

Transformation and Expression Conditions

E. coli BL21 Star (DE3) was chosen as the expression strain because it is specifically designed for the expression of T7-regulated genes. It contains the T7 RNA polymerase gene, which is regulated in this strain by the *lacUV5* promoter. Upon addition of the allolactose homolog isopropyl β-D-thiogalactoside (IPTG), expression of the T7 RNA polymerase (and hence of the T7 promoter-regulated gene insert) is induced. In the pET101/D-TOPO vector, the T7 promoter contains a *lac* operator sequence (Figure 4.2), which binds the lac repressor encoded by *lacI* in *E. coli* BL21 Star (DE3). This provides additional control of gene expression, and prevents transcription of the gene insert even when low basal levels of T7 RNA polymerase are present in the cell.

Transformation of purified pAA2 plasmid DNA into chemically competent *E. coli* BL21 Star (DE3) was carried out using the heat shock method as per manufacturer instructions, with the addition of 10 ng plasmid DNA in 1 μL volume to one vial of *E. coli* cells. The products of the transformation reaction were grown overnight in 10 mL of LB broth containing 200 μg/mL ampicillin, then inoculated at 1% (v/v) in fresh (identical) broth to begin each expression assay.

In initial attempts, *E. coli* CHMO expression cultures were grown at 37°C and induced with 1 mM (final conc.) IPTG once they reached an OD_{600} of 0.5-0.7, as per the manufacturer instructions. Two hours post-induction, the cultures were pelleted and

resuspended to an OD_{600} of approximately 10 in KP buffer, as in the resting cell assays described in Chapter III. Resting cell suspensions (1 mL) were placed in 20 mL glass serum bottles and sealed with Teflon-coated rubber stoppers and crimp caps. Ambient pressure gas-phase ethene (0.1 mL, 4.1 μmoles) was added to the appropriate cell assays with 0.22 μM pore-size filtered syringes; cDCE and cyclohexanone were dissolved in ethanol and added (to the selected bottles) to a range of final concentrations from 0.5 to10 mM (1% ethanol v/v). Ethanol stocks were used in order to ensure accurate substrate concentration in assay bottles (serial dilution instead of measurement of tiny volumes), and the substrates involved in both Chapter IV and V are more soluble in ethanol than in water. Negative control bottles with cells from uninduced *E. coli* Bl21 (Star) DE3 cultures were used for each substrate.

Analytical Methods

Headspace samples (100 μL) were taken from the cDCE- and ethene-containing cultures at selected time points (0-24 hrs), and analyzed by GC; cDCE on a J&W Scientific GSQ column, and ethene and epoxyethane on a Supelco 1% SP-1000 column, both with FID and N_2 carrier gas. Cyclohexanone and caprolactone were extracted and quantified using methods discussed thoroughly in Chapter V.

Total cell extracts for SDS-PAGE analysis were prepared using French press, as described in Chapter III. For soluble/insoluble protein fraction analysis, EPICENTRE's EasyLyse Bacterial Protein Extraction Solution was adapted as in the protocol by Burns (2004). Figure 4.6 provides an illustration of this technique. Protein fractions were prepared for SDS-PAGE by resuspending in SDS loading buffer and heating at 95°C for one minute, and gel electrophoresis was run as described in Chapter III.

Results and Discussion

Protein Expression Troubleshooting

Following successful transformation of the *E. coli* expression strain with the vector containing the CHMO gene, initial expression assays (using manufacturer-recommended conditions) did not show any activity on cDCE, ethene, or cyclohexanone, the CHMO enzyme's normal substrate. Several possible causes of this were considered. First, it was possible that the CHMO gene was not functional, either in strain JS666 or in its *E. coli* host. This seemed unlikely, however, given strain JS666's ability to grow using cyclohexanone as a carbon source. A second possibility was that some error had been made in construction of the expression vector, making it impossible for the host cell to express the desired gene sequence. This option was investigated by extracting the total protein from *E. coli* cells before and after induction with IPTG, then visualizing the results using SDS-PAGE. The resulting gel (Figure 4.3) showed a marked increase in the intensity of a protein band of the CHMO's expected size (~60 kDa) following induction. This indicated that a protein of the CHMO's approximate length was being produced, and as no obvious error in the vector was found, it appeared most likely that the CHMO gene was being transcribed and translated in the *E. coli* cells, but some factor was preventing the protein from achieving an active form. This could be due to improper folding of the protein, aggregation of over-produced proteins, or the elimination of some post-translational protein modification step catalyzed by strain JS666 but not by the *E. coli* host. Post-translational modification of the CHMO enzyme had been proposed by Jennings, et al. (2009) because of their observation of "spot chains" in 2D SDS-PAGE analysis. Protein misfolding and aggregation were the easier of the possible causes to evaluate, so specialized protein extraction was undertaken to investigate the solubility of the heterologously expressed CHMO.

An adapted protocol for the EPICENTRE EasyLyse Bacterial Protein Extraction Solution (Burns, 2004) was utilized to separate soluble proteins from insoluble proteins in the *E. coli* cell extracts (see "Analytical Methods," below, and Figure 4.6). Figure 4.4 is an SDS-PAGE gel illustrating the soluble and insoluble protein fractions in the *E. coli* host strain over time as the cells are induced to manufacture CHMO. This gel was consistent with the gel in Figure 4.3, in that it showed a marked increase in CHMO protein following induction. However, the addition of soluble/insoluble protein fractionation made it clear that under manufacturer-recommended conditions, almost all of the CHMO protein was not soluble in the cytoplasm of the cell, and therefore could not be active.

The generalized cause of insoluble protein aggregates (or "inclusion bodies") in heterologous expression systems is overloading of the host cell's ability to correctly process the recombinant enzyme (Kane & Hartley, 1988). Numerous copies of the single polypeptide clog the cell's protein folding apparatus (chaperones and foldases), resulting in aggregation of many mis-folded, insoluble proteins, which are often inactive even if extracted and re-solubilized (Baneyx, 1999; Miroux & Walker, 1996). Some studies have indicated that inducing the *E. coli* host cells to also over-express foldase genes improves the solubility of the heterologous protein (D. H. Lee, Kim, Lee, Kweon, & Seo, 2004), but a simpler initial approach is to adjust the expression conditions (temperature and IPTG concentration) to slow the expression of the heterologous protein (W. Lee, Park, Lee, Park, & Seo, 2005).

Growth temperature was varied from 37°C to room temperature (23°C), and IPTG concentration was varied from 1.0 mM to 0.01 mM in a series of optimization experiments. The gel in Figure 4.5 is identical to the gel in Figure 4.4, but was run with fractionated protein from *E. coli* cells expressing the CHMO at 30°C, induced with 0.01 mM IPTG. It can clearly be seen that less overall CHMO protein is produced by the later timepoints under these conditions than at 37°C and 1.0 mM IPTG. On close inspection,

it can also be seen that there is some CHMO protein present in the soluble fraction here, along with some in the insoluble fraction. A group of these SDS-PAGE gels was used to identify improved expression conditions, and subsequent activity assays narrowed down the most appropriate conditions to room temperature and 0.1 mM IPTG (Lee, et al. (2005) reported 25°C and 0.01 mM IPTG as the best conditions for their recombinant CHMO). *Polaromonas* sp. strain JS666 grows best between 20°C and 25°C, with no detectable growth at 30°C or above, so it makes sense that the CHMO from strain JS666 would exhibit optimum activity at room temperature. Results achieved with the expression system at these optimized conditions are discussed below.

Following the work of Lee, et al. (2005), it was also discovered that actively growing cells had higher activity than resting cells, so the method described above was modified to eliminate the KP buffer resuspension step. Instead, 4 mL of the actively growing culture (in LB broth with ampicillin) was sealed in the serum bottles with the substrate two hours after induction with IPTG (which occurred once an OD_{600} of 0.5-0.7 had been reached).

Assessment of Alkene Oxidation

Once expression conditions that yielded soluble protein were finally discovered, our cyclohexanone monooxygenase expression system achieved success in oxidizing cyclohexanone, the natural (expected) substrate of the CHMO, to ε-caprolactone. This proved that strain JS666's CHMO was not only soluble in the cytoplasm of its *E. coli* host, but also active. Representative resting cell results for this oxidation can be seen in Figure 4.7. Given an initial 10 mM cyclohexanone concentration, approximately 0.5 mM of caprolactone was accumulated in the reaction medium after 18 hours, 80% of which was produced in the first three hours. An approximate maximum enzyme activity from this data is a 0.004 mM increase in caprolactone concentration per minute by the 4 mL of

growing cells in the reaction bottle, or 16 nmoles/mL-min (the protein concentration varied over the course of each reaction, and the whole cell extracts would contain many non-CHMO proteins, so a specific activity could not be calculated). This yield could probably be improved through further optimization of reaction conditions and elimination of more insoluble protein aggregates, but was enough to demonstrate that the CHMO from strain JS666 was active in its *E. coli* host. A reliably detectable protein activity was sufficient for our studies with the CHMO expression system, but future use of this system in biocatalysis applications would likely require more optimization to achieve its highest potential activity.

Under conditions in which the heterologously-expressed *Polaromonas* CHMO readily converted cyclohexanone to ε-caprolactone, no activity was observed with either ethene or cDCE. This result suggested the need to reevaluate our past hypotheses about the initial enzymatic attack on ethene and cDCE in strain JS666. A recent report of cDCE oxidation by strain JS666's P450 monooxygenase confirms that our focus on the CHMO's possible involvement in alkene oxidation was incorrect (Shin, 2010). However, the discovery that strain JS666's CHMO is not involved in cDCE or ethene oxidation allows new interpretation of the results discussed in Chapter III. The observed upregulation of the CHMO gene during cDCE degradation may be a result of regulatory linkage with an adjacent gene encoding a putative epoxide hydrolase, which has been proposed to act on 2,3-dichlorooxirane (cDCE epoxide) during cDCE assimilation (Jennings et al., 2009). The upregulation of this putative hydrolase gene in response to cDCE has also been confirmed by microarray (Jennings et al., 2009) and proteomics (Alexander & Mattes, Unpublished data). It is also possible that the upregulation occurs because the CHMO itself serves a beneficial purpose when the cell is confronted with a mixture of xenobiotic compounds including cDCE. Future investigations into cDCE oxidation in strain JS666 will likely focus on downstream processing of the product(s) of

the P450 monooxygenase, including the potential role of the CHMO operon-encoded epoxide hydrolase.

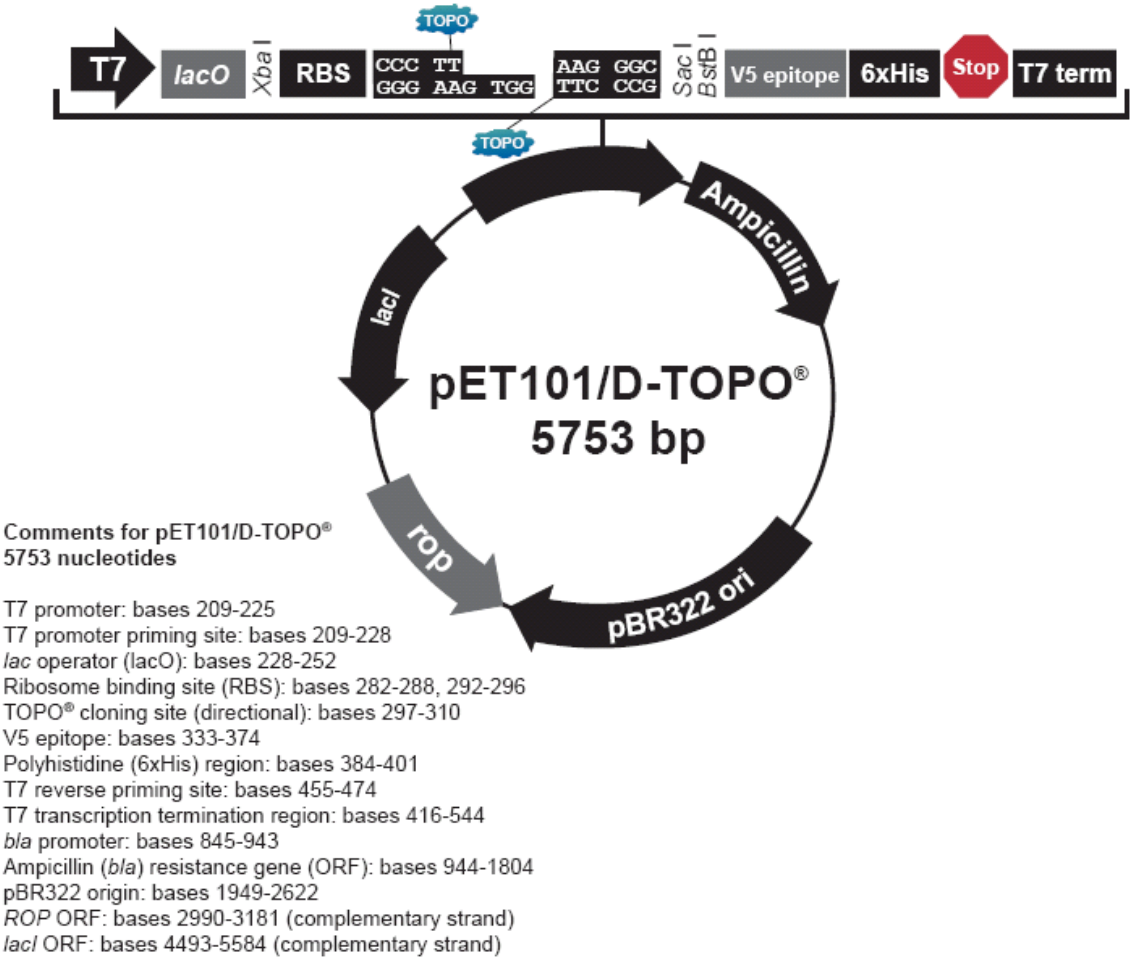

Comments for pET101/D-TOPO®
5753 nucleotides

T7 promoter: bases 209-225
T7 promoter priming site: bases 209-228
lac operator (lacO): bases 228-252
Ribosome binding site (RBS): bases 282-288, 292-296
TOPO® cloning site (directional): bases 297-310
V5 epitope: bases 333-374
Polyhistidine (6xHis) region: bases 384-401
T7 reverse priming site: bases 455-474
T7 transcription termination region: bases 416-544
bla promoter: bases 845-943
Ampicillin (*bla*) resistance gene (ORF): bases 944-1804
pBR322 origin: bases 1949-2622
ROP ORF: bases 2990-3181 (complementary strand)
lacI ORF: bases 4493-5584 (complementary strand)

Figure 4.1. pET101/D-TOPO vector map (Invitrogen, 2010b).

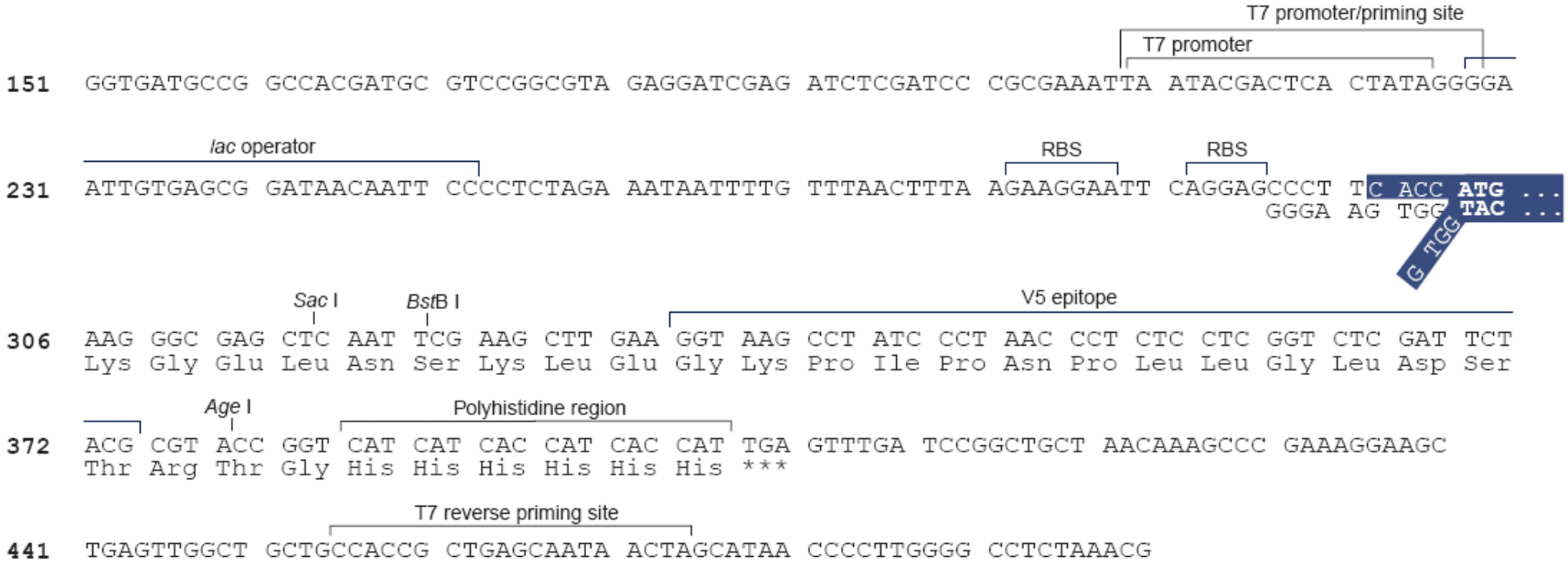

Figure 4.2. pET101/D-TOPO vector sequence near the gene insertion site (Invitrogen, 2010a).
The base pairs highlighted in blue represent the beginning of the cloned gene (ATG = start codon).
T7 priming sites: Recognized by T7 primers for sequencing of the gene insert
RBS: Ribosomal binding site
T7 promoter: Strong promoter recognized by T7 RNA Polymerase (produced by expression host)
V5 epitope, Polyhistidine region: Protein fusion tags not translated in the JS666 CHMO vector due to the inclusion of the native stop codon in the cloned gene sequence.

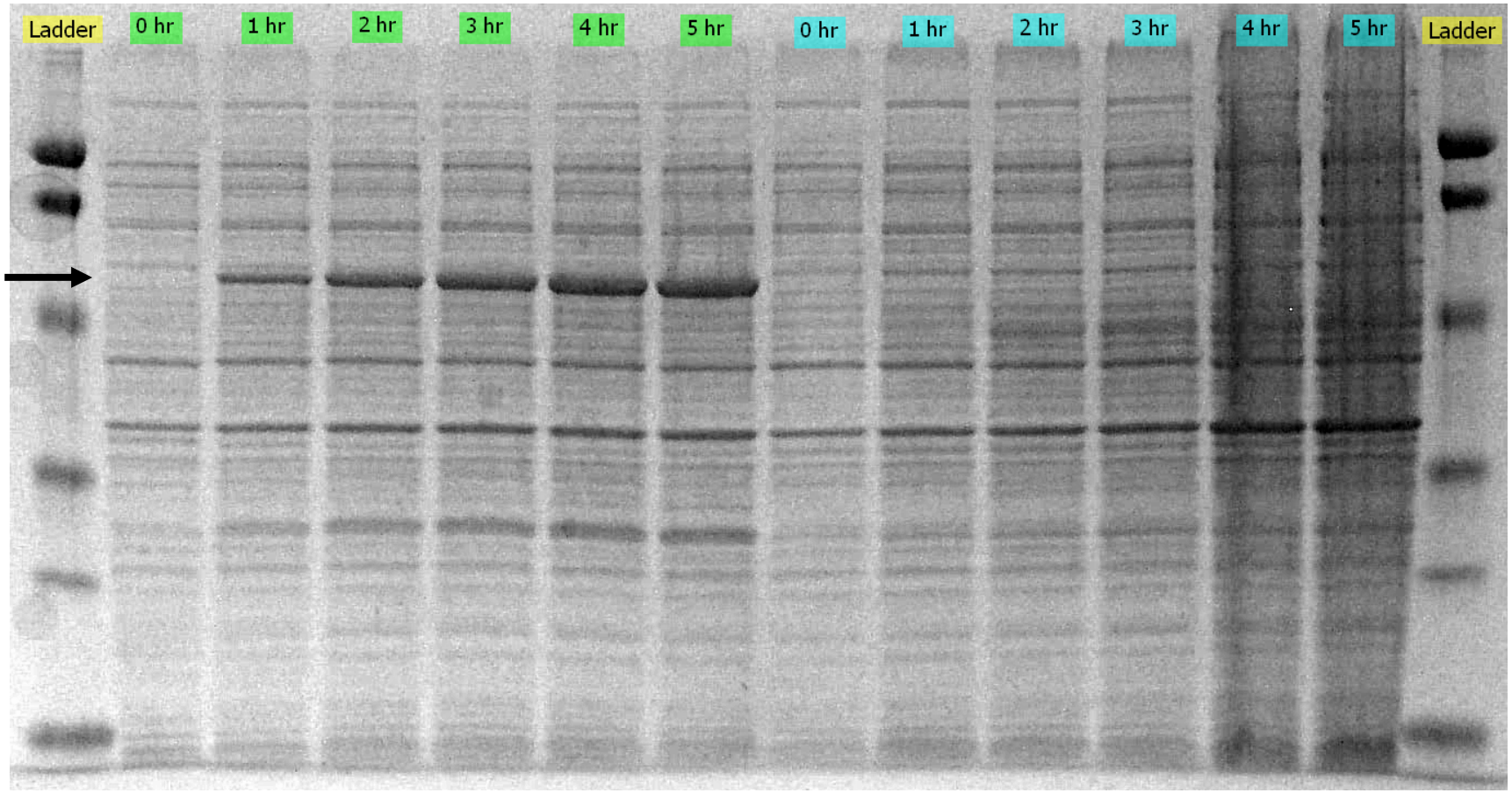

Figure 4.3. SDS-PAGE gel with total protein extracts from *E. coli* BL21 Star (DE3) cultures containing the JS666 CHMO pET101 vector. Lane labels (hours) denote time from induction with 1 mM IPTG.
Ladder: DNA size reference ladder
Green-labeled lanes (left half) are extracts from induced cultures.
Blue-labeled lanes (right half) are extracts from uninduced cultures.
The arrow marks the expected size (~60 kDa) of the CHMO protein.

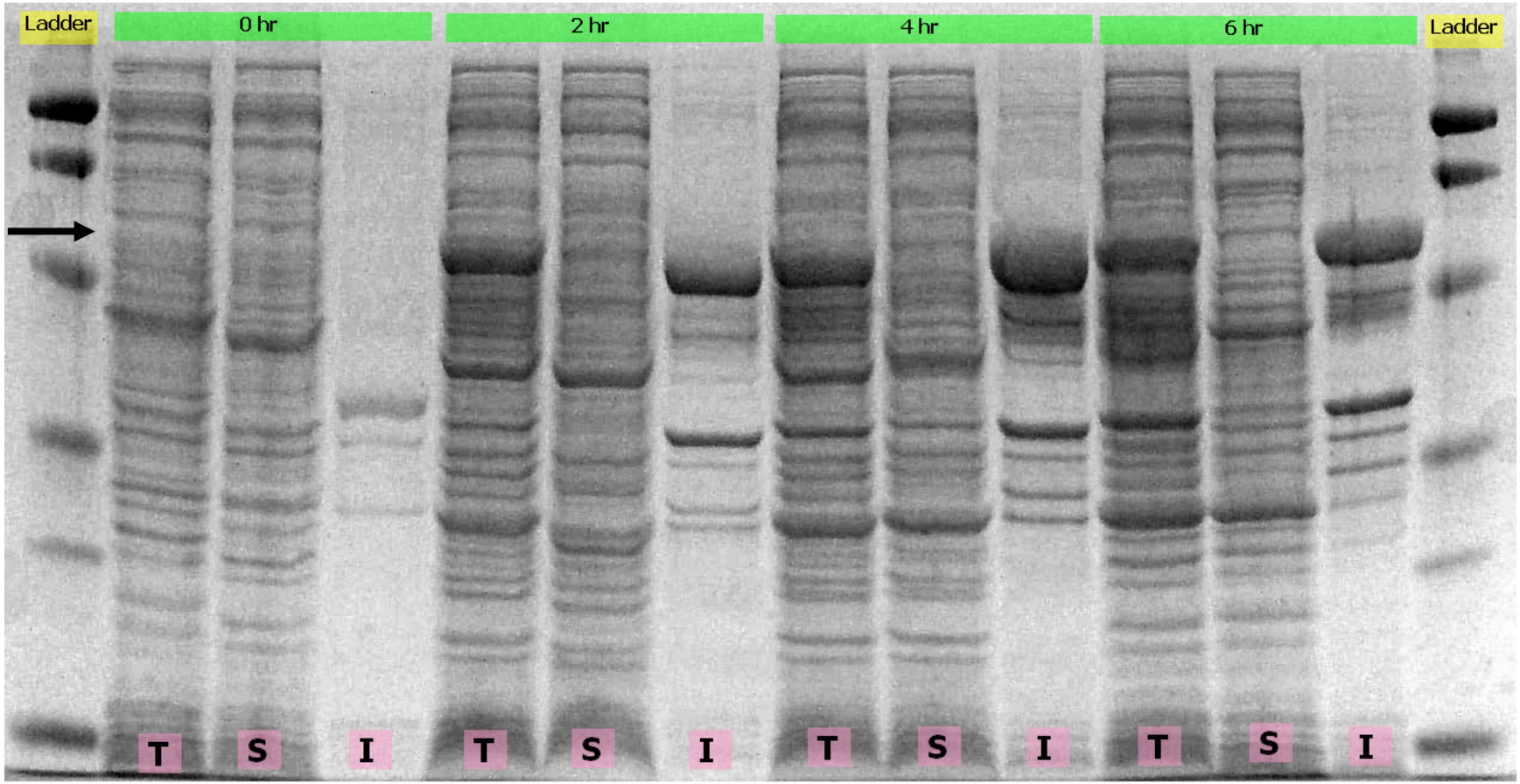

Figure 4.4. SDS-PAGE gel with fractionated protein extracts from *E. coli* BL21 Star (DE3) cultures containing the JS666 CHMO pET101 vector, grown at 37°C and induced with 1.0 mM IPTG. Time labels denote time from induction; "T" lanes contain the total protein extract, "S" lanes contain the soluble protein fraction, and "I" lanes contain the insoluble protein fraction.

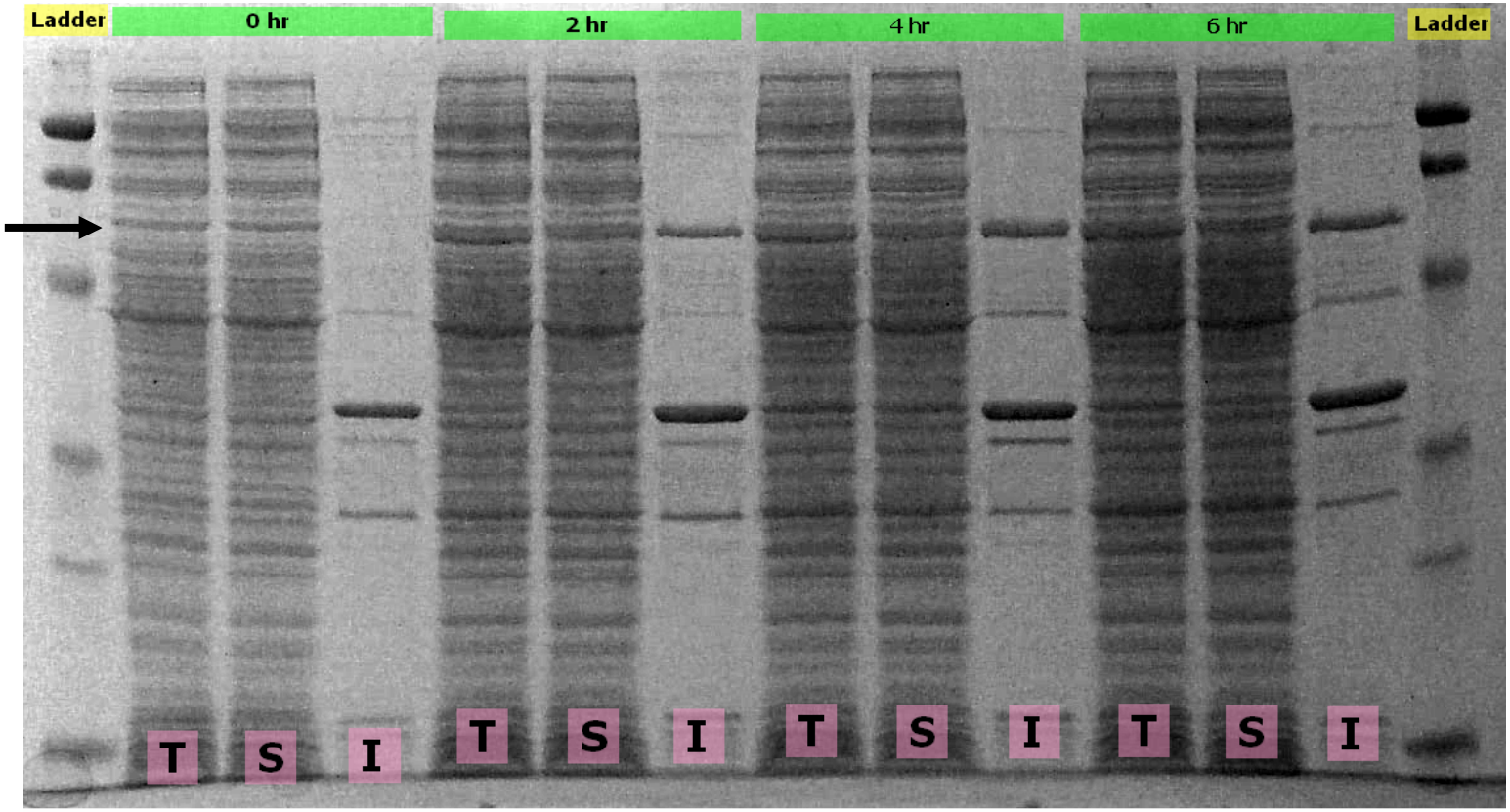

Figure 4.5. SDS-PAGE gel with fractionated protein extracts from *E. coli* BL21 Star (DE3) cultures containing the JS666 CHMO pET101 vector, grown at 30°C and induced with 0.01 mM IPTG. Time labels denote time from induction; "T" lanes contain the total protein extract, "S" lanes contain the soluble protein fraction, and "I" lanes contain the insoluble protein fraction.

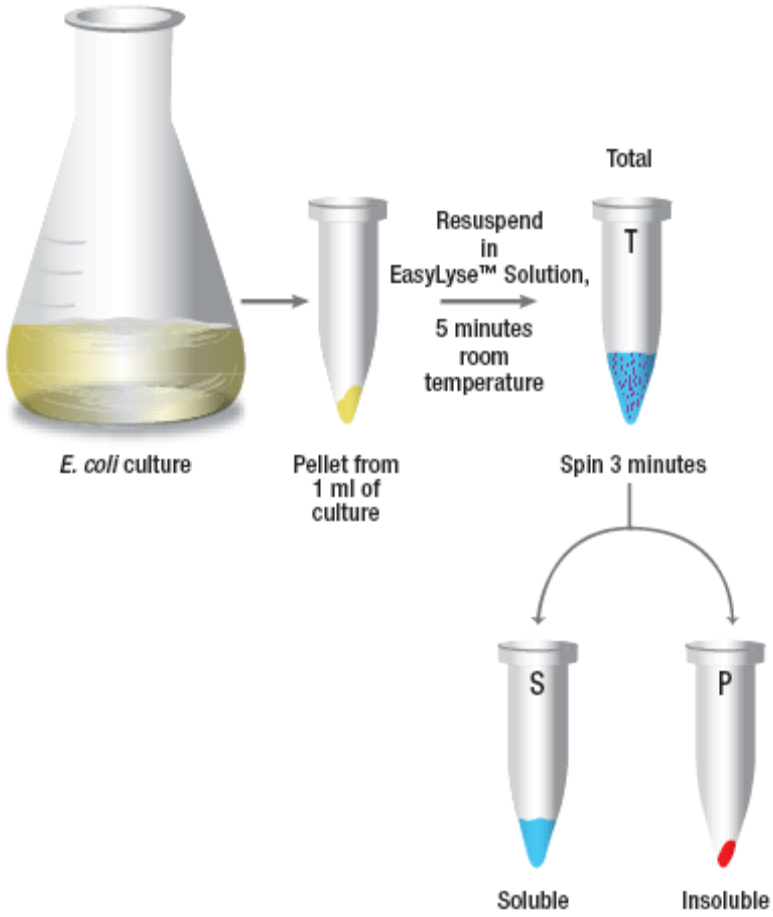

Figure 4.6. Illustration of solubility testing procedure using EasyLyse Bacterial Protein Extraction Solution (Burns, 2004).
"Total" protein fraction is removed from the "T" tube,
"Soluble" protein fraction is removed from the "S" (supernatant) tube, and
"Insoluble" protein fraction is removed from the "P" (pellet) tube.

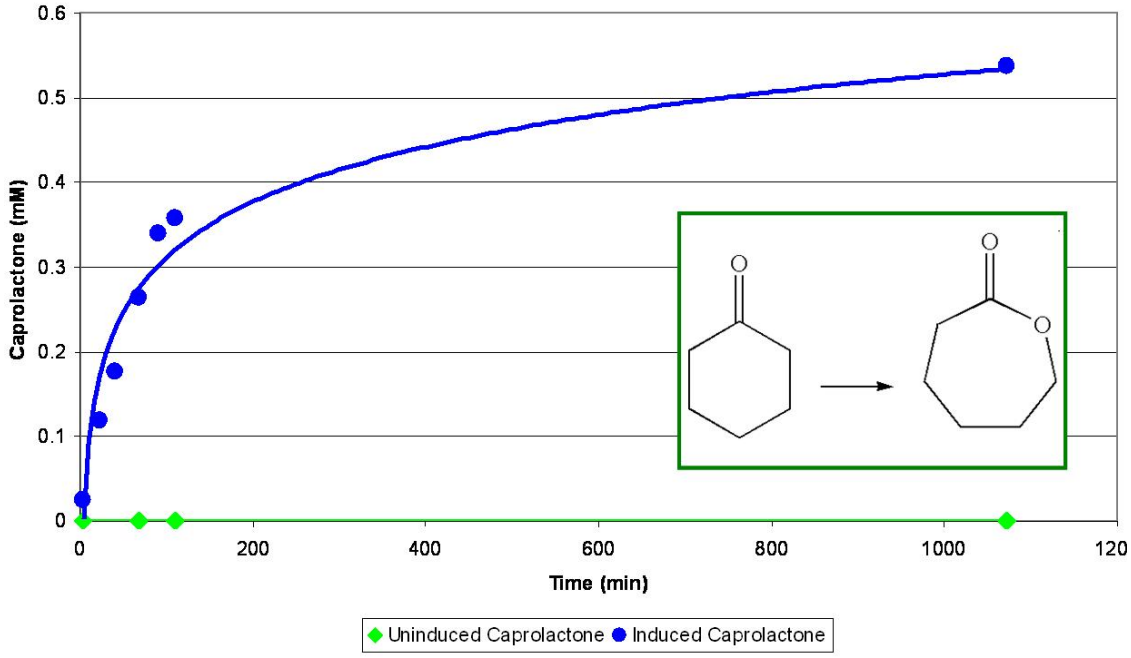

Figure 4.7. Production of caprolactone from 10 mM cyclohexanone by *E. coli* resting cells expressing the JS666 CHMO. Induced cells (blue) can catalyze the reaction, while uninduced cells (green) cannot.

CHAPTER V

BIOCATALYTIC PRODUCTION OF CHIRAL LACTONES

Background

Cyclohexanone monooxygenases (CHMOs) are a subset of the family of enzymes known as Baeyer-Villiger monooxygenases (BVMOs; E.C. 1.4.13.22), so named because they perform the classical Baeyer-Villiger oxidation illustrated in Figure 5.1. BVMOs are the focus of a significant amount of research in the field of oxidative biocatalysis, and some are already in industrial use today (Kamerbeek et al., 2003). Enzymatic Baeyer-Villiger oxidations have several advantages over their traditional chemical counterparts; namely, they can achieve greater regio- and enantioselectivity while avoiding the use of hazardous organic peracids and organometallic catalysts (Mirza et al., 2009). They also can catalyze oxidations at benign temperatures and neutral pH, making them a sustainable alternative to energy-intensive chemical oxidations, which frequently require high temperatures and extremes in pH, as well as multiple protection and deprotection steps to avoid undesired oxidations (Kamerbeek et al., 2003; Thomas et al., 2002). Baeyer-Villiger monooxygenases have been a popular target of study over the last few decades because of their versatility and enantiopure production of chiral lactones, which are valuable building blocks in the pharmaceutical industry (Alphand, Carrea, Wohlgemuth, Furstoss, & Woodley, 2003).

The CHMO found in *Acinetobacter* sp. NCIMB 9871 is the most extensively-researched enzyme in this group, and has exhibited activity on over 100 ketone substrates (Li et al., 2002). Novel CHMOs have been discovered and characterized more recently through genome mining and heterologous expression; this increased enzyme availability has provided opportunities to discover diverse activities and selectivities and to explore

the effects of changes in particular regions of the protein sequence (Kyte et al., 2004; Szolkowy, Eltis, Bruce, & Grogan, 2009). Investigations into CHMO sequence/function relationships have been made more fruitful with the fairly recent publication of the first CHMO crystal structure (of the CHMO from *Rhodococcus* sp. strain HI-31) (Mirza et al., 2009). Analysis of this crystal structure identified FAD- and $NADP^+$-binding domains, which were expected for this type of monooxygenase, and also identified amino acid residues that make up the predicted substrate binding pocket of the enzyme (Mirza et al., 2009). One unique characteristic of the CHMO substrate binding pocket is the presence of a flexible, solvent-exposed loop (approx. 18 amino acid residues) that has a defined structure only when a substrate is bound. The authors hypothesized that the flexible nature of this segment contributes to the wide variety of CHMO substrates by adjusting its "closed" structure to accommodate compounds of various shapes and sizes (Mirza et al., 2009).

Our expression system for the CHMO from *Polaromonas* sp. strain JS666 is a novel addition to the group of heterologously expressed CHMOs due to the xenobiotic degradation abilities of its host strain and the unusual location of the CHMO gene on a plasmid. The CHMOs that have been studied so far show a variety of substrate acceptance and enantioselectivity profiles (Kyte et al., 2004), so our new expression system is likely to shed light on new substrates and enantioselectivities, or at least provide more information for protein sequence/function interpretation. Protein sequence alignment was performed with all sequenced, heterologously expressed CHMOs, including strain JS666's, to look for associations between key amino acid residue changes and differences in enantioselectivity. This alignment also permitted the construction of a phylogenetic tree illustrating the perceived evolutionary distance between various CHMO enzymes. Most strains with a sequenced and heterologously expressed CHMO did not have an available 16S rRNA sequence, so a proper bacterial strain phylogenetic tree could not be constructed for comparison. Significant differences between a 16S-based

tree and a CHMO-based tree could indicate that horizontal gene transfer had contributed to the distribution of CHMO genes in the environment.

Four model 2-substituted cyclohexanones (2-methyl-, 2-ethyl-, 2-allyl-, and 2-phenyl-cyclohexanone) were chosen to provide an initial investigation into the enantioselectivity of the CHMO from *Polaromonas* strain JS666. These four compounds were selected because they are structurally simple (with only one chiral center), they are closely related to a compound for which the enzyme already had demonstrated activity (cyclohexanone), they have been studied with almost all previously expressed CHMOs so results can be directly compared among species, and they exist in racemic mixtures, allowing an investigation of kinetic resolution by the CHMO enzyme. The varying side-group size also provided a framework with which to evaluate the impact of steric forces on enantioselectivity. The *E. coli* expression system described in Chapter IV was necessary for this work because products of CHMO oxidation in strain JS666 cells would be consumed by downstream reactions.

Materials and Methods

Expression Conditions

The expression conditions for this heterologous system were as described in Chapter IV, after optimization for the production of soluble protein. In short, a freshly-transformed overnight culture was inoculated at 1% (v/v) in LB broth with 200 μg/mL ampicillin to begin each expression assay. Cultures were grown at 23 ± 1°C (room temperature) with shaking at 200 rpm until an OD_{600} of 0.5-0.7 was reached, at which point they were induced with 0.1 mM (final concentration) isopropyl β-D-1-thiogalactopyranoside (IPTG) and transferred to 20 mL glass serum bottles sealed with

PTFE-coated rubber septa (4 mL per bottle). The ketone substrates were dissolved in ethanol and added to a final concentration of 2.5 mM (1% ethanol v/v) two hours post-induction.

E. coli cells containing plasmid pMM4 (encoding the *Acinetobacter* NCIMB 9871 CHMO) were provided by Dr. Marko Mihovilovic of the Technical University in Vienna. These cells were cultured and induced in the same way as the JS666 CHMO expression system, and were presented with the same four 2-substituted cyclohexanones. Since the enantiomer preference of the *Acinetobacter* CHMO is known for these ketones, these cultures were used to provide confirmation of enantiomer identity in GC analysis.

Analytical Methods

At selected time points (up to ~24 hours), 0.5 mL of culture medium was extracted with 0.5 mL ethyl acetate plus 1 g/L methyl benzoate as internal standard. The organic phase was separated by centrifugation and dried over 0.05 g $MgSO_4$, then analyzed by chiral GC with an Agilent 6897N gas chromatograph fitted with a Cyclodextrin E column (Solutions and Tools GmbH, 25m x 0.25mm x 0.125 μm), flame ionization detector (FID), and H_2 carrier gas. Expected lactone peaks were identified through *meta*-chloroperbenzoic acid (*m*CPBA) oxidation of the racemic ketones, using a biphasic reaction protocol adapted from Mohan and Whalen (1993). 10 mL of dichloromethane with 1 g/L methyl benzoate as internal standard was stirred in an ice bath with 20 mL aqueous 10% sodium carbonate and 0.09 mmoles of the ketone, as 20 mL dichloromethane (with 1 g/L methyl benzoate) containing 1.5 mmoles *m*CPBA was added dropwise. Following this addition, the mixture was stirred overnight in the ice bath. 2 mL of the organic layer was then removed and washed with 10% aqueous sodium carbonate (5 x 2 mL), then saturated aqueous sodium chloride solution (1 x 1 mL). 0.4 mL of the remaining organic layer was transferred to an autosampler vial and dried over

50 mg anhydrous magnesium sulfate. This diluted, dropwise addition method was designed for safe use of the highly reactive *m*CPBA, and the many sodium carbonate washing steps were included to neutralize any remaining *m*CPBA in the reaction mixture (to avoid introducing it to the chiral GC column). The sodium chloride and magnesium sulfate steps were included to remove water from the organic layer, because water can damage a highly sensitive chiral GC column.

GC peak area was correlated with ketone concentrations, but could not reliably be done for lactone products, given the highly variable yields from the biphasic oxidation protocol. GC temperature programs and carrier gas flow rates were adjusted to provide clear resolution of both ketone and lactone enantiomers; run times were between 30 and 45 minutes.

Enantioselectivity values were calculated using *Selectivity* software (Faber, Hönig, & Kleewein, 1994). This software makes use of the equations developed by Charles Sih to describe enantioselectivity during the kinetic resolution of a racemic mixture of enantiomers (Chen, Fujimoto, Girdaukas, & Sih, 1982). These equations permit the calculation of the enantioselectivity, E, which is the ratio of the specificity constants for the fast- and slow-reacting enantiomers.

$$E = \frac{V_A / K_A}{V_B / K_B}$$ where V and K are the maximal velocities and Michaelis constants of the fast (A) and slow (B) -reacting enantiomers, respectively

$$\frac{V_A / K_A}{V_B / K_B} = \frac{\ln[(1 - c)(1 - ee\{S\})]}{\ln[(1 - c)(1 + ee\{S\})]}$$ where c is the extent of conversion and ee(S) is the enantiomeric excess of the recovered substrate fraction

$$c = 1 - [(A + B) / (A_0 + B_0)]$$ where A and B are the two substrate enantiomers

$$ee(S) = (B - A) / (A + B)$$

To calculate E, only the extent of conversion (c) and the amounts of remaining substrate enantiomers must be known. This is ideal for our system, given that absolute

quantification of the product enantiomers was not possible. Enantioselectivity (E) values can be compared among different biocatalysts, regardless of overall reaction rate and absolute substrate concentrations. Differences in E values greater than 200 are not statistically significant, and are generally reported as E > 200.

Amino acid sequence alignment of heterologously expressed CHMOs and phylogenetic tree calculation were conducted in the MEGA4 program, using the neighbor-joining method (Tamura, Dudley, Nei, & Kumar, 2007).

Results and Discussion

Four 2-substituted cyclohexanones were chosen to examine the effect of side group size on yield and enantioselectivity, and to provide an initial basis of comparison of our new expression system with more thoroughly studied CHMOs. The expected kinetic resolution of these 2-substituted cyclohexanones is illustrated in Figure 5.2, and the results are summarized in Table 5.1. Figure 5.3 shows raw results for the oxidation of 2-methylcyclohexanone (which was not very well resolved) and 2-phenylcyclohexanone (which was highly resolved). The graphs in Figure 5.3 illustrate the simultaneous conversion of ketone to lactone and enrichment in specific enantiomers over time. As the side group size increased (from methyl to phenyl), the percent conversion from ketone to lactone in 24 hours decreased, and enantioselectivity was lowest for the fastest-reacting 2-methylcyclohexanone. Preference for the *(S)*-ketones (or *(R)*-ketones with higher-priority side groups) was consistent with the majority of previously studied CHMOs (Kyte et al., 2004; Mirza et al., 2009).

The lower enantioselectivity observed with 2-methylcyclohexanone (E = 7.5) was comparable to that of *Acinetobacter* NCIMB9871, *Xanthobacter flavus*, and other

CHMOs (Mirza et al., 2009; Rial, Cernuchova, van Beilen, & Mihovilovic, 2008); it is significantly exceeded (E > 200) by *Rhodococcus ruber* SC1, whose BVMO has been characterized as a cyclododecanone monooxygenase and does not group closely with the CHMOs (Kyte et al., 2004). The enantioselectivity of the JS666 CHMO toward 2-ethyl, 2-allyl, and 2-phenylcyclohexanone was extremely high; to our knowledge, it is the only CHMO to date that has exhibited E values greater than 200 for all three of these ketones. It is matched by *Rhodococcus* SC1 and *Acinetobacter* NCIMB9871 for 2-ethylcyclohexanone (Kyte et al., 2004), several species including *Acinetobacter* NCIMB9871 for 2-allylcyclohexanone (Kyte et al., 2004), and by *Xanthobacter flavus* for 2-phenylcyclohexanone (Rial et al., 2008).

The phylogenetic relationships of sequenced cyclohexanone monooxygenases whose activities have been verified through heterologous expression are shown in Figure 5.4. The CHMO from strain JS666 is most similar to the CHMO from *Brachymonas petroleovorans* (66% amino acid identity), and is also very close to the CHMOs from *Xanthobacter flavus* and *Acidovorax* sp. JS42; however, all enzymes in this tree are closely related. The *Polaromonas* JS666 CHMO has 62% amino acid identity with the well-studied *Acinetobacter* sp. NCIMB 9871 CHMO. All share the consensus $NADP^+$-binding motif and conserved substrate binding pocket residues identified by Mirza, et al. (2009), but there are differences in the "mobile loop" sequence hypothesized to flexibly close around the substrate in the binding pocket. (Figure 5.5) Variation in these residues is a possible source of diversity in substrate acceptance, and is a logical target of future research into CHMO substrate range and enzyme engineering. The *Polaromonas* sp. strain JS666 CHMO shares much of the sequence of this flexible loop with the other sequenced CHMOs, but has three glycine residues in places where most other enzymes have residues with larger side groups, such as glutamate, asparagine, and alanine. The size and identity of amino acid residues in this flexible portion of the protein may affect the substrate profile of each enzyme, since these residues are hypothesized to close

around the substrate in the binding pocket. Glycine has the smallest side group of any amino acid (-H), so more glycine residues in this region may allow the accommodation of larger substrates in the enzyme's binding pocket. Strain JS666's CHMO also is unique among all CHMOs characterized so far in that it has a tyrosine residue in the mobile loop region. Further in-depth work to correlate CHMO peptide sequence with substrate acceptance and/or enantiospecificity is needed to elucidate the effects of changes in these and other residues.

The newly expressed cyclohexanone monooxygenase from *Polaromonas* sp. strain JS666 is an intriguing target for further study in the field of novel and enantiospecific biooxidations, given its origin in a xenobiotic-degrading species and its high enantioselectivity with the compounds tested so far. This *E. coli*-based expression system and initial comparison to other CHMOs in the literature should facilitate future in-depth research into the potential applications of this enzyme. Specifically, this work indicates that the CHMO from strain JS666 should be tested for enantioselective oxidation of large and/or complex ketone substrates to take advantage of its potentially more sterically-accommodating substrate binding pocket.

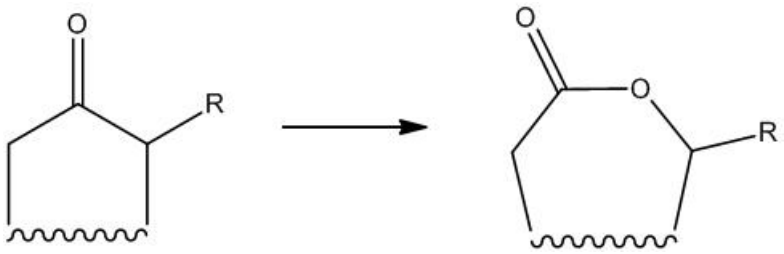

Figure 5.1. General Baeyer-Villiger reaction.

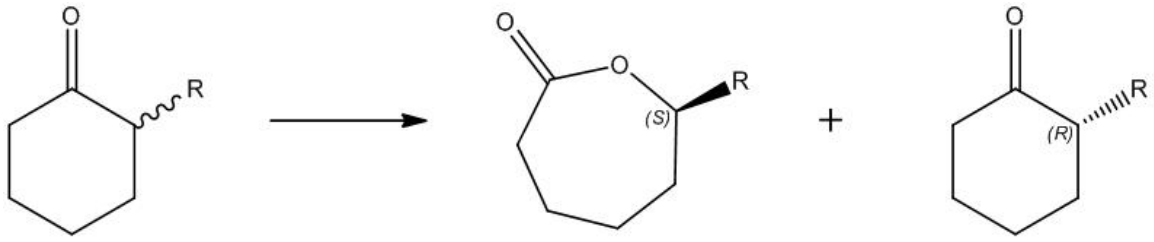

Figure 5.2. Kinetic resolution of 2-substituted cyclohexanones

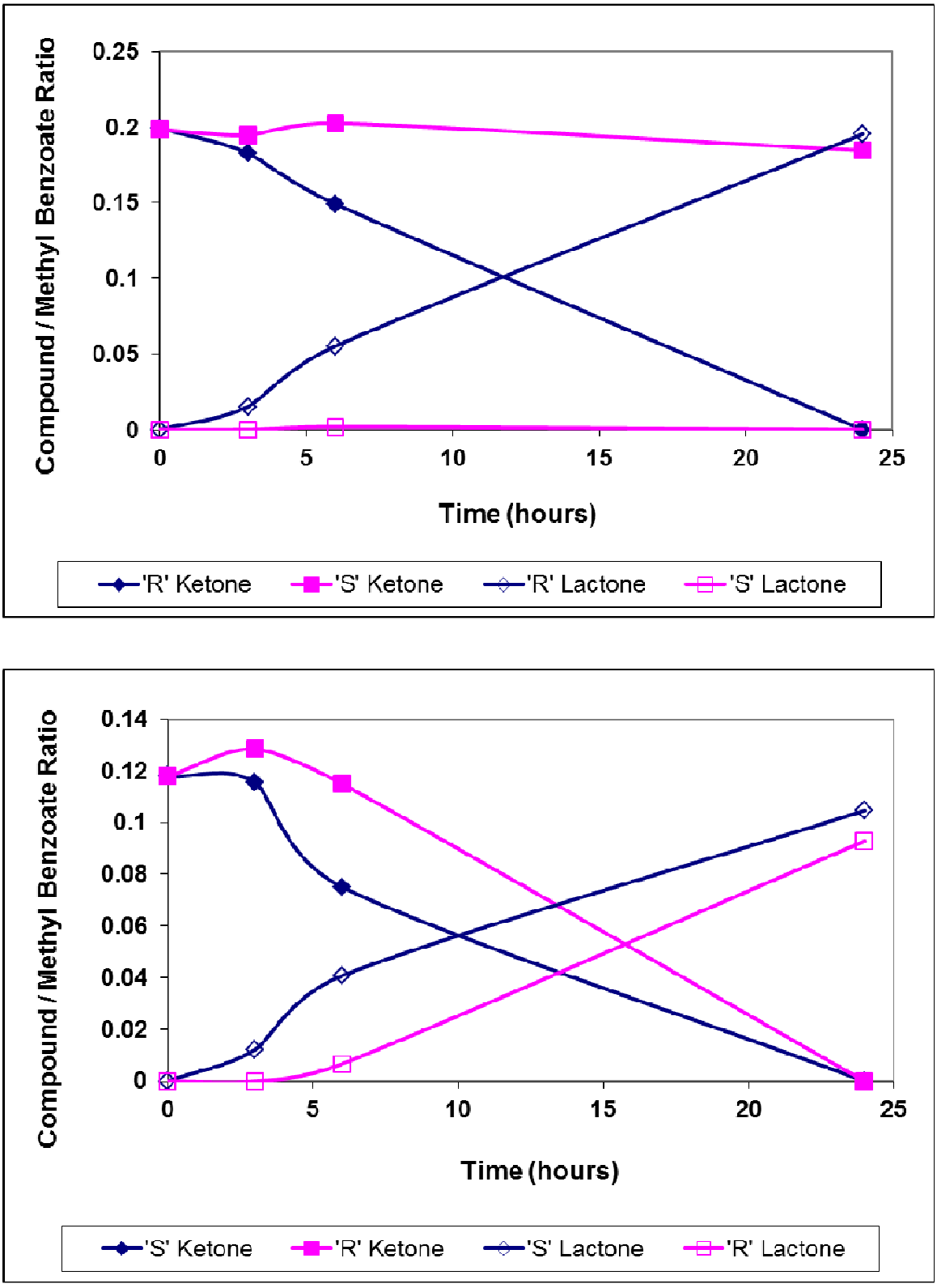

Figure 5.3. Kinetic resolution graphs for 2-phenylcyclohexanone (top) and 2-methylcyclohexanone (bottom)).

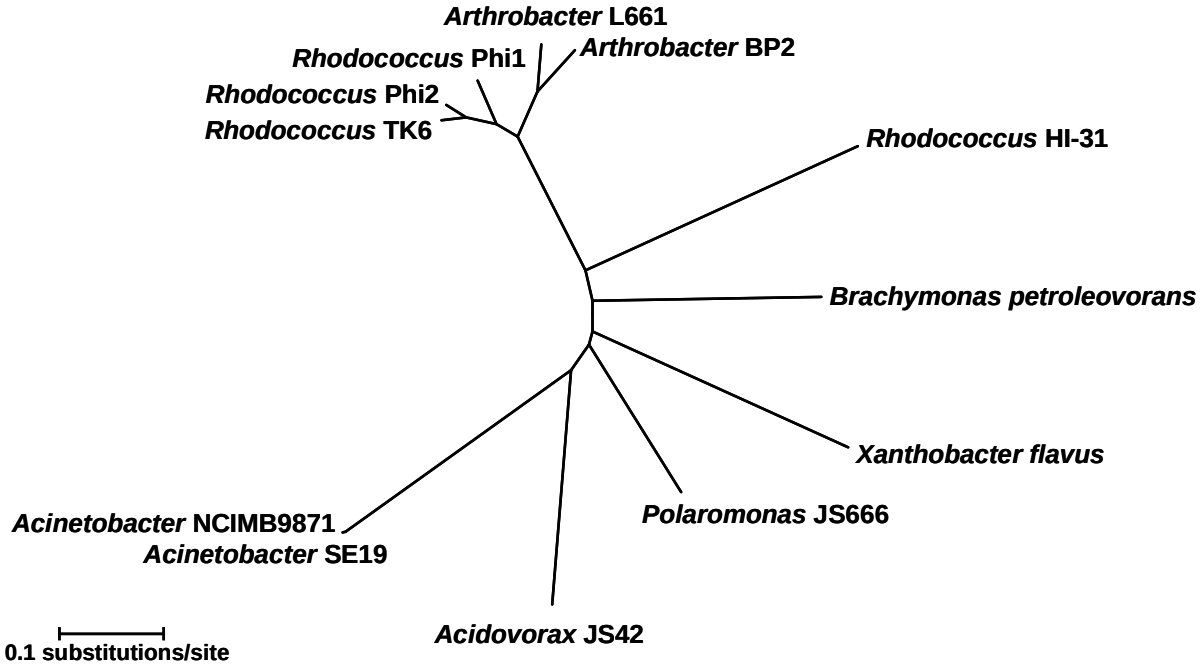

Figure 5.4. Phylogenetic relationships between CHMO protein sequences, where branch length is proportional to inferred evolutionary distance. Sequences were aligned over 512 positions using the neighbor-joining method and MEGA4 (Tamura et al., 2007). The JS666 CHMO has 539 residues.

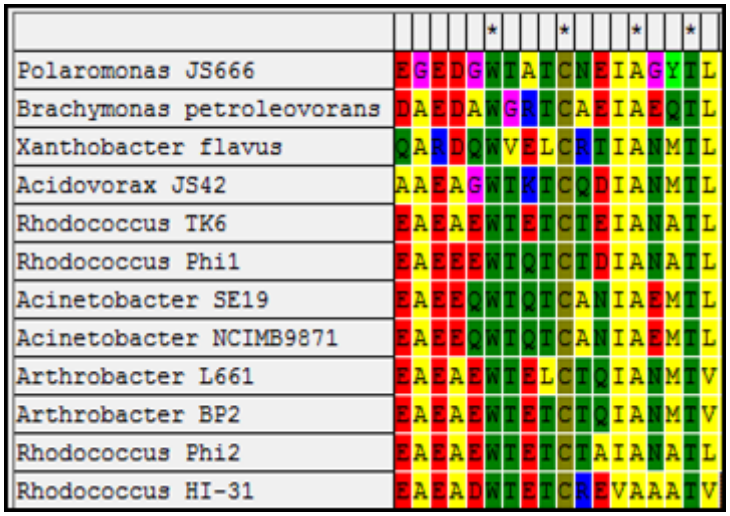

Figure 5.5. Alignment of flexible loop regions of characterized CHMOs, created in MEGA4 (Tamura et al., 2007).
Letters are standard amino acid abbreviations, and asterisks denote residues conserved across all strains.
The conserved "W" (tryptophan) residue is hypothesized to be an integral part of the substrate binding pocket when the flexible loop is in the closed position (Mirza et al., 2009).

Table 5.1. Kinetic resolution of 2-substituted cyclohexanones by the JS666 CHMO expressed in E. coli.

Side Group (R)	**% Conversion after 24 hours**	**Preferred Enantiomer[a]**	**Enantioselectivity "E"[b]**
None (-H)	100	N/A	N/A
Methyl ($-CH_3$)	100	S	7.5
Ethyl ($-CH_2CH_3$)	92	S	200
Allyl ($-CH_2CH=CH_2$)	75	R	200
Phenyl ($-C_6H_6$)	54	R	200

a) Note that the spatial orientation of the preferred enantiomer is the same for all substrates; the difference in nomenclature is due to a change in substituent priorities.

b) "E" values were calculated using enantiomeric excesses observed when substrate conversions were <50%, as required by Sih's kinetic resolution equations (Chen et al., 1982).

CHAPTER VI

CONCLUSIONS

Chapter II described proof-of-concept laboratory experiments that addressed Hypothesis #1: The genome of *Polaromonas* sp. strain JS666 can be used to predict its substrate range, efficiently adding to the collection of interesting enzymes that can be examined for use in bioremediation and biocatalysis.

This hypothesis was confirmed by results showing growth of strain JS666 on substrates predicted by genome analysis. Many of these compounds were xenobiotic in nature (e.g., *n*-octane, *n*-heptane, and chloroacetate), some were of interest for industrial biocatalysis (e.g., ferulate and cyclohexanol), and most would not have been suspected growth substrates without genome-based prediction techniques. While some predicted substrates were unable to support growth under laboratory conditions, the success rate was much greater than would have been achieved through a more traditional approach. Genome-based substrate prediction allows researchers to cast a wide net over a range of bacterial species to look for specific catalytic abilities, or to extensively investigate a single species to uncover many possible pathways, as was done in this study. It should be an important technique in future searches for biocatalysts and pollutant-degrading microbes, especially as the availability of sequenced genomes continues to grow.

Chapters III and IV addressed Hypothesis #2: Alkene oxidation activity observed in cDCE-grown JS666 cells is catalyzed by the cyclohexanone monooxygenase encoded by gene ABE47414.1 on plasmid pPol338.

Chapter III detailed the investigation into alkene oxidation by *Polaromonas* sp. strain JS666 using reverse transcriptase PCR, proteomics, and kinetic assays. The general conclusions drawn from this work were that strain JS666's plasmid-encoded cyclohexanone monooxygenase (CHMO) is upregulated in response to cDCE and

cyclohexanol exposure, and that these growth substrates promote ethene epoxidation. These conclusions provided the incentive for the construction of a heterologous CHMO expression system, which was described in Chapter IV. Our heterologous system was optimized to express an active CHMO enzyme, whose activity on cDCE and ethene was tested. This work proved that the CHMO was incapable of cDCE or ethene oxidation activity under conditions that promoted its activity on other substrates. A recently published dissertation corroborates this result, reporting cDCE degradation by strain JS666's P450 monooxygenase (Shin, 2010).

While Hypothesis #2 appears to have been disproven by this research, the results still provide some valuable insight. Cyclohexanol was discovered to promote ethene oxidation, and while we initially suspected that this was due to upregulation of the CHMO for its monooxygenase activity, it now seems more likely that growth on cyclohexanol improves the ethene oxidation rate because it also increases the expression of an epoxide hydrolase, co-regulated with the CHMO and possibly responsible for toxic chlorinated epoxide mediation. This epoxide hydrolase enzyme may be strain JS666's answer to the epoxide toxicity problem, analogous to the importance of CoM transferases in vinyl chloride assimilating microbes. Its function could be tested using heterologous expression and exposure to epoxyethane, or by assessing ethene oxidation activity in a JS666 strain with an epoxide hydrolase gene knockout.

Future research into cDCE degradation by *Polaromonas* sp. strain JS666 will focus on the various pathway possibilities downstream of the P450 monooxygenase, as the previously mentioned dissertation indicated that both cDCE epoxide and 1,1-dichloroacetaldehyde were produced by this enzyme (Shin, 2010). Our research suggests that epoxide hydration is important in cDCE degradation, but the preferred pathway may be highly dependent upon growth conditions. As discussed in Chapter III, dichotomous good and bad cDCE degradation behavior is observed in strain JS666; this may be indicative of two competing pathways for cDCE in the cell, with the dominant pathway

dependent on regulatory cues gleaned from previous growth substrates. More work is needed to determine the mechanism of cDCE degradation in contaminated environments, both to make informed use of strain JS666 in bioaugmentation and to assist in the search for other cDCE-degrading strains.

Another future direction of this research is sequence comparison of P450 monooxygenases. Many bacteria contain these enzymes, but so far, *Polaromonas* sp. strain JS666 is the only one to exhibit activity on cDCE. Protein alignment and 3D-modeling should be used to investigate possible changes in the P450 protein that allow this activity in strain JS666.

The work described in Chapter V tested Hypothesis #3: The plasmid-encoded cyclohexanone monooxygenase in *Polaromonas* sp. strain JS666 has enantioselective activity on industrially relevant compounds.

This hypothesis was confirmed when we observed very high enantioselectivity by our heterologously-expressed CHMO during kinetic resolution of several model 2-substituted cyclohexanones to their lactone products. Chiral lactones are valuable building blocks in the pharmaceutical industry, and since this CHMO was among the most enantioselective of those studied with these compounds, it holds promise for highly enantioselective behavior with more complex ketones, as well. The construction of this expression system also adds another active CHMO to the toolbox of enzymes being studied for use in biocatalysis, and contributes to the sequence/function information available for future application in rational enzyme design.

The discovery of enantioselective lactone production by our cyclohexanone monooxygenase expression system highlights the overlap between bioremediation research and biocatalyst discovery. Our work with the CHMO enzyme in strain JS666 was originally begun in order to learn more about its role in bioremediation of xenobiotic compounds, but led to valuable research results in the field of industrial biocatalysis. This is not unexpected, as both bioremediation and biocatalysis make use of xenobiotic-

degrading organisms and unique enzymes, but many studies in bioremediation do not venture into the possible application of the results to biocatalysis, and vice versa. Further integration of these two areas and recognition of shared goals will lead to beneficial discoveries in both disciplines, and improvement of environmental remediation and sustainable chemical production.

REFERENCES

Abe, Y., Aravena, R., Zopfi, J., Shouakar-Stash, O., Cox, E., Roberts, J. D., & Hunkeler, D. (2009). Carbon and chlorine isotope fractionation during aerobic oxidation and reductive dechlorination of vinyl chloride and *cis*-1,2-dichloroethene. *Environmental Science & Technology, 43*(1), 101-107.

Abrahamsson, K., Ekdahl, A., Collen, J., & Pedersen, M. (1995). Marine Algae-A Source of Trichloroethylene and Perchloroethylene. *Limnology and Oceanography, 40*(7), 1321-1326.

Alexander, A. K., & Mattes, T. E. (Unpublished data)

Alfreider, A., Vogt, C., & Babel, W. (2002). Microbial diversity in an in situ reactor system treating monochlorobenzene contaminated groundwater as revealed by 16S ribosomal DNA analysis. *Syst. Appl. Microbiol., 25*(2), 232-240.

Alphand, V., Carrea, G., Wohlgemuth, R., Furstoss, R., & Woodley, J. M. (2003). Towards large-scale synthetic applications of Baeyer-Villiger monooxygenases. *Trends in Biotechnology, 21*(7), 318.

Arciero, D., Vannelli, T., Logan, M., & Hopper, A. B. (1989). Degradation of trichloroethylene by the ammonia-oxidizing bacterium *Nitrosomonas europaea*. *Biochemical and Biophysical Research Communications, 159*(2), 640-643.

Arp, D., Sayavedra-Soto, L., & Hommes, N. (2002). Molecular biology and biochemistry of ammonia oxidation by *Nitrosomonas europaea*. *Archives of Microbiology, 178*(4), 250-255.

Balasundram, N., Sundram, K., & Samman, S. (2006). Phenolic compounds in plants and agri-industrial by-products: Antioxidant activity, occurrence, and potential uses. *Food Chemistry, 99*(1), 191-203.

Baneyx, F. (1999). Recombinant protein expression in *Escherichia coli*. *Current Opinion in Biotechnology, 10*(5), 411-421.

Bhatt, P., Kumar, M. S., Mudliar, S., & Chakrabarti, T. (2007). Biodegradation of Chlorinated Compounds--A Review. *Critical Reviews in Environmental Science and Technology, 37*(2), 165-198.

Bradley, P. M., & Chapelle, F. H. (2000). Aerobic microbial mineralization of dichloroethene as sole carbon source. *Environ. Sci. Technol., 34,* 221-223.

Brown, J. F., Bedard, D. L., Brennan, M. J., Carnahan, J. C., Feng, H., & Wagner, R. E. (1987). Polychlorinated Biphenyl Dechlorination in Aquatic Sediments. *Science, 236*(4802), 709-712.

Brzostowicz, P. C., Walters, D. M., Jackson, R. E., Halsey, K. H., Ni, H., & Rouviere, P. E. (2005). Proposed involvement of a soluble methane monooxygenase homologue in the cyclohexane-dependent growth of a new *Brachymonas* species. *Environ. Microbiol., 7*(2), 179-90.

Burns, C. M. (2004). A Rapid Method to Assess Protein Overproduction and Solubility in *E. coli* Using EasyLyse Bacterial Protein Extraction Solution. *EPICENTRE Forum, 11*(3), 6-7.

Bustin, S. A., Benes, V., Nolan, T., & Pfaffl, M. W. (2005). Quantitative real-time RT-PCR - a perspective. *Journal of Molecular Endocrinology, 34*(3), 597-601.

Carrea, G., Redigolo, B., Riva, S., Colonna, S., Gaggero, N., Battistel, E., & Bianchi, D. (1992). Effects of substrate structure on the enantioselectivity and stereochemical course of sulfoxidation catalyzed by cyclohexanone monooxygenase. *Tetrahedron: Asymmetry, 3*(8), 1063-1068.

Chain, P. S. G., Denef, V. J., Konstantinidis, K. T., Vergez, L. M., Agullo, L., Reyes, V. L., Hauser, L., Cordova, M., Gomez, L., Gonzalez, M., Land, M., Lao, V., Larimer, F., LiPuma, J. J., Mahenthiralingam, E., Malfatti, S. A., Marx, C. J., Parnell, J. J., Ramette, A., Richardson, P., Seeger, M., Smith, D., Spilker, T., Sul, W. J., Tsoi, T. V., Ulrich, L. E., Zhulin, I. B., & Tiedje, J. M. (2006). Inaugural Article: *Burkholderia xenovorans* LB400 harbors a multi-replicon, 9.73-Mbp genome shaped for versatility. *PNAS, 103*(42), 15280-15287.

Chartrand, M. M., Waller, A., Mattes, T. E., Elsner, M., Lacrampe-Couloume, G., Gossett, J. M., Edwards, E. A., & Lollar, B. S. (2005). Carbon isotopic fractionation during aerobic vinyl chloride degradation. *Environ Sci Technol, 39*(4), 1064-70.

Chen, C. S., Fujimoto, Y., Girdaukas, G., & Sih, C. J. (1982). Quantitative analyses of biochemical kinetic resolutions of enantiomers. *Journal of the American Chemical Society, 104*(25), 7294-7299.

Cheng, Q., Thomas, S. M., Kostichka, K., Valentine, J. R., & Nagarajan, V. (2000). Genetic Analysis of a Gene Cluster for Cyclohexanol Oxidation in *Acinetobacter* sp. Strain SE19 by In Vitro Transposition. *The Journal of Bacteriology, 182*(17), 4744-4751.

Christ, J. A., Ramsburg, C. A., Abriola, L. M., Pennell, K. D., & Löffler, F. E. (2005). Coupling Aggressive Mass Removal with Microbial Reductive Dechlorination for Remediation of DNAPL Source Zones: A Review and Assessment. *Environmental Health Perspectives, 113*(4), pp. 465-477.

Chu, K., Mahendra, S., Song, D. L., Conrad, M. E., & Alvarez-Cohen, L. (2004). Stable carbon isotope fractionation during aerobic biodegradation of chlorinated ethenes. *Environmental Science and Technology, 38*(11), 3126-3130.

Chuang, A. S., & Mattes, T. E. (2007). Identification of polypeptides expressed in response to vinyl chloride, ethene, and epoxyethane in *Nocardioides* sp. strain JS614 by using peptide mass fingerprinting. *Appl. Environ. Microbiol., 73*(13), 4368-4372.

Cohen, M. L. (1992). Epidemiology of drug resistance: Implications for a post-antimicrobial era. *Science, 257*(5073), 1050-1055.

Coleman, N. V., Mattes, T. E., Gossett, J. M., & Spain, J. C. (2002a). Biodegradation of *cis*-dichloroethene as the sole carbon source by a beta-proteobacterium. *Appl. Environ. Microbiol., 68*(6), 2726-2730.

Coleman, N. V., Mattes, T. E., Gossett, J. M., & Spain, J. C. (2002b). Phylogenetic and kinetic diversity of aerobic vinyl chloride-assimilating bacteria from contaminated sites. *Appl. Environ. Microbiol., 68*(12), 6162-6171.

Coleman, N. V., & Spain, J. C. (2003). Distribution of the coenzyme M pathway of epoxide metabolism among ethene- and vinyl chloride-degrading *Mycobacterium* strains. *Appl. Environ. Microbiol., 69*(10), 6041-6046.

Coleman, N. V., Spain, J. C., & Duxbury, T. (2002). Evidence that RDX biodegradation by *Rhodococcus* strain DN22 is plasmid-borne and involves a cytochrome p-450. *J. Appl. Microbiol., 93*(3), 463-472.

Connon, S. A., Tovanabootr, A., Dolan, M., Vergin, K., Giovannoni, S. J., & Semprini, L. (2005). Bacterial community composition determined by culture-independent and -dependent methods during propane-stimulated bioremediation in trichloroethene-contaminated groundwater. *Environ. Microbiol., 7*(2), 165-178.

Danko, A. S., Luo, M., Bagwell, C. E., Brigmon, R. L., & Freedman, D. L. (2004). Involvement of linear plasmids in aerobic biodegradation of vinyl chloride. *Appl. Environ. Microbiol., 70*(10), 6092-6097.

de Bont, J. A. M. (1976). Oxidation of ethylene by soil bacteria. *Antonie Van Leeuwenhoek, 42*, 59-71.

De Wildeman, & Verstraete. (2003). The quest for microbial reductive dechlorination of C_2 to C_4 chloroalkanes is warranted. *Applied Microbiology and Biotechnology, 61*(2), 94-102.

DiStefano, T. D., Gossett, J. M., & Zinder, S. H. (1991). Reductive dechlorination of high concentrations of tetrachloroethene to ethene by an anaerobic enrichment culture in the absence of methanogenesis. *Appl.Environ.Microbiol., 57*(8), 2287-2292.

Distefano, T. D. (1999). The effect of tetrachloroethene on biological dechlorination of vinyl chloride: Potential implication for natural bioattenuation. *Water Research, 33*(7), 1688-1694.

Elango, V., Liggenstoffer, A., & Fathepure, B. (2006). Biodegradation of vinyl chloride and *cis*-dichloroethene by a *Ralstonia* sp. strain TRW-1. *Appl Microbiol Biotechnol, 72*(6), 1270.

Eleaume, H., & Jabbouri, S. (2004). Comparison of two standardisation methods in real-time quantitative RT-PCR to follow *Staphylococcus aureus* genes expression during in vitro growth. *Journal of Microbiological Methods, 59*(3), 363-370.

Ellis, L. B. M., Roe, D., & Wackett, L. P. (2006). The University of Minnesota Biocatalysis/Biodegradation Database: the first decade. *Nucl. Acids Res., 34*(Suppl 1), D517-521.

Elsner, M., Zwank, L., Hunkeler, D., & Schwarzenbach, R. P. (2005). A new concept linking observable stable isotope fractionation to transformation pathways of organic pollutants. *Environmental Science & Technology, 39*(18), 6896-6916.

Faber, K., Hönig, H., & Kleewein, A. (1994). *Selectivity*. http://borgc185.kfunigraz.ac.at./:

Fathepure, B. Z., Elango, V. K., Singh, H., & Bruner, M. A. (2005). Bioaugmentation potential of a vinyl chloride-assimilating *Mycobacterium* sp., isolated from a chloroethene-contaminated aquifer. *FEMS Microbiol. Lett., 248*(2), 227.

Fey, A., Eichler, S., Flavier, S., Christen, R., Hofle, M. G., & Guzman, C. A. (2004). Establishment of a real-time PCR-based approach for accurate quantification of bacterial RNA targets in water, using *Salmonella* as a model organism. *Appl. Environ. Microbiol., 70*(6), 3618-3623.

Freedman, D. L., & Gossett, J. M. (1989). Biological reductive dechlorination of tetrachloroethylene and trichloroethylene to ethylene under methanogenic conditions. *Appl. Environ. Microbiol., 55*, 2144-2151.

Gasson, M. J., Kitamura, Y., McLauchlan, W. R., Narbad, A., Parr, A. J., Parsons, E. L. H., Payne, J., Rhodes, M. J. ., & Walton, N. J. (1998). Metabolism of Ferulic Acid to Vanillin. *J. Biol. Chem., 273*(7), 4163-4170.

Gavaskar, A. R. (1999). Design and construction techniques for permeable reactive barriers. *Journal of Hazardous Materials, 68*(1-2), 41-71.

Giddings, C. G., Jennings, L. K., & Gossett, J. M. (2010). Microcosm Assessment of a DNA Probe Applied to Aerobic Degradation of cis-1,2-Dichloroethene by *Polaromonas* sp. Strain JS666. *Ground Water Monitoring & Remediation, 30*(2), 97-105.

Giddings, C. G. S., Liu, F., & Gossett, J. M. (2010). Microcosm Assessment of *Polaromonas* sp. JS666 as a Bioaugmentation Agent for Degradation of cis-1,2-dichloroethene in Aerobic, Subsurface Environments. *Ground Water Monitoring & Remediation, 30*(2), 106-113.

Gillam, E. M. (2005). Exploring the potential of xenobiotic-metabolising enzymes as biocatalysts: Evolving designer catalysts from polyfunctional cytochrome P450 enzymes. *Clinical and Experimental Pharmacology and Physiology, 32*(3), 147-152.

Gorontzy, T., Drzyzga, O., Kahl, M. W., Bruns-nagel, D., Breitung, J., von Loew, E., & Blotevogel, K. (1994). Microbial Degradation of Explosives and Related Compounds. *Critical Reviews in Microbiology, 20*(4), 265.

Grandel, S., & Dahmke, A. (2004). Monitored Natural Attenuation of Chlorinated Solvents: Assessment of Potential and Limitations. *Biodegradation, 15*(6), 371-386.

Gygi, S. P., Rochon, Y., Franza, B. R., & Aebersold, R. (1999). Correlation between Protein and mRNA Abundance in Yeast. *Molecular and Cellular Biology, 19*(3), 1720-1730.

Habets-Crützen, A. Q. H., Brink, L. E. S., van Ginkel, C. G., de Bont, J. A. M., & Tramper, J. (1984). Production of epoxides from gaseous alkenes by resting-cell suspensions and immobilized cells of alkene-utilizing bacteria. *Appl. Microbiol. Biotechnol., 20*, 245-250.

Habets-Crützen, A. Q. H., & de Bont, J. A. M. (1985). Inactivation of alkene oxidation by epoxides in alkene- and alkane-grown bacteria. *Appl. Microbiol. Biotechnol., 22*, 428-433.

Hartmans, S., & de Bont, J. A. M. (1992). Aerobic vinyl chloride metabolism in *Mycobacterium aurum* L1. *Appl. Environ. Microbiol., 58*, 1220-1226.

Hubner, A., Danganan, C. E., Xun, L., Chakrabarty, A. M., & Hendrickson, W. (1998). Genes for 2,4,5-trichlorophenoxyacetic acid metabolism in *Burkholderia cepacia* AC1100: Characterization of the *tftC* and *tftD* genes and locations of the *tft* operons on multiple replicons. *Appl.Environ.Microbiol., 64*(6), 2086-2093.

Hunkeler, D., Aravena, R., & Cox, E. (2002). Carbon isotopes as a tool to evaluate the origin and fate of vinyl chloride: Laboratory experiments and modeling of isotope evolution. *Environmental Science and Technology, 36*(15), 3378-3384.

Invitrogen. (2010a) *pET/D-TOPO Vector Polylinker*, from http://tools.invitrogen.com/content/sfs/vectors/pet101dtopo_mcs.pdf

Invitrogen. (2010b) *pET101/D-TOPO Vector Map*, from http://tools.invitrogen.com/content/sfs/vectors/pet101dtopo_map.pdf

Irgens, R. L., Gosink, J. J., & Staley, J. T. (1996). *Polaromonas vacuolata* gen. nov., sp. nov., a psychrophilic, marine, gas vacuolate bacterium from Antarctica. *Int. J. Syst. Bacteriol., 46*(3), 822-6.

Janssen, D. B., Pries, F., & Van der Ploeg, J. R. (1994). Genetics and biochemistry of dehalogenating enzymes. *Annu.Rev.Microbiol., 48*(1), 163-191.

Jennings, L. K., Chartrand, M. M. G., Lacrampe-Couloume, G., Lollar, B. S., Spain, J. C., & Gossett, J. M. (2009). Proteomic and transcriptomic analyses reveal genes upregulated by *cis*-dichloroethene in *Polaromonas* JS666. *Applied and Environmental Microbiology, 75*(11), 3733-3744.

Jeon, C. O., Park, W., Padmanabhan, P., DeRito, C., Snape, J. R., & Madsen, E. L. (2003). Discovery of a bacterium, with distinctive dioxygenase, that is responsible for in situ biodegradation in contaminated sediment. *Proc. Natl. Acad. Sci. USA, 100*(23), 13591-13596.

Jin, Y. O., & Mattes, T. E. (2008). Adaptation of aerobic, ethene-assimilating *Mycobacterium* strains to vinyl chloride as a growth substrate. *Environ.Sci.Technol., 42*(13), 4784-4789.

Johnson, D. R., Lee, P. K. H., Holmes, V. F., & Alvarez-Cohen, L. (2005). An internal reference technique for accurately quantifying specific mRNAs by real-time PCR with application to the *tceA* reductive dehalogenase gene. *Appl. Environ. Microbiol., 71*(7), 3866-3871.

Kalb, V. F.,and R.W.Bernlohr. (1977). A new spectrophotometric assay for protein in cell extracts. *Anal. Biochem., 82*, 362-371.

Kamerbeek, N. M., Janssen, D. B., van Berkel, W. J. H., & Fraaije, M. W. (2003). Baeyer-Villiger Monooxygenases, an Emerging Family of Flavin-Dependent Biocatalysts. *Adv. Synth. Catal.,* , 667-678.

Kampfer, P., Busse, H., & Falsen, E. (2006). *Polaromonas aquatica* sp. nov., isolated from tap water. *Int J Syst Evol Microbiol, 56*(3), 605-608.

Kane, J. F., & Hartley, D. L. (1988). Formation of recombinant protein inclusion bodies in *Escherichia coli*. *Trends in Biotechnology, 6*(5), 95-101.

Krum, J. G., & Ensign, S. A. (2001). Evidence that a linear megaplasmid encodes enzymes of aliphatic alkene and epoxide metabolism and coenzyme M (2-mercaptoethanesulfonate) biosynthesis in *Xanthobacter* strain Py2. *J. Bacteriol., 183*(7), 2172-7.

Küver, J., Xu, Y., & Gibson, J. (1995). Metabolism of cyclohexane carboxylic acid by the photosynthetic bacterium *Rhodopseudomonas palustris*. *Archives of Microbiology, 164*(5), 337-345.

Kyte, B. G., Rouvière, P., Cheng, Q., & Stewart, J. D. (2004). Assessing the Substrate Selectivities and Enantioselectivities of Eight Novel Baeyer-Villiger Monooxygenases toward Alkyl-Substituted Cyclohexanones. *The Journal of Organic Chemistry, 69*(1), 12-17.

Leak, D. J., Sheldon, R. A., Woodley, J. M., & Adlercreutz, P. (2009). Biocatalysts for selective introduction of oxygen. *Biocatalysis and Biotransformation, 27*(1), 1-26.

Lee, D. H., Kim, M. D., Lee, W. H., Kweon, D. H., & Seo, J. H. (2004). Consortium of fold-catalyzing proteins increases soluble expression of cyclohexanone monooxygenase in recombinant *Escherichia coli*. *Applied Microbiology and Biotechnology, 63*(5), 549-552.

Lee, P. K. H., Conrad, M. E., & Alvarez-Cohen, L. (2007). Stable carbon isotope fractionation of chloroethenes by dehalorespiring isolates. *Environmental Science & Technology, 41*(12), 4277-4285.

Lee, W., Park, Y., Lee, D., Park, K., & Seo, J. (2005). Simultaneous biocatalyst production and Baeyer-Villiger oxidation for bioconversion of cyclohexanone by recombinant *Escherichia coli* expressing cyclohexanone monooxygenase. *Applied Biochemistry and Biotechnology, 123*(1), 827-836.

Leisinger, T. (1983). General aspects: Microorganisms and xenobiotic compounds. *Cellular and Molecular Life Sciences, 39*(11), 1183-1191.

Lewis, D. F. V., & Wiseman, A. (2005). A selective review of bacterial forms of cytochrome P450 enzymes. *Enzyme and Microbial Technology, 36*(4), 377-384.

Li, Z., van Beilen, J. B., Duetz, W. A., Schmid, A., de Raadt, A., Griengl, H., & Witholt, B. (2002). Oxidative biotransformations using oxygenases. *Curr. Opin. Chem. Biol., 6*(2), 136-144.

Lipscomb, J. D. (1994). Biochemistry of the soluble methane monooxygenase. *Annu.Rev.Microbiol., 48*(1), 371-399.

Lloyd, J. R., Nolting, H. F., Sole, V. A., Bosecker, K., & Macaskie, L. E. (1998). Technetium Reduction and Precipitation by Sulfate-Reducing Bacteria. *Geomicrobiology Journal, 15*, 45-58.

Lorah, M. M., & Voytek, M. A. (2004). Degradation of 1,1,2,2-tetrachloroethane and accumulation of vinyl chloride in wetland sediment microcosms and in situ porewater: biogeochemical controls and associations with microbial communities. *Journal of Contaminant Hydrology, 70*(1-2), 117.

Louarn, E., Aulenta, F., Levantesi, C., Majone, M., & Tandoi, V. (2006). Modeling substrate interactions during aerobic biodegradation of mixtures of vinyl chloride and ethene. *Journal of Environmental Engineering, 132*(8), 940-948.

Lovley, D. R., & Phillips, E. J. (1992). Reduction of uranium by *Desulfovibrio desulfuricans*. *Applied and Environmental Microbiology, 58*(3), 850-856.

Loy, A., Beisker, W., & Meier, H. (2005). Diversity of Bacteria Growing in Natural Mineral Water after Bottling. *Applied and Environmental Microbiology, 71*(7), 3624.

Magic-Knezev, A., Wullings, B., & Van der Kooij, D. (2009). *Polaromonas* and *Hydrogenophaga* species are the predominant bacteria cultured from granular activated carbon filters in water treatment. *Journal of Applied Microbiology, 107*(5), 1457-1467.

Matrix Science. (2010). *MASCOT Peptide Mass Fingerprint*, from www.matrixscience.com

Mattes, T. E. (Unpublished data).

Mattes, T. E., Coleman, N. V., Gossett, J. M., & Spain, J. C. (2005). Physiological and molecular genetic analyses of vinyl chloride and ethene biodegradation in *Nocardioides* sp. strain JS614. *Arch. Microbiol., 183*, 95-106.

Mattes, T. E., Alexander, A. K., & Coleman, N. V. (2010). Aerobic biodegradation of the chloroethenes: pathways, enzymes, ecology, and evolution. *FEMS Microbiology Reviews, 34*(4), 445-475.

Mattes, T. E., Alexander, A. K., Richardson, P. M., Munk, A. C., Han, C. S., Stothard, P., & Coleman, N. V. (2008). The Genome of *Polaromonas* sp. Strain JS666: Insights into the Evolution of a Hydrocarbon- and Xenobiotic-Degrading Bacterium, and Features of Relevance to Biotechnology. *Applied and Environmental Microbiology, 74*(20), 6405-6416.

Mattes, T. E., Coleman, N. V., Chuang, A. S., Rogers, A. J., Spain, J. C., & Gossett, J. M. (2007). Mechanism controlling the extended lag period associated with vinyl chloride starvation in *Nocardioides* sp. strain JS614. *Arch. Microbiol., 187*(3), 217-226.

McCarty, P. L., Goltz, M. N., Hopkins, G. D., Dolan, M. E., Allan, J. P., Kawakami, B. T., & Carrothers, T. J. (1998). Full-scale evaluation of in situ cometabolic degradation of trichloroethylene in groundwater through toluene injection. *Environ. Sci. Technol., 32*, 88-100.

Meinhardt, F., Scharath, R., & Larsen, M. (1997). Microbial linear plasmids. *Appl Microbiol Biotechnol, 47*, 329-336.

Miroux, B., & Walker, J. E. (1996). Over-production of proteins in *Escherichia coli*: mutant hosts that allow synthesis of some membrane proteins and globular proteins at high levels. *J Mol Biol, 260*(3), 289-98.

Mirza, I. A., Yachnin, B. J., Wang, S., Grosse, S., Bergeron, H., Imura, A., Iwaki, H., Hasegawa, Y., Lau, P. C. K., & Berghuis, A. M. (2009). Crystal Structures of Cyclohexanone Monooxygenase Reveal Complex Domain Movements and a Sliding Cofactor. *Journal of the American Chemical Society, 131*(25), 8848-8854.

Myneni, S. C. B. (2002). Formation of Stable Chlorinated Hydrocarbons in Weathering Plant Material. *Science, 295*(5557), 1039-1041.

Osborne, T., Jamieson, H., Hudson-Edwards, K., Nordstrom, D. K., Walker, S., Ward, S., & Santini, J. (2010). Microbial oxidation of arsenite in a subarctic environment: diversity of arsenite oxidase genes and identification of a psychrotolerant arsenite oxidiser. *BMC Microbiology, 10*(1), 205.

Page, K. A., Connon, S. A., & Giovannoni, S. J. (2004). Representative Freshwater Bacterioplankton Isolated from Crater Lake, Oregon. *Applied and Environmental Microbiology, 70*(11), 6542.

Poelarands, G. J., Zandstra, M., Bosma, T., Kulakov, L. A., Larkin, M. J., Marchesi, J. R., Weightman, A. J., & Janssen, D. B. (2000). Haloalkane-utilizing *Rhodococcus* strains isolated from geographically distinct locations possess a highly conserved gene cluster encoding haloalkane catabolism. *J. Bacteriol., 182*(10), 2725-2731.

Polo, S., Guerini, O., Sosio, M., & Deho, G. (1998). Identification of two linear plasmids in the actinomycete *Planobispora rosea*. *Microbiology, 144*(10), 2819-2825.

Premier Biosoft International. (2010) *NetPrimer*, from http://www.premierbiosoft.com/netprimer/index.html

Pries, F., Wijngaard, A. J. v. d., Bos, R., Pentenga, M., & Janssen, D. B. (1994). The role of spontaneous cap domain mutations in haloalkane dehalogenase specificity and evolution. *J. Biol. Chem., 269*(26), 17490-17494.

Rial, D. V., Cernuchova, P., van Beilen, J. B., & Mihovilovic, M. D. (2008). Biocatalyst assessment of recombinant whole-cells expressing the Baeyer-Villiger monooxygenase from *Xanthobacter* sp. ZL5. *Journal of Molecular Catalysis B: Enzymatic, 50*(2-4), 61-68.

Rosazza, J. P. N., Huang, Z., Dostal, L., Volm, T., & Rousseau, B. (1995). Review: Biocatalytic transformations of ferulic acid: An abundant aromatic natural product. *Journal of Industrial Microbiology & Biotechnology, 15*(6), 457-471.

Rozen, S., & Skaletsky, H. J. (2000). Primer3 on the WWW for general users and for biologist programmers. In S. Krawetz, & S. Misener (Eds.), *Bioinformatics Methods and Protocols: Methods in Molecular Biology* (pp. 365-386). Totowa, NJ: Humana Press.

Saeki, H., Akira, M., Furuhashi, K., Averhoff, B., & Gottschalk, G. (1999). Degradation of trichloroethene by a linear-plasmid-encoded alkene monooxygenase in *Rhodococcus corallinus* (*Nocardia corallina*) B-276. *Microbiology, 145*(Pt 7), 1721-30.

Saeki, Y., & Emura, T. (2002). Technical progresses for PVC production. *Progress in Polymer Science, 27*(10), 2055-2131.

Seth-Smith, H. M. B., Rosser, S. J., Basran, A., Travis, E. R., Dabbs, E. R., Nicklin, S., & Bruce, N. C. (2002). Cloning, sequencing, and characterization of the hexahydro-1,3,5-trinitro-1,3,5-triazine degradation gene cluster from *Rhodococcus rhodochrous*. *Appl. Environ. Microbiol., 68*(10), 4764-4771.

Shin, K. (2010). *Biodegradation of diphenylamine and cis-dichloroethene.* (Ph.D., Georgia Institute of Technology).

Stecker, C., Johann, A., Herzberg, C., Averhoff, B., & Gottschalk, G. (2003). Complete nucleotide sequence and genetic organization of the 210-kilobase linear plasmid of *Rhodococcus erythropolis* BD2. *J. Bacteriol., 185*(17), 5269-5274.

Steele, H. L., & Streit, W. R. (2005). Metagenomics: Advances in ecology and biotechnology. *FEMS Microbiology Letters, 247*(2), 105-111.

Stewart, J. D., Reed, K. W., Zhu, J., Chen, G., & Kayser, M. M. (1996). A "Designer Yeast" That Catalyzes the Kinetic Resolutions of 2-Alkyl-Substituted Cyclohexanones by Enantioselective Baeyer-Villiger Oxidations. *The Journal of Organic Chemistry, 61*(22), 7652-7653.

Stroud, J., Paton, G., & Semple, K. (2007). Microbe-aliphatic hydrocarbon interactions in soil: implications for biodegradation and bioremediation. *Journal of Applied Microbiology, 102*(5), 1239-1253.

Swanson, P. E. (1999). Dehalogenases applied to industrial-scale biocatalysis. *Current Opinion in Biotechnology, 10*(4), 365-369.

Szolkowy, C., Eltis, L. D., Bruce, N. C., & Grogan, G. (2009). Insights into Sequence-Activity Relationships amongst Baeyer-Villiger Monooxygenases as Revealed by the Intragenomic Complement of Enzymes from *Rhodococcus jostii* RHA1. *ChemBioChem, 10,* 1208-1217.

Tamura, K., Dudley, J., Nei, M., & Kumar, S. (2007). MEGA4: Molecular Evolutionary Genetics Analysis (MEGA) software version 4.0. *Molecular Biology and Evolution, 24,* 1596-1599.

Thomas, S. M., DiCosimo, R., & Nagarajan, V. (2002). Biocatalysis: applications and potentials for the chemical industry. *Trends in Biotechnology*, *20*(6), 238-242.

Thompson, I. P., Van Der Gast, C. J., Ciric, L., & Singer, A. C. (2005). Bioaugmentation for bioremediation: the challenge of strain selection. *Environmental Microbiology, 7*(7), 909-915.

Tiehm, A., Schmidt, K. R., Pfeifer, B., Heidinger, M., & Ertl, S. (2008). Growth kinetics and stable carbon isotope fractionation during aerobic degradation of *cis*-1,2-dichloroethene and vinyl chloride. *Water Research, 42*(10-11), 2431-2438.

Top, E. M., & Springael, D. (2003). The role of mobile genetic elements in bacterial adaptation to xenobiotic organic compounds. *Curr. Opin. Biotechnol., 14*(3), 262.

University of Iowa Carver College of Medicine DNA Facility. *Real-Time PCR Primer and Probe Design*, 2010, from http://dna-9.int-med.uiowa.edu/?q=node/42

USEPA. (2006). *Global Anthropogenic Non-CO2 Greenhouse Gas Emissions: 1990-2020.*, 2010, from http://www.epa.gov/climatechange/economics/downloads/GlobalAnthroEmissionsReport.pdf

USEPA. (2010). *Pollutants/Toxics.*, 2010, from http://www.epa.gov/ebtpages/pollutants.html

van Beilen, J. B., Holtackers, R., Luscher, D., Bauer, U., Witholt, B., & Duetz, W. A. (2005). Biocatalytic production of perillyl alcohol from limonene by using a novel *Mycobacterium* sp. cytochrome P450 alkane hydroxylase expressed in *Pseudomonas putida*. *Appl. Environ. Microbiol., 71*(4), 1737-1744.

van der Meer, J. R., & Sentchilo, V. (2003). Genomic islands and the evolution of catabolic pathways in bacteria. *Curr. Opin. Biotechnol., 14*(3), 248.

van der Ploeg, J., Willemsen, M., van Hall, G., & Janssen, D. B. (1995). Adaptation of *Xanthobacter autotrophicus* GJ10 to bromoacetate due to activation and mobilization of the haloacetate dehalogenase gene by insertion element IS1247. *J. Bacteriol., 177*, 1348-1356.

van der Ploeg, J. R., Kingma, J., De Vries, E. J., Van der Ven, J. G., & Janssen, D. B. (1996). Adaptation of *Pseudomonas* sp. GJ1 to 2-bromoethanol caused by overexpression of an NAD-dependent aldehyde dehydrogenase with low affinity for halogenated aldehydes. *Arch. Microbiol., 165*(4), 258-64.

van Hylckama Vlieg, J. E. T., de Koning, W., & Janssen, D. B. (1996). Transformation kinetics of chlorinated ethenes by *Methylosinus trichosporium* OB3b and detection of unstable epoxides by on-line gas chromatography. *Appl. Environ. Microbiol., 62*, 3304-312.

Verce, M. F., Ulrich, R. L., & Freedman, D. L. (2000). Characterization of an isolate that uses vinyl chloride as a growth substrate under aerobic conditions. *Appl. Environ. Microbiol., 66*, 3535-3542.

Verce, M. F., Ulrich, R. L., & Freedman, D. L. (2001). Transition from cometabolic to growth-linked biodegradation of vinyl chloride by a *Pseudomonas* sp. isolated on ethene. *Environ. Sci. Technol., 35*, 4242-4251.

Widada, J., Nojiri, H., & Omori, T. (2002). Recent developments in molecular techniques for identification and monitoring of xenobiotic-degrading bacteria and their catabolic genes in bioremediation. *Applied Microbiology and Biotechnology, 60*(1), 45-59.

Wiegel, J., & Wu, Q. (2000). Microbial reductive dehalogenation of polychlorinated biphenyls. *FEMS Microbiology Ecology, 32*(1), 1-15.

Zhang, Z., Schwartz, S., Wagner, L., & Miller, W. (2000). A greedy algorithm for aligning DNA sequences. *Journal of Computational Biology, 7*(1-2), 203.